FORUM HOLZBAU INTERNATIONAL

28th International Wood Construction Conference (IHF)
Master Colloquium
Volume III December 5, 2024
Practical experience – Practical application



Content MASTER COLLOQUIUM

Displacement-based Design of Highly Ductile Anchored CLT Walls using the N2 Method 07
Jonas Wacker, Bern University of Applied Sciences, Biel/Bienne, Switzerland
WaltGalmarini, Zurich, Switzerland

FE-modeling and calibration of a long-span wooden beam floor by means of vibration measurement 19
Valentin Knöpfle, Biberach University of Applied Sciences, Biberach, Germany

Investigations of the load-bearing behaviour of resin impregnated compressed wood dowels in a double shear timber connection 31
Max Jeschkowski, Mittelhessen/Giessen University of Applied Sciences, Germany

Künstliche Intelligenz im Holzbau
Entwicklung und Training eines Künstlichen Neuronalen Netzes zur Vorhersage der Biegefestigkeit von Pappelholz 39
Pascal Fröhlich, Biberach University of Applied Sciences, Kempten, Germany

Sustainable Development and Adaption of the Historic Tachenhausen Farm Estate 53
Eliese Helmig, Frankfurt University of Applied Sciences, Frankfurt am Main, Germany

A Systems Thinking Approach to Production Optimisation in the Prefabricated Housing Industry 61
Lorenz Weiß, Rosenheim Technical University of Applied Sciences, Rosenheim, Germany; Rubner Haus, Bruneck, Italy

Enhancing design and production in modular timber architecture with computational design tools 73
Joaquim Escoda, Bern University of Applied Sciences, Biel/Bienne, Switzerland

Moderation

Prof. Heinzmann Andreas
Rosenheim Technical University
of Applied Sciences
Hochschulstrasse 1
83024 Rosenheim, Germany

+49 8031 805 23 08
andreas.heinzmann@fh-rosenheim.de

Prof. Dr. Lehmann Martin
Bern University of Applied Sciences
Solothurnstrasse 102
2504 Biel/Bienne, Switzerland

+41 32 344 03 21
martin.lehmann@bfh.ch

Speakers

Escoda Joaquim
Bern University of Applied Sciences
Solothurnstrasse 102
2504 Biel/Bienne, Schweiz

joaquim.escodallorens@bfh.ch

Fröhlich Pascal
Biberach University of Applied Sciences
Karlstrasse 6-11
88400 Biberach, Germany

pas.froehlich@gmail.com

Helmig Eliese
Frankfurt University of Applied Sciences
Nibelungenplatz 1
60318 Frankfurt am Main, Germany

eliese.helmig@aol.com

Jeschkowski Max
Mittelhessen/Giessen University
of Applied Sciences
Wiesenstrasse 14
35390 Giessen, Germany

max.jeschkowski@bau.thm.de

Knöpfle Valentin
Biberach University of Applied Sciences
Karlstrasse 6-11
88400 Biberach, Germany

knoepfle@hochschule-bc.de

Wacker Jonas
Bern University of Applied Sciences
Solothurnstrasse 102
2504 Biel/Bienne, Switzerland

jonas.wacker@waltgalmarini.ch

Weiß Lorenz
Rosenheim Technical University
of Applied Sciences
Hochschulstrasse 1
83024 Rosenheim, Germany

lorenz-weiss@outlook.com

Displacement-based Design of Highly Ductile Anchored CLT Walls using the N2 Method

Jonas Wacker
WaltGalmarini AG
Bern University of Applied Sciences
Zürich, Switzerland



Displacement-based Design of Highly Ductile Anchored CLT Walls using the N2 Method

1. Introduction

In Switzerland the seismic design of new buildings is usually carried out using a force-based approach. A more sophisticated analysis may be achieved by means of a displacement-based approach. In the scope of the presented Master Thesis [1] the N2 method as proposed in the Eurocode 8 draft prEC8 of the second generation was used [2,3]. This method represents a simplification of the N2 method, as developed by Peter Fajfar [4].

With cross laminated timber CLT, a wood-based panel suitable for bracing walls is available. The most challenging part of the design is the transfer of tensile forces from the CLT into the concrete foundation. Using off-the-shelf solutions, a capacity of approximately 100 kN per anchorage component can be achieved. With the aim to develop a simple and high-performing anchorage system, the University of Applied Sciences Bern BFH and Ancotech AG launched an Innosuisse Project in 2018. It aims to apply the principles of slender concrete shear walls while using highly ductile B500C steel bars as anchorage for CLT walls.

2. Material and Method

2.1. Material

In the Master Thesis [1] the CLT was modelled with strength properties according to ETA-06/0138 from KLH Massivholz GmbH [5]. This European Technical Assessment accounts for the favourable influence of decreasing lamella thickness on the in-plane net shear strength $f_{v.xy.k}$ as documented by Hirschmann [6]. This allows for a built-up with thin horizontal lamellas and thick vertical lamellas, maximizing both tensional and in-plane shear strength. The modulus of elasticity of the lamellas was assumed to be E_0 = 11’500 MPa and the in plane shear modulus of the cross section with G_{xy} = 450 MPa cf. Bernasconi [7].

The stiffness and strength properties of the steel bars acting as anchorage were modelled according to prEC8-1-1 [2] as well as data from experimental tests carried out at BFH. Since the steel bars act as an anchorage of a timber element, they were tested using a protocol suitable for timber connections [8]. From these testing data mean values were derived that have been used to model the properties of the steel bars.

2.2. Construction

Conventionally, CLT buildings are braced with all walls built from CLT in platform framing (indicated with Type A in Figure 1). This conflicts with the preference of modern architecture for a minimal number of bracing walls. An alternative approach are buildings braced with CLT, labeled as Type B in Figure 1. Here, only suitable walls are constructed in CLT and used as bracing elements. This construction method is well suited to balloon framing. The constructions examined in the Master Thesis [1] fall under Type B.

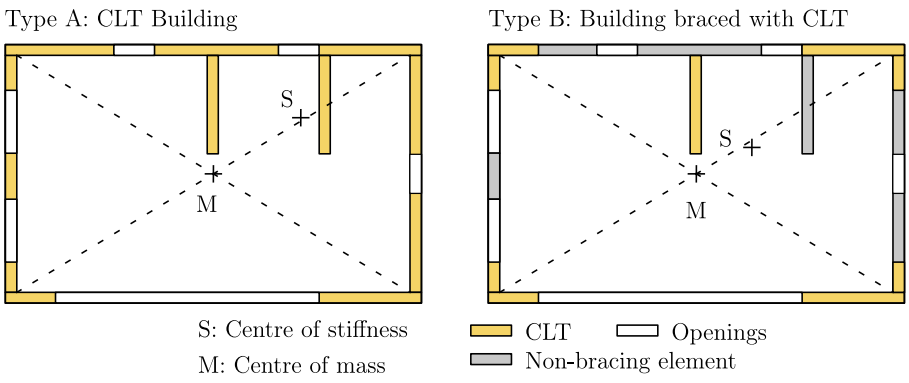


Figure 1: Types of CLT bracing systems based on Lignatec [9]

The aforementioned bracing Type B is suitable for slender bracing walls with a flexural dissipative mechanism. An example of such a system is the highly ductile anchored CLT walls shown in Figure 2. Around the eyes (see Figure 3b) the forces exert tension, while a shear plane forms below them. This necessitates an optimized built-up design that enhances shear as well as tensile resistance. Subsequently, the forces are transferred as compression forces from the CLT to the steel plate through contact.

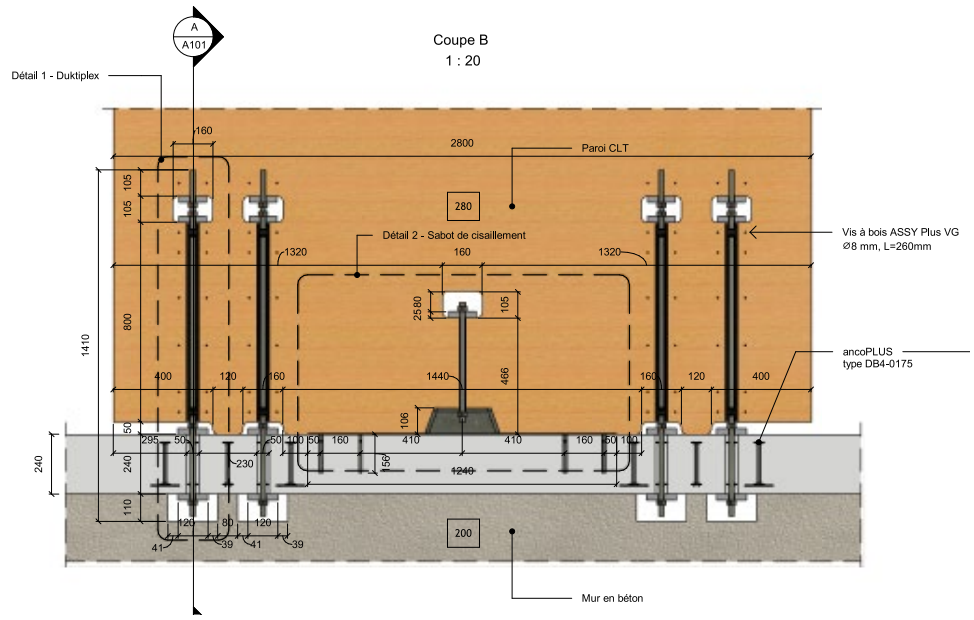
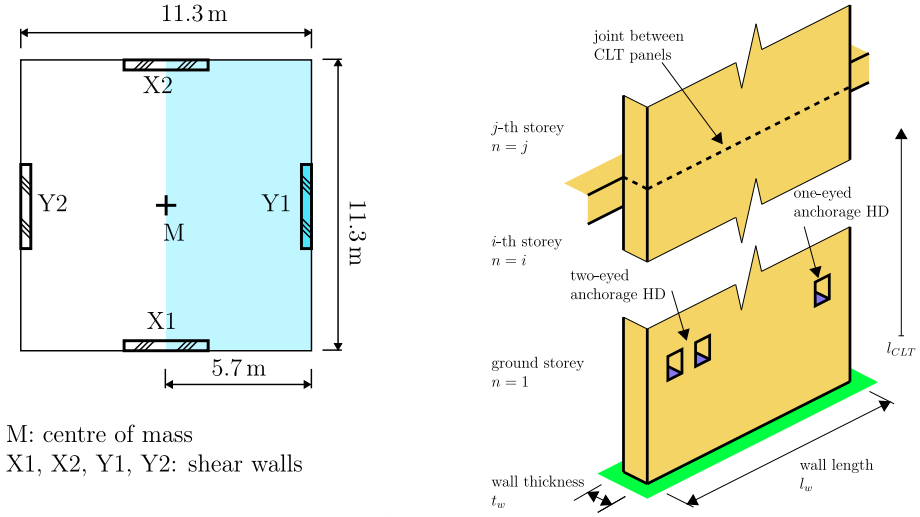


Figure 2: Highly ductile anchored CLT wall as shown by Geiser/Maître [10]

The ductile mechanism of these walls requires them to develop a rocking behaviour. At the time of writing, no detail could be developed that introduces vertical loads into the bracing wall without preventing it from developing a rocking behaviour. The investigated example building, as seen in Figure 3, is assumed to be a skeleton construction regardng the vertical load path. In order to introduce horizontal actions without preventing the rocking behaviour, a detail was developed in the scope of the research project CLT Dynamics [11]. Furthermore the following boundary conditions for the examined building are:

- Story height h_i = 3 m
- Quasi-permanent mass 7 kN/m^2 with a load introduction area of approximately 64 m^2
- Load introduction area in elevation per storey of 17 m^2 for wind action
- Overstrength factor γ = 1.6



(a) (b)

Figure 3: Examined object (a) floor map (b) axonometry of wall with example of one-eyed and two-eyed hold downs HD

For the anchorage, one-eyed and two-eyed layouts were examined, with two steel bars positioned in each eye. The following steel bars were considered:

- Steel bar B500C d = 16 mm
- Steel bar B500C d = 20 mm

For the CLT panels, the built-ups as shown in Table 1 have been examined. The width of the CLT panel, expressed as wall width l_w, was limited by the requirement for transportation. For the length of the CLT panel a length of l_{CLT} = 12 m and a storey wise segmentation l_{CLT} = h_i = 3 m was considered.

Table 1: Examined cross section for CLT walls

Wall dimension t_w x l_w [mm]	Thickness of single layer t_i [mm]											t_0 [mm]	t_{90} [mm]
	L_1	Q_1	L_2	Q_2	L_3	Q_3	L_4	Q_4	L_5	Q_5	L_6		
220 x 2’200	40	20	40	20	40	20	-	-	-	-	-	160	60
280 x 2’800	40	20	40	20	40	20	40	20	-	-	-	200	80
340 x 3’400	40	20	40	20	40	20	40	20	40	20	40	240	100

The connection of the CLT elements was designed to be a non-dissipative element. The connection of the CLT wall elements between each other was designed using a two-sided Rothoblaas WHT Plate T with HBS Plate d8x100 mm, a four shear plane connection with Dowels d10 mm or a steel bar connection, such as the anchorage to the embedment level. In this case, the connection can be simplified since it remains elastic.

2.3. Displacement-based Approach

The displacement-based approach as proposed in prEC8 [2,3] estimates the response based on the fundamental period T_1. The structure is modelled using mean values and the components that remain in the elastic regime are modelled linear-elastic, while the ductile-dissipative components are modelled non-linear. A flow chart of the procedure is shown in Figure 4.

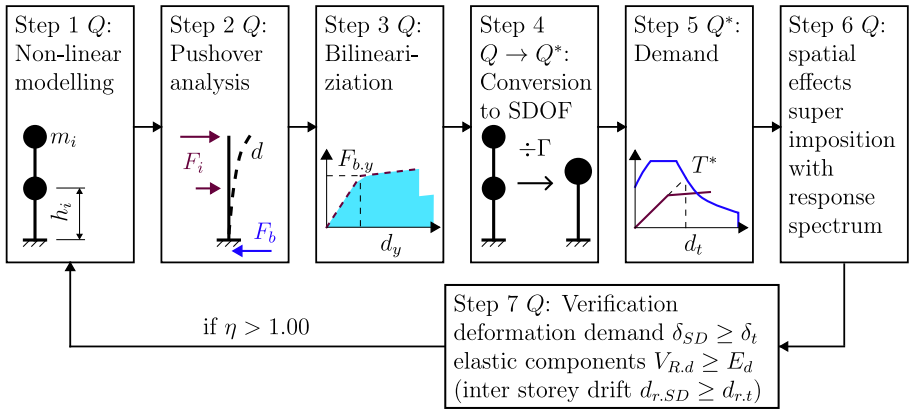


Figure 4: Flow chart of N2 method according to prEC8 [2,3]

In a force-based approach, the ductile-dissipative components are verified using forces, whereas in the displacement-based approach, these components are verified using deformations or displacements. The demand is estimated by using an equivalent single degree of freedom system SDOF for the first mode. This SDOF represents a simplification of the multi degree of freedom system MDOF. As shown in Figure 5, the acceleration displacement response spectrum ADRS allows to superimpose the properties of the SDOF with the seismic action. The properties of the SDOF are represented with the pushover curve. The response spectrum is plotted with the spectral acceleration $S_e(T)$ on the ordinate and the spectral displacement $S_u(S_e)$ on the abscissa. A definition of a yield point is necessary in order to derive the deformation demand d_t^*. In most cases the fundamental period of the MDOF T_1 and the SDOF T^* are similar or equal. For medium and long period ($T^* > T_C$), the elastic displacement demand d_{et}^* is equal to the inelastic displacement demand d_t^*. For short periods ($T^* \leq T_C$) the inelastic displacement demand is to be increased $d_t^* \geq d_{et}^*$.

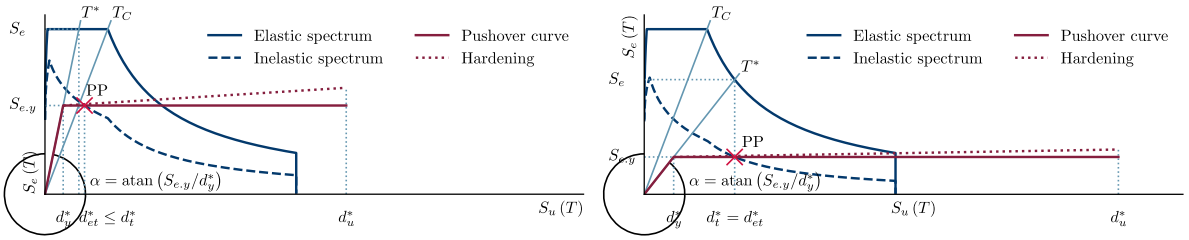


Figure 5: Determination of displacement demand using the ADRS format for short periods (a) and medium to long period (b)

Non-linear modelling in a three dimensional manner is challenging. Therefore, it is challenging to account for spatial effects using the displacement-based approach. The current Eurocode 8 EC8-1 [12] proposes for regular structures to do a two dimensional modelling for both main directions and accounting for torsion in plane. Essentially, the same procedure as for the equivalent force method. In prEC8-1-1 [2], it is proposed to superpose the results of the N2 method with the results of the response spectrum method.

The current chapter aims to give the reader a brief overview of the N2 method, as it was used in the presented Master Thesis [1]. For further information, the reader is referred to technical literature such as Fajfar [4] as well as the Master Thesis.

2.4. Examined Limit States

The structure was modelled according to prEC8 [2,3] and the actions according to SIA 260 and 261 [13,14]. With the updates of seismic actions from prEC8-1-1 [2] already incorporated into SIA 261 this is a feasible approach. The following limit state criteria LSC have been defined for the Master Thesis:

- LSC I: maximal wind (GK II and q_{p0} = 1.3 kN/m^2) and maximal seismic actions (BGK E and Z3b)
- LSC II: minimal wind (GK IV and q_{p0} = 0.9 kN/m^2) and maximal seismic actions (BGK E and Z3b)
- LSC III: maximal seismic actions (BGK E and Z3b)
- LSC IIIb: minimal seismic actions (BGK A and Z1a)

LSC III could represent the narrow side of a building, where seismic actions are clearly governing. In addition to the verifications according to prEC8-1-2 [3] the fundamental period was limited to $T_1 \leq 2$ s in order to examine only relevant scenarios.

3. Results and Discussion

In a first step, the influence of stiffness components, lever arm of anchorage and normal force were examined. The first two parameters were used to check the model for plausibility. For the latter no favourable influence on the verification could be identified. Due to the small spans in timber floors, a limited amount of normal force can be introduced into a wall. Furthermore due to the restrictions due to detailing, this construction would have to be designed conventionally with q = 1.5. This trade off between added overbearing load and loss in ductility results in an overall much higher utilization of verifications. This chapter discusses going forward the results regarding the following examinations:

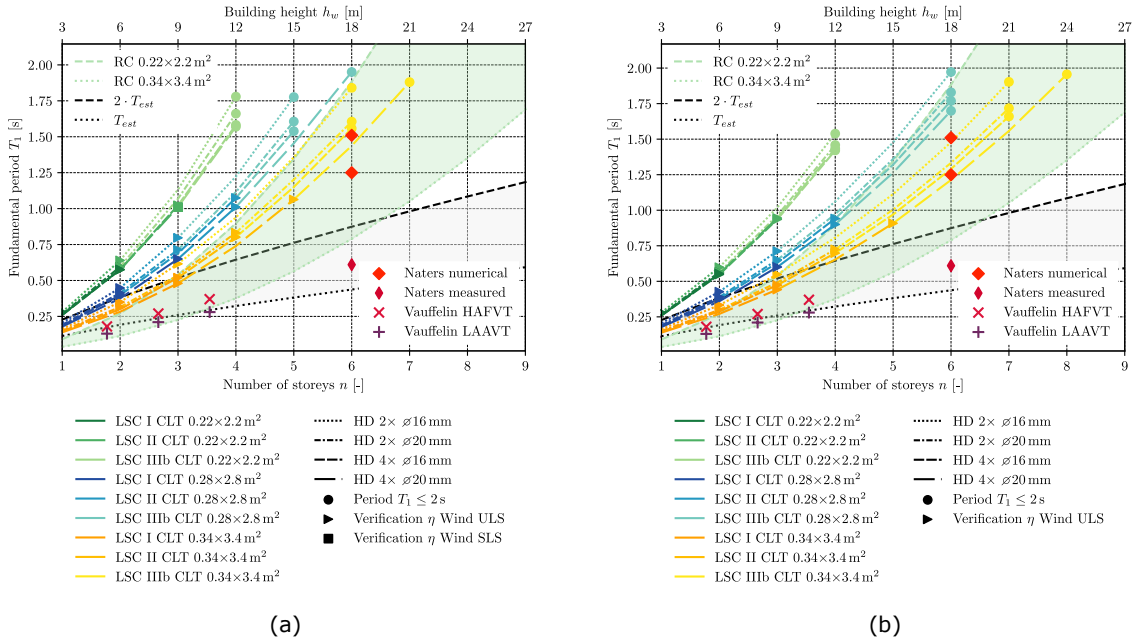
- Fundamental period T_1
- Derived behaviour factor q_{SD} (at limit state significant damage SD cf. prEC8-1-1 [2])
- Verification according to prEC8 [2,3]

3.1. Fundamental Period

For the force-based as well as the displacement-based approach, the fundamental period T_1 is a crucial parameter. In the scope of the new earthquake design guideline of Lignum [15], measurements of the buildings braced with timber have been carried out. It was shown that the fundamental period T_1 typically does not exceed $2 \cdot T_{est}$. The value for T_{est} can be calculated using formula (1) with the building height h_w as the only input parameter [3]. This range is marked in grey in Figure 6.

$$T_{est} = 0.05 \cdot h_w^{0.75} \quad (1)$$

Two of the aforementioned measurements are of particular interest for the Master Thesis [1]. First, there are the measurements carried out during a testing of a CLT structure in Vauffelin CH [15]. LAAVT are measurements using small amplitudes and ambient vibrations, whereas HAFVT uses high amplitudes and forced vibrations. The latter is suitable to estimate a fundamental period T_1 used in seismic design. The test building in Vauffelin CH was designed to be stiffer than the structures examined for the Master Thesis [1]. Secondly, there is a building in Naters CH which is braced with slender CLT walls (building type B in Figure 1). The anchorage is done conventionally and not with the here examined anchorage system. The difference between numerically estimated and measured fundamental period T_1, termed as $\eta_{t.k} \cdot X$, is significant. The green, blue and yellow curves in Figure 6 represent the highly ductile anchored CLT walls that were examined. It can be seen that they are in a similar range and show a similar shape as concrete walls RC with the same geometry and mass. In Figure 6 it, is shown that joint at every storey with l_{CLT} = 3 m has a significant influence on the fundamental period T_1.



(a) (b)

Figure 6: Fundamental period T_1 as function of number of storeys n and building height h_w: highly ductile anchored CLT walls with LSC I, II and IIIb with l_{CLT} = 3 m (a) and l_{CLT} = 12 m (b), range for empirical formula T_{est}…2 · T_{est}, RC wall and measurements from Lignum Earthquake Documentation [15]

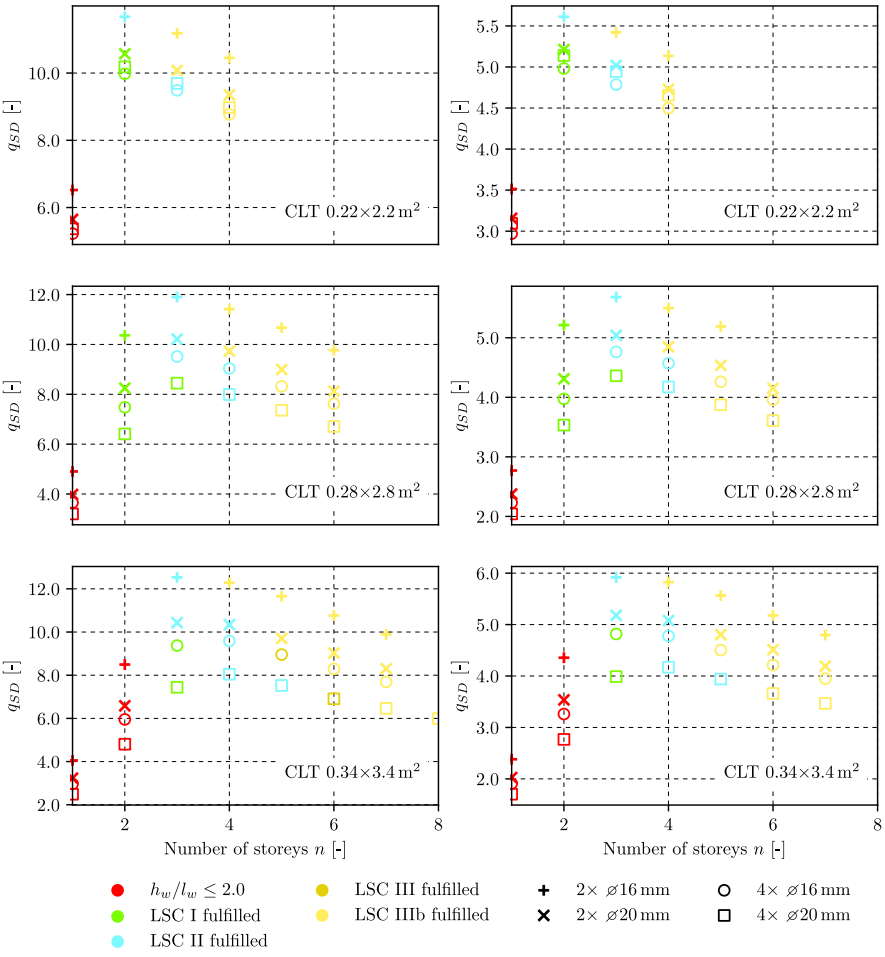
In the scope of the presented Master Thesis [1] the bracing walls were modelled as beam elements neglecting any contribution of non-bracing elements. The same approach was used for the seismic design of the building in Naters CH [15], which can lead to an underestimation of the stiffness. For the calculation of the fundamental period, the stiffness is taken into account under the square root. Therefore, the stiffness increase $\eta_{t.k} \cdot X$ to take into account the contribution of non-bracing elements can be estimated by squaring the ratio of numerical and measured period T_1. This way a factor of $\eta_{t.k} \cdot X \approx 4.2…6.1$ can be derived for the building in Naters CH. Increasing the stiffness in this manner places the fundamental periods of the highly ductile anchored CLT walls in the range of T_{est}…2 · T_{est}. Since an overestimation of stiffness is on the non-conservative side in the case of a displacement-based approach, this increase in stiffness has been neglected in the scope of the Master Thesis [1].

3.2. Derived Behaviour Factor

Using the ratio of displacement capacity d_{SD} for the limit state SD and yield displacement d_y a behaviour factor q_{SD} for a structure can be derived. In prEC8 [2,3] the behaviour factor q is defined as the product of the components for overstrength q_S, ductility q_D and redistribution q_R. Using the displacement-based approach, the first two components are included in the model and the latter can be conservatively assumed to be unity. In Figure 7 behaviour factors q_{SD} for the example building in Figure 3 are shown. A joint in the wall is placed using a CLT length of l_{CLT} = 12 m.

In Figure 7a the results when modelling the anchorage with the experimental properties are shown, whereas Figure 7b visualizes the results with properties of the anchorage according to prEC8-1-1 [2,3] are shown. For both, the post-elastic range is reduced by 50 % as prescribed by prEC8-1-1 [1]. Using this reduction, the structures modelled with the experimentally determined properties for the anchorage exhibit a local ductility of μ_ε = μ_φ = 20.5. The ratio between local and global ductility is in the range of 1.6…3.5. The local and global ductility is reduced by approximately 50 % if the anchorage is modelled using the properties for the anchorage according to prEC8-1-1 [2]. If joints are placed at every storey with l_{CLT} = 3 m the ductility is reduced by 17 % or less. The green, azure, ochre and yellow colors in Figure 7 indicate the limit state criteria LSC that is fulfilled. The undershooting of the minimum slenderness for a capacity design according to SIA 262 [16] is indicated in red. With an increasing number of storeys at first an increase in ductility

can be observed and then it decreases. Ductility increases with the wall's slenderness. The bending stiffness decreases cubically with height, while the base fixation follows a quadratic relationship. Initially, the effect of increased ductility due to greater slenderness prevails; however, from the third or fourth story onward, the increase in yield displacement becomes the dominant factor.



(a) (b)

Figure 7: Behaviour factor q_{SD} with (a) experimentally determined properties for anchorage and (b) properties according to prEC8-1-1 [1]

For slender concrete walls, SIA 262 [16] proposes a behaviour factor of q = 4 and prEC8-1-2 [3] q = 3.6. Using the properties of the steel bar according to prEC8-1-1 [2] as well as neglecting the relatively low possible masses for timber buildings, a minimum value for the behaviour factor of q = *4* can be confirmed. In Figure 7 solely results that fulfil the defined limit state criteria LSC are plotted. It can be observed that only in isolated cases the number of possible storeys is reduced if the properties of the anchorage are modelled according to prEC8-1-1 [2]. For q > 6…8 the displacement-based approach may underestimate the demand cf. Fajfar [4]. However, the results show that a behaviour factor of q > 6 is not needed for the design.

3.3. Verification in prEC8

In the current EC8-1 [12] the safety level for the displacement-based approach is in general lower than in prEC8 [2,3]. The calculation of the displacement demand d_t remains unchanged. The calculation of the capacity differs, however. For structures that exhibit a local yielding, such as highly ductile anchored CLT walls, prEC8-1-1 [2] allows for a verification of the deformation demand rather than displacement demand. This is more favourable, as the local ductility is bigger than the global ductility. Furthermore, the partial

safety factor is more favourable in prEC8-1-1 [2] than in EC8-1 [12]. The change, that makes the verification less favourable, is the requirement to reduce the post-elastic component of the deformation by 50 % when calculating the capacity for the limit state SD cf. prEC8-1-1 [2].

As the name highly ductile anchored CLT walls implies, the principles of capacity design may be applied. For the force-based approach, clear guidance is given in prEC8 [2,3] on how to prevent premature brittle failure. In the Master Thesis [1] the utilization for the displacement-based approach has been compared with the force-based approach using the principles of capacity design. For the examined walls the utilization for the displacement-based approach was approximately more favorable by the overstrength factor γ_{Rd}.

When doing the pushover analysis the forces may be applied in different shapes (Step 2 in Figure 4). The modal shape resembles the first mode, while the linear shape approximates it. Both standards propose to use one of them. Additionally, in EC8-1 [12] the uniform shape shall be used. For shear controlled failure mechanisms of elastic components the uniform shape leads to a higher utilization.

4. Conclusion and Outlook

It can be concluded that the displacement-based approach according to prEC8 [2,3] can be applied to timber structures. The procedure allows for a more realistic assessment of the seismic behaviour than a force-based approach. The process of bilinearizing the load-deformation behaviour of highly ductile anchored CLT walls was straightforward. In the case of conventional i.e. laterally loaded dowel-type fasteners the process is challenging. Open questions such as the verification of elastic components and the shape for the pushover analysis remain. For novel construction types without an established behaviour factor q the displacement-based approach offers an efficient design methodology. A potential solution to simplify the complex consideration of spatial effects is to determine the behaviour factor q for the least ductile bracing walls. This behaviour factor q can then be used for the entire building in a force-based approach.

When using highly ductile anchored CLT walls, it could be shown that the hazard scenario earthquake is in exceptional cases the governing horizontal action. The bracing system exhibits several of the advantageous characteristics of a slender concrete wall, including a ductile failure mechanism. For the examined geometry, it was shown that bracing up to five stories is possible. Open points, especially concerning the construction remain, including the connection between floor and wall as well as the placement of joints within the wall.

5. Acknowledgement

I would like to express my gratitude to my supervisors Prof. Martin Geiser, Prof. Dr. Pierino Lestuzzi and Prof. Dr. Martin Lehmann, for their continuous support throughout my Master Thesis. I am also deeply thankful to my friends for the invaluable insight that I could gain through our many discussions on the subject. Last but not least I thank Kilian Paul for proof reading this conference contribution.

6. References

[1] J. Wacker, Verschiebungsbasierte Bemessung von hochduktil verankerten Wänden in Brettsperrholz mithilfe der N2-Methode. Berner Fachhochschule BFH, 2024

[2] prEN 1998-1-1:2022, Eurocode 8: Design of structures for earthquake resistance – part 1-1: General rules and seismic action (Standard), CEN – European Committee for Standardization Brussels, Sep. 2022.

[3] prEN 1998-1-2:2022, Eurocode 8: Design of structures for earthquake resistance part 1-2: Buildings (Standard), CEN – European Committee for Standardization Brussels, Dec. 2022.

[4] P. Fajfar, The Story of the N2 Method.
Tokyo: IAEE International Association for Earthquake Engineering, 2021.

[5] ETA-06/0138, Massive plattenförmige Holzbauelemente für tragende Bauteile in Bauwerken, KLH Massivholzbau GmbH (Europäische Technische Bewertung), Österreichisches Institut für Bautechnik (OIB), Jan. 2021.

[6] B. Hirschmann, Ein Beitrag zur Bestimmung der Scheibenschubfestigkeit von Brettsperrholz. Verlag der Technischen Universität Graz, 2011.

[7] A. Bernasconi, «Grundlagen der Bemessung von Brettsperrholz,» in Von der Forschung zur Praxis – Erweiterung der Möglichkeiten im modernen Holzbau – Erdbebensicherheit und Brettsperrholz, (Biel/Bienne), A. Müller and B. Franke, Eds., S-WIN, May 2021, pp. 51–60, isbn: 978-906703-57-2.

[8] B. Sunier, Détermination de la ductilité cyclique des assemblages agrafés et cloués selon différents protocoles de chargement ainsi que sa méthode d'évaluation.
Berner Fachhochschule BFH, 2021.

[9] G. Gysel et al., Brettsperrholz aus Schweizer Produktion (Lignatec 32).
Zürich: Lignum Holzwirtschaft Schweiz, 2020, vol. 32.

[10] M. Geiser and K. Maître, «Hochduktile Verankerungen für den Holzbau,» in Von der Forschung zur Praxis – Erweiterung der Möglichkeiten im modernen Holzbau – Erdbebensicherheit und Brettsperrholz, (Biel/Bienne), A. Müller and B. Franke, Eds., S-WIN, May 2021, pp. 39–49, isbn: 978-906703-57-2.

[11] U. Oberbach and L. Furrer, «CLT Dynamics – Forschungsbericht,» Berner Fachhochschule BFH, Bern, Tech. Rep. R-010132-10-71FE-PB01, Dec. 2020.

[12] EN 1998-1:2004+AC:2009, Eurocode 8: Design of structures for earthquake resistance – part 1: General rules, seismic action and rules for buildings (Standard), CEN – European Committee for Standardization Brussels, Jul. 2009.

[13] SIA 261:2013, Grundlagen der Projektierung von Tragwerken (Standard), SIA Schweizer Ingenieur- und Architektenverein e.V. Zürich, Aug. 2013.

[14] SIA 261:2020, Einwirkungen auf Tragwerke (Standard), SIA Schweizer Ingenieurund Architektenverein e.V. Zürich, Aug. 2020.

[15] M. Geiser, L. Furrer, P. Lestuzzi, G. Ratsch, and N. Wirz, Erdbebengerechte Holzbauten. Zürich: Lignum Holzwirtschaft Schweiz, 2023.

[16] SIA 262:2013, Betonbau (Standard), SIA Schweizer Ingenieur- und Architektenverein e.V. Zürich, Jan. 2013.

FE-modeling and calibration of a long-span wooden beam floor by means of vibration measurement

Valentin Knöpfle
Institut für Holzbau/Hochschule Biberach
Biberach, Deutschland



FE-modeling and calibration of a long-span wooden beam floor by means of vibration measurement

1. Abstract

The objective of this master's thesis was to use an FE model to predict the vibration behavior of a wide-span wood joist floor as accurately as possible. As a result, a better economic efficiency of these floors should be achieved, since the vibration verification is often decisive for these floors. In the course of a research project, measurements from November 2021 to July 2022 identified a large number of influences on the vibration behavior that need to be considered. According to the current state of standardization and technology, these influences have not yet been included in the hand calculation, so the different but related individual topics have to be investigated for a realistic prognosis.
It was shown that a simulation of the structural behavior by means of FE models, especially under special boundary conditions, can be carried out much more accurately. Based on investigations of the individual material properties, an extensive calibration of the model was carried out and significant influences and dependencies were identified and considered accordingly.
During calibration, it was important to build up the model step by step in order to consider better the individual material properties. But even despite this approach, many material parameters had to be constantly readjusted. In this case, the calibration was performed only on the natural frequencies. Some aspects of the measurements were also discovered in the model. However, in order to use this model for an assessment of the vibrations of the floor, further investigations are necessary. At the same time, the velocities and accelerations should also be considered.
The in-depth study of this topic has made it clear that the calibration of an FE model is associated with a high level of effort. Nevertheless, it is subsequently possible to predict the vibration behavior of the floor in the model without the need for costly erection or reconstruction of the floor on construction site and to investigate it subsequently by measurements.

Keywords: vibrations, long-span wooden floors, FE-modeling, calibration

2. Introduction and motivation

From January 2021 to June 2023, Biberach University of Applied Sciences worked in cooperation with PIRMIN JUNG Deutschland GmbH, Remagen, on the development of a lightweight, vibration-optimized timber floor system with joists for large spans. Previous research work has already investigated the vibration behavior of wooden floors. The new focus in this project is primarily on the size of the system under investigation. Buildings such as schools, administration and office buildings require floors with very large column spacing and therefore very large spans. Different floor systems with different superstructures, support conditions and spans were measured and evaluated. The research project included theoretical and practical considerations of the vibration and damping behavior of wooden floors with large spans and beams.

With large spans, the frequency criterion becomes decisive, as can be seen in Figure 1. It is therefore of great importance to examine floors with large spans more intensively with regard to their actual vibration behavior. This is to be done using a test rig on a scale of 1:1, which is explained in the following chapter 4.

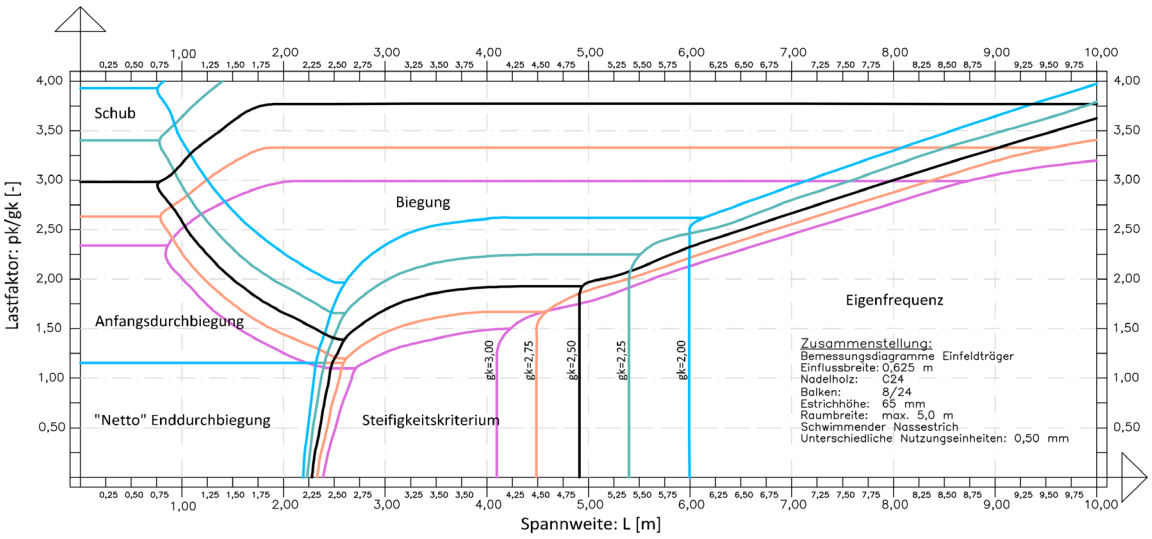


Figure 1: Design-relevant verification for floors as a function of the span, based on [2], taken from [5].

3. Existing design rules in codes and literature

3.1. Previous research

Based on the vibration analysis that has long existed in Eurocode 5 [1], a research project was carried out at the Technical University of Munich from 2007 to 2009 [2]. The research project showed that floors with natural frequencies below the limit frequency of f_{lim}= 8 Hz are satisfactory in terms of their serviceability if two conditions are met:
The frequency must be greater than the minimum frequency of f_{min} = 4.5 Hz and the acceleration, when walking in resonance with the second or third harmonic, must be less than a limiting acceleration a_{grenz}.

However, the acceleration can only be verified for heavy floors, such as wood-concrete composite systems or systems with large spans. The following flow chart (see Figure 1) shows the verification of vibrations according to [2].

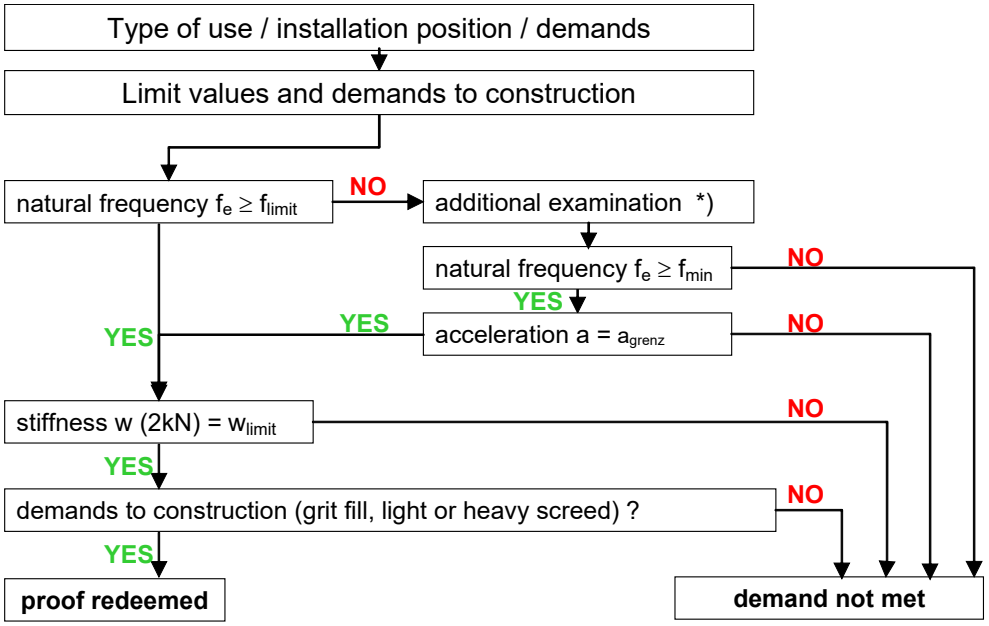


Figure 2: Design and dimensioning rules according to [2]

3.2. Draft Eurocode 5

The basic idea of the new draft of Eurocode 5 [3] is to modify the rules in such a way that human perception is significantly incorporated into the design. The response factor R was therefore introduced. The sensitivity of perception depends – as shown in ISO 10137 [9] – on the natural frequency of the floor. The limit values and verifications are therefore carried out depending on the natural frequency and the requirements (see Table 1).

Table 1: Limit values and response factor R according to performance level according to [3]

	Floor performance levels					
Criteria	I	II	III	IV	V	VI
Response factor R	4	8	12	24	36	48
Stiffness criteria for all floors w_{1kN} [mm] ≤	0,25		0,5	1,0	1,5	2,0
Frequency criteria for all floors f_1 [Hz] ≥	4,5					
Acceleration criteria for resonant vibration (f_1 < 8 [Hz]) a_{rms} [m/s²] ≤	0,005 R					
Velocity criteria for transient vibration (f_1 ≥ 8 [Hz]) v_{rms} [m/s] ≤	0,0001 R					

Table 1 shows the response factor R as a function of a floor performance level to be selected, as well as the limit values for deflection due to a static concentrated load, acceleration and velocity, see [3].
Figure 2 shows the principle path and the most important equations of the verification (see also [4]).

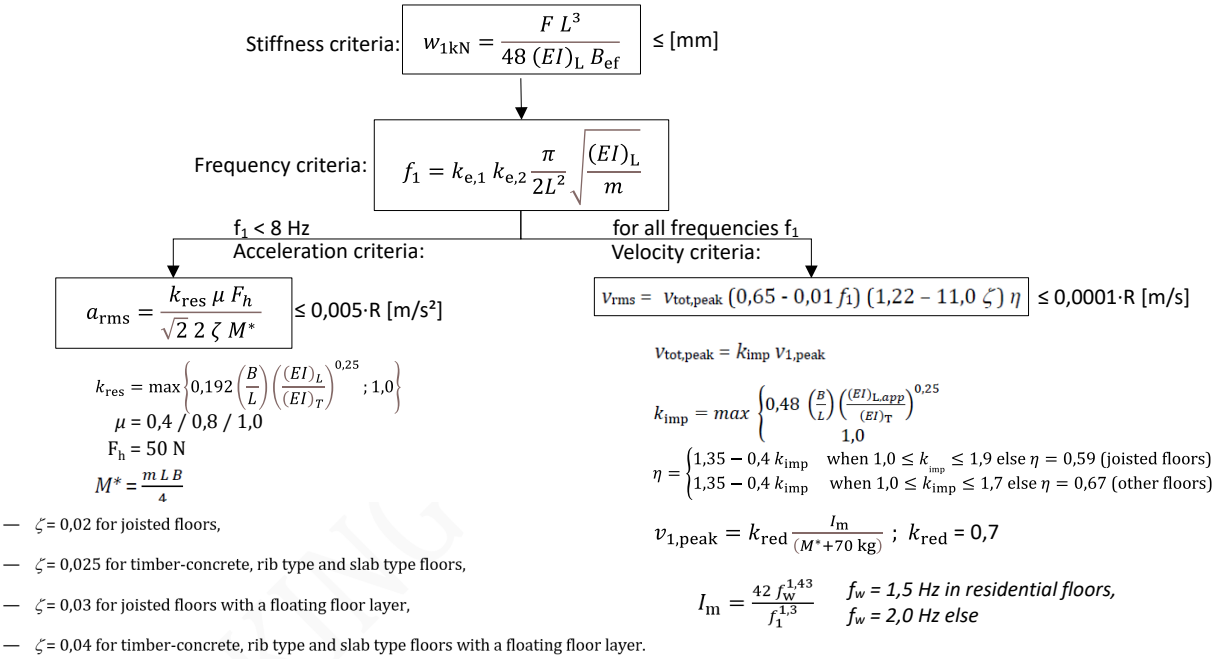


Figure 3: Flow chart and equation according to [3]

4. Test bench

4.1. Design

The vibration verification is a verification in the serviceability limit state. The focus here is on the safety and well-being of the users of the floors. To find out how people feel on the floor, a test stand is built on a 1:1 scale so that all effects can be measured and felt. This test stand measures 12.5 m x 12.5 m and consists of box elements. The construction of the test stand is shown in Figures 4 to 6. Detailed information on planning and construction can be found in [6].



Figure 4: Raw floor without top planking



Figure 5: Raw floor with top planking

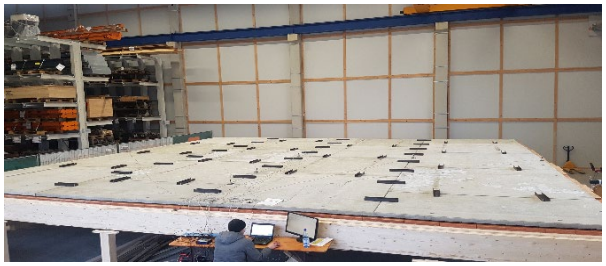


Figure 6: Test bench with mass and screed elements, type 3

4.2. Measurements

The test stand was designed to be flexible in order to be able to reproduce different floor structures and storage situations. The various superstructures and combinations can be seen in [6]. With the help of the test stand, the span width could be varied between 8 m and 12 m. Another special feature was the variation of the bearing situation: it is possible to represent both a two-sided (Zs) and a four-sided (Vs) bearing on walls. In addition, an elastic support can be represented by a wooden beam (Uz) as well as by a steel beam.

Different methods were used to excite the floor. First, a heel drop was carried out to measure the natural frequencies and damping. Everyday use was depicted with a person walking. With this measurement, the velocity (v_{rms}) is considered.

In addition to the impulse and random walking, the floor was excited to resonant vibrations by jogging at natural frequency. A shaker was also used. This shaker can be used to generate a defined force and thus determine the resonating mass.

One of the most important points is the subjective evaluation of the vibrations. The vibrations were assessed by the test subjects JR and VK and compared with visitor groups and other participants. The scores used are based on the research report [2] and the work of Kreuzinger/Mohr [7].

5. FE-modeling

After many measurements and their evaluations have been carried out, the next step is FE modeling. The modeling procedure is dictated by the measurements. This means that the model is created step by step in the same way as the structure of the floor. The modeling was carried out using the «*Mechanical APDL*» program from «*Ansys Inc.*». The advantage of this program is that the data can be entered using *Ansys*' own scripting language (*Ansys Parametric Design Language*). This ensures that the parameters entered are used and not standardized parameters from a database. At the same time, automation is possible without major effort. All parameters used are stored as variables and linked to each other. If a parameter is changed, most of the values are adjusted immediately so that almost no further editing is necessary. For this reason, the span can be changed without great effort or the four-sided bearing can also be considered. Due to the complexity of the calibration, only the 12 m span and a two-sided support are considered in this work, whereby the downstand beam (elastic support) is underpinned and therefore not active.

The target is defined as a deviation of the natural frequencies of a maximum of 3 %. The calibration in this work is limited to the natural frequencies. Other important aspects such as acceleration are not considered, as this is dependent on the existing damping, which can only be investigated by measurement. Due to the still relatively large deviation of the damping in the measurement data, the acceleration will be considered at a later stage. The exact input of the program is not discussed in this paper, but only the essential settings are presented. The complete scripts can be found in [8]. To simplify the documentation, a program code was written that creates screenshots with defined program settings at the points used and automatically saves them with the desired file name and file location. If changes are made to the program code, all images are always up to date. At the same time, it is no longer necessary to look at every step; instead, the complete program code can be executed and the individual steps can be viewed at leisure afterwards.

5.1. Sensitivity analyses of the model

In order to be able to examine the sensitivity of the model, this is explained and carried out in more detail here. One or more specific parameters are changed for the same boundary conditions in order to be able to show their influence on the result, based on [10]. This has been described in detail in [8]. The deviation was also specified there, whereby the variance V differs from this. It can identify non-linear model deviations. The correction or improvement can be made possible by the individual steps. In an ideal model, the variance is 0.
At the same time, a mean deviation b can also be used to quantify the model inaccuracy, which indicates linear, global deviations of the model. For an ideal model, the mean deviation is 1.

6. Results

After many measurements had been carried out and evaluated, the FE model could be calibrated. It became apparent that this was important and necessary in order to increase accuracy. The scattering of the material parameters alone revealed inaccuracies. At the same time, there is a measurement uncertainty that was not considered in detail.
In order to transfer the measurement results to the calculations of future long-span timber floors, it must be ensured that the measured values match the calculation. This was done with the help of an FE model, see Figures 7 to 9. The model was built up step by step, analogous to the test bench. This allowed all individual conditions such as modulus of elasticity, mass etc. to be considered. The modeling was carried out with the «Mechanical APDL» program from «Ansys Inc.».

It has been shown that a simulation of the structural behavior can be carried out very precisely with the help of FE models, especially under special boundary conditions (see Table 2). In a first step, a calibration was carried out on the natural frequencies. In order to use this model for an evaluation of the vibrations of floors, further investigations are necessary. For this purpose, for example, the speeds and accelerations caused by walking and running people will also be considered in the numerical model.

Table 2: Comparison of the measured and calculated natural frequencies of the first modes

construction	Measured frequencies [Hz]			calculated frequencies [Hz]		
	Mode 1	Mode 2	Mode 3	Mode 1	Mode 2	Mode 3
beam	7,32	-	-	7,32	-	-
One element	6,85	14,4	19,4	6,79	14,4	19,4
Raw floor; Type 1b	6,20	7,43	8,62	6,24	7,43	8,65
Raw floor with mass;Type 2b	4,56	5,23	6,15	4,07	5,04	5,75
Floor with mass and screed; Type 3b	4,20	4,95	5,09	4,35	4,64	5,20

Such calibrated models make it possible to determine the vibration behavior of another (similar) wooden floor in the model without the need for a complex test rig and on-site conversion. For detailed information on the FE model and calibration, see [8].

Table 3: Overview of the mean deviations and variances of all scenarios

Type of measurement	**Mean value deviation b**	**Variance V**
beam	1,000	-
One element	1,000	0,0054
Raw floor	0,999	0,0050
Vertification one element	1,108	0,0315
Vertification beam	1,055	-
Raw floor with mass	1,066	0,0478
Vertification raw floor	0,996	0,0139
Vertification raw floor with mass	1,070	0,0386
Raw floor with mass and screed	0,884	0,0870
Raw floor with mass and screed-new	0,889	0,0880
Raw floor with mass and screed – Option 2	1,002	0,0558

It was shown that a simulation of the structural behavior using FE models, especially under special boundary conditions, can be much more accurate. Based on investigations of the individual material parameters, an extensive calibration of the model was carried out and significant influences and dependencies were identified and considered accordingly. Only time will tell whether the model is sufficient for future forecasts. Some of the aspects observed during the tests and measurements could also be recognized in the model. It was also shown which material parameters could be investigated in more detail in order to further optimize the model. As expected, some parameters have only a minor influence on the result, whereas other parameters have a greater influence than assumed.
Nevertheless, good results were achieved in the modeling, which is also shown by the mean deviation b and the variance V (see Table 3). Except for the raw slab with mass, there is a larger deviation, but this is also limited.

For the second natural frequency, the results of the measurements and calculations are even closer together. No values are available for the beam, as there is only one measured natural frequency. The situation is almost analogous to the second natural frequency for the third natural frequency although the deviations are even smaller in this case (see Table 2).

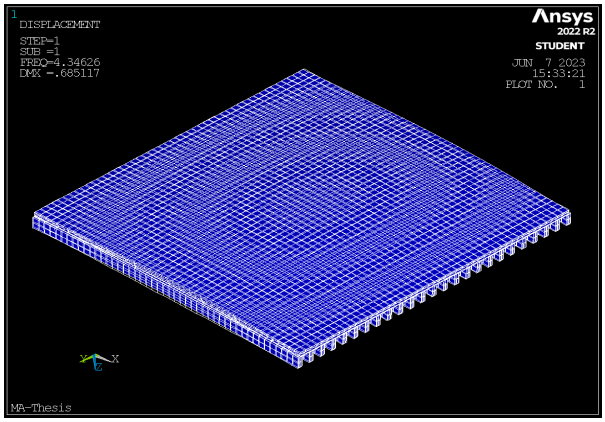


Figure 7: FE model showing the first mode

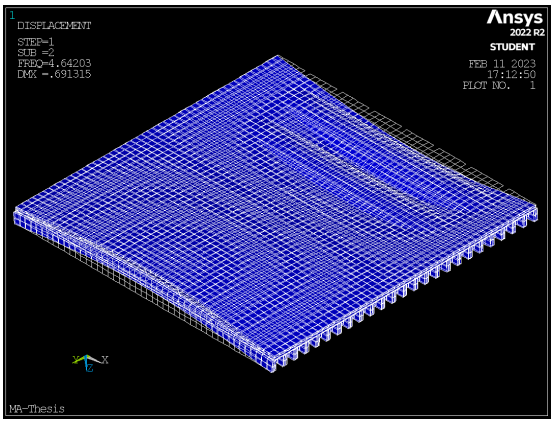


Figure 8: FE model showing the second mode

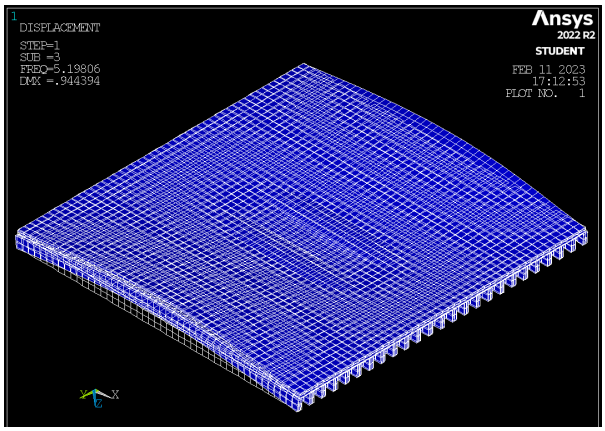


Figure 9: FE model showing the third mode

The research and results of this work have made it clear that creating and calibrating a model involves a great deal of effort, but it is worth it for this research floor. This effort will not be worthwhile for conventional floors. The aim of the work was to use the FE model to make the most accurate possible predictions of the vibration behavior of a long-span wooden beam by allowing the model to reflect several measured situations.
During calibration, it was also important to build up the model step by step in order to better consider the individual material parameters. However, even with this approach, many material parameters had to be constantly readjusted. However, in order to use this model to assess the vibrations of the floor, further investigations are necessary.

7. Outlook

The aim of the research project is to develop an extended design concept for long-span timber floors. As a result, it can be stated that wide-span wooden floors can be excited to vibrate despite their large mass. The subjective assessment and the newly introduced floor performance level were recorded. More precise values for Lehr's damping coefficient for wide-span floors and findings on modal mass were obtained. The possibility of installing tuned mass dampers is still being investigated.

It was shown that a simulation of the structural behavior using FE models, especially under special boundary conditions, can be much more accurate than with manual calculations. Nevertheless, FE models will only be able to represent a simplification of the actual observed vibration behavior of structures in the future. It will still be the task and responsibility of the engineer to identify and model the relevant properties that are relevant for a given problem. At the same time, he must know the assumptions and the possibilities of the models in order to be able to draw conclusive conclusions. Furthermore, appropriate laboratory and field tests are important in order to compare the results of the model with reality. This increases the accuracy enormously compared to manual calculations.

At the same time, other aspects must be considered in order to be able to use the model for detailed vibration assessment. For the frequencies considered here, these are the accelerations generated by walking. To do this, a pedestrian walking across the floor must be implemented in the model. The result is the reactions of the floor. In addition, the existing damping must be stored so that it can also be considered. In addition, the basis was created for checking other geometric conditions. These include the variation of the span width, which can be easily changed using the variable-based input. A four-sided support of the floor can also be further investigated in the model. Another influence that should not be neglected is the activation of the downstand beam, which was not carried out in this work. This increases the potential for improving the vibration behavior, but the flexible floor plan design is easier to implement.

With these additional aspects, another comprehensive calibration should be carried out in order to adapt the model to the new aspects. Subsequently, a damper should be integrated into the model, which has already been investigated metrologically. This has already contributed to a significant improvement in the subjective perception of the floor, which can also be determined by measuring the prevailing acceleration values. Despite all this, the floor has not yet achieved satisfactory results for use in office buildings or apartment blocks. This could be due to the fact that the damper was only tuned to the first natural frequency of the floor. In this model, however, it was also apparent that some natural frequencies occurred in the transverse direction, which are excited by the low frequencies due to walking and can therefore be disturbing. As a result of these findings, beams were added to the test bench for transverse stiffening, which significantly improved the subjective perception. Without the model, this would not have been recognized. Furthermore, it has made it clear that there is still a need for research into the influence of transverse stiffness on the vibration behavior of floor.

By implementing the damper in the model, it is expected that this interaction will be further optimized so that a configuration with satisfactory results can be achieved, which should then provide metrological evidence to achieve a satisfactory result of the vibration behavior for this floor system.

8. Acknowledgments

The research project has been carried out at Biberach University of Applied Sciences in cooperation with PIRMIN JUNG Deutschland GmbH, Remagen from 01.01.2021 to 30.06.2023. It was financed by ZIM. «ZIM» stands for «Zentrales Innovationsprogramm Mittelstand», which means «Central Innovation Programme for small and medium-sized enterprises (SMEs)». It is a funding programme of the Federal Ministry for Economic Affairs and Cllimate Action. Thanks to the entire team at Pirmin Jung and Biberach University of Applied Sciences for the great cooperation.

9. References

[1] Eurocode 5: EN 1995-1-1: Eurocode 5: Bemessung und Konstruktion von Holzbauten – Teil 1-1: Allgemeines – Allgemeine Regeln und Regeln für den Hochbau. Deutsche Fassung. Dezember 2010.

[2] Hamm, P., Richter, A., Winter, S.: Floor vibrations – new results. In: WCTE World Conference in Timber Engineering. 20. – 24. Juni 2010. Riva del Garda, Italy.

[3] Eurocode 5: pr EN 1995-1-1:20XX: Design of timber structures – Common rules and rules for buildings – Part 1-1: General. Noch nicht veröffentlicht.

[4] Hamm, P., Marcroft, J., Toratti, T.: Vibrations of floors – Comparison of measured data and suggested design. In: INTER - International Network on Timber Engineering Research. 17. – 19. August 2020, Kap. 53-20-1, 14 S. (http://holz.vaka.kit.edu/540.php), Planned to be held in Chile, because of Covid-19 held as an Online meeting. Editor: Karlsruher Institut für Technologie (KIT), Holzbau und Baukonstruktionen, Karlsruhe.

[5] Bender, M.: Bemessungsdiagramme für Holzbalkendecken bei unterschiedlichen Anforderungen an den Schwingungsnachweis. Masterthesis. Biberach University. 2016.

[6] Ruf, J.: Planung, Aufbau und Durchführung eines Prüfstandes für weitgespannte Holzdecken zur Untersuchung des Schwingungsverhaltens. Masterthesis. Biberach University of Applied Sciences. 2022.

[7] Kreuzinger, H., Mohr B.: Gebrauchstauglichkeit von Wohnungsdecken aus Holz; Abschlussbericht Januar 1999. TU München, Fachgebiet Holzbau. Forschungsvorhaben durchgeführt für die EGH in der DGfH.

[8] Knöpfle, V.: Planung, FE-Modellierung und Kalibrierung einer weitgespannten Holzbalkendecke mittels Schwingungsmessungen. Masterthesis. Biberach University of Applied Scienes. 2023.

[9] ISO 10137: Berechnungsgrundlagen für Bauten – Gebrauchstauglichkeit von Gebäuden und Stegen bei Vibrationen. 2007-11.

[10] M. Herten, R. Schwab, A. Richter: Parameter für Stoffgesetze bei FE-Berechnungen, FuE-Abschlussbericht A39520205613, Karlsruhe: Bundesanstalt für Wasserbau, 2015.

Investigations of the load-bearing behaviour of resin impregnated compressed wood dowels in a double shear timber connection

Max Jeschkowski
Technische Hochschule Mittelhessen
Gießen, Germany



Investigations of the load-bearing behaviour of resin impregnated compressed wood dowels in a double shear timber connection

Abstract

As part of this master's thesis, tests were carried out on 80 glulam and wood-based material joints in combination with a dowel made of reinforced densified veneer wood. The aim of this study was to investigate the load-bearing behaviour of the connection. The influence of different panel thicknesses was considered in order to obtain the different failure mechanisms according to EC5 for double-shear connections. In addition, the calculation approaches for connections with dowels made of compressed synthetic resin wood are to be checked. Deviant behaviour was observed as all tests resulted in a brittle failure of the dowel.

1. Introduction

In principle, timber construction is undoubtedly a climate-neutral construction method. In comparison to steel and concrete construction, material-uniform timber-timber connections are rarely common in timber construction nowadays; the connections are primarily characterized by the use of steel. It is currently not possible to build pure timber buildings in Europe without the use of steel elements or metal fasteners, for example. A pure timber construction would be easier and less risky to separate in the sense of a recycling- and cycle-orientated design. The existing structure would be less damaged and reuse would be possible. Therefore connections using modified timber-based materials can be an alternative to commonly used steel in steel-to-timber connections. Densified veneer wood reinforced with a resole phenolic resin (RDVW) can be used as one option.
The current Eurocode 5-2010 [1] does not provide for connections with dowels made of wood-based materials. It is therefore necessary to check whether such connections can also be calculated with the previous calculation models according to Johansen's yield theory. Due to the brittle material behaviour of RDVW, it is reasonable to assume that no plastic hinges can form in the fastener and thereby leading to other failure mechanisms.

2. Experimental Setup

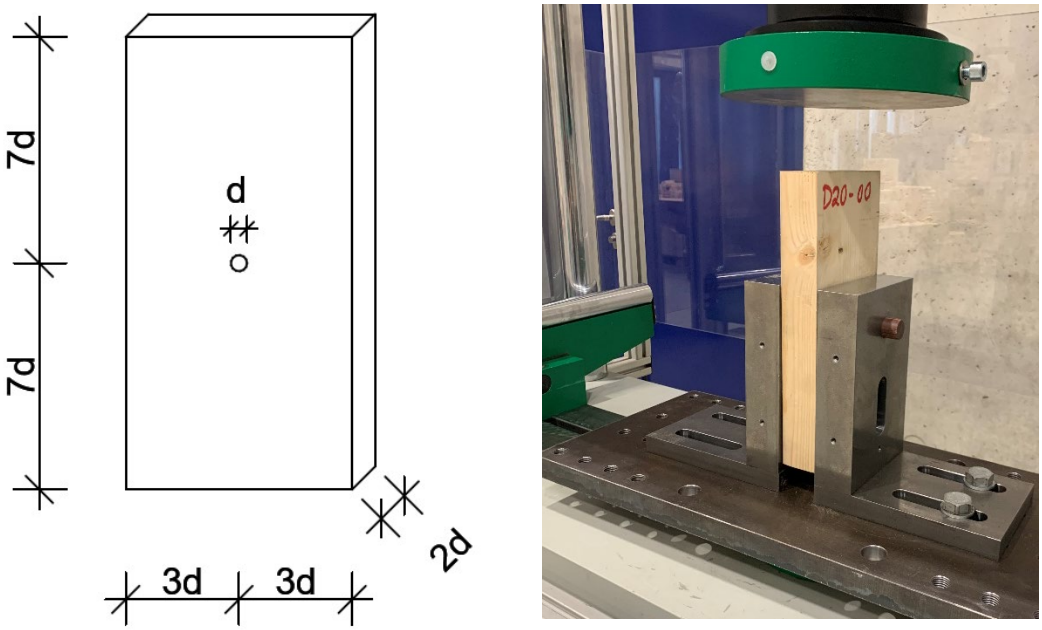
On the basis of previous tests on the material properties of RDVW, it was found that compared to other wood-based materials the density is significantly higher with 1.35 g/cm and the strength values are exceptionally high.

2.1. RDVW dowel properties

The material properties of dowels made of RDVW with a diameter of 12 mm were examined in previous tests. Both radial and tangential fibre directions were investigated. The characteristic bending strength radial was determined to 273 N/mm² and tangential to 261 N/mm². As the difference of the bending strengths of the dowels for radial and tangential direction was rather minor it was simplified to the mean value. The failure moment was calculated to
$M_{y,rk} = 45.312\ Nmm.$

2.2. Embedment tests

40 tests were carried out to investigate the embedment strength of glulam with a dowel made of RDVW according to DIN EN 383 [2]. Four different diameters were considered: 6mm, 12mm, 16mm and 20mm with ten tests each. The thickness of the tab was chosen with $2 \cdot d$. Figure 1 shows the dimensions of the specimen and how it was configurated in the testing machine.



(a) Dimensions of the specimen (b) Specimen with dowel

Figure 1: Embedment specimen

According to DIN EN 383 [2] the test is finished after a displacement of 5 mm. Most of the tests were stopped then but two with diameter 6 mm and one with diameter 16 mm failed earlier due to a breakage of the dowel. All three tests had the highest load in their series. In the following figure the series of the embedment tests with diameter 12 mm are pictured. The highest load was 13.0 kN and the lowest load was 8.9 kN.

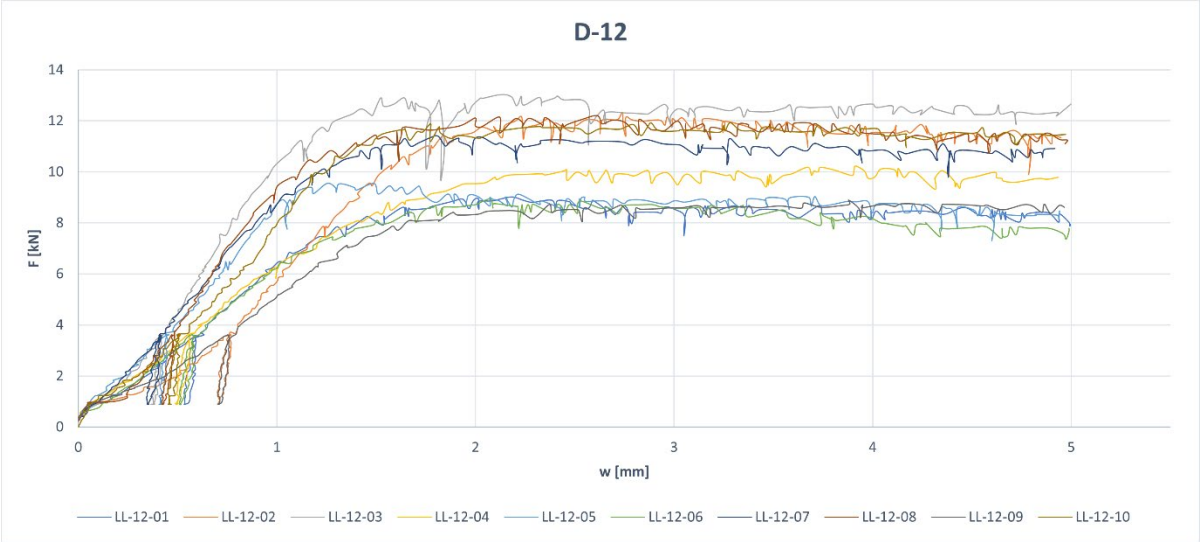


Figure 2: Force-displacement-diagram of the embedment tests with d = 12 mm

The equation for the embedment strength of the EC5 [1] for timber is described as: $f_{h,0,k} = 0{,}082 \cdot \rho_c \cdot (1 - 0{,}01 \cdot d)$.

In addition to the density of the timber and the diameter of the dowel, other parameters influence the embedment strength, such as the steel grade of the bolt. Therefore, it is assumed that a different equation is needed for a connection with a dowel made of timber. According to Blaß et al. [3], the embedment strength of timber with dowels made of timber can be calculated as:

$f_{h,0,k} = \rho_{dowel,c} \cdot \rho_{timber,c} \cdot 10^{-4} \cdot 1{,}1 \cdot (1 - 0{,}01 \cdot d)$.

RDVW dowels have a much higher strength and density than typically used timber dowels and exhibit different mode of failure than steel bolts. The test results were compared with various approaches.

The density of the glulam used was determined from 20 specimens, yielding a mean value of 414 g/cm³. The characteristic value was calculated according to DIN EN 1990 D.7 [4] as 348 g/dm³.

To compare the test results with the calculation approaches, characteristic values were established. The following table shows the results of all embedment tests.

Table 1: Results of the embedment tests

diameter	mean value f_h [N/mm²]	characteristic value $f_{h,k}$ [N/mm²]
6	43.17	34.06
12	37.24	27.50
16	38.23	23.59
20	34.17	38.13

The best approach was the one of the Eurocode 5. According to the equations, a new formula has been proposed:

$f_{h,0,k} = 0{,}101 \cdot \rho_k \cdot (1 - 0{,}0145 \cdot d)$

The range of individual test results in the series with diameter of 16 mm is rather large, which leads to a significant reduction when calculating the characteristic values. This may indicate a stronger influence of the diameter. This new calculation approach needs to be verified through further tests.

For the calculations in chapter 2, the characteristic value for dowels with diameter of 12 mm of 27.50 N/mm² was used.

2.3. Double-shear connection

The current calculation approaches for double-shear timber-to-timber connections are defined by the Eurocode 5 through four different modes of failure [1]. The modes describe a failure of the timber tab or a plastic deformation of the bolt. The parameters that are included in the calculation of the load capacity of the connection are:

$f_{h,i,k}$ characteristic embedment strength of the timber *i*
t_i embedment depths of the timber tab *i*
d diameter of the fastener
$M_{y,Rk}$ yield moment of the fastener

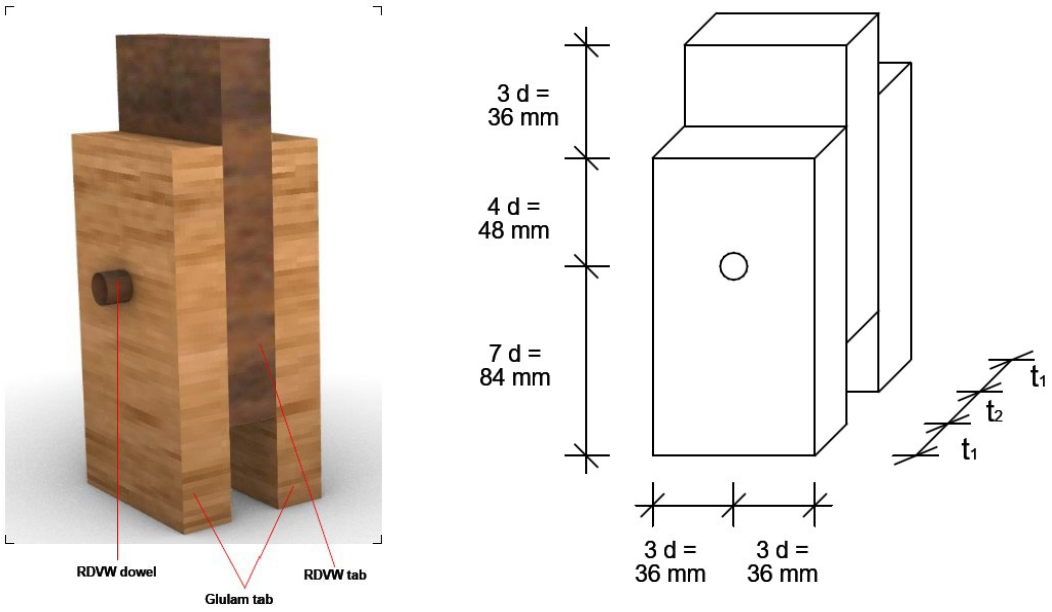
For this investigation a double-shear timber-to-timber connection with external glulam tabs and an internal RDVW tab with a RDVW dowel was used.

40 tests were carried out, 4 different setups with 10 tests each. The following table shows the setups. All tests used RDVW dowels with a diameter of 12 mm.

Table 2: Double shear tab thicknesses

	t_1 [mm]	t_2 [mm]
Series 1	40	20
Series 2	20	10
Series 3	20	20
Series 4	15	10

The edge distances were chosen as the minimum distances according to EC5 [1]. The tests were carried out by push-out-tests according to DIN EN 26891 [5]. The tab thicknesses were chosen to achieve different modes of failure according to the equations of EC5.



(a) Double-shear specimen (b) Specimen dimensions

Figure 3: Double-shear specimen

3. Results

All tests failed due to a brittle breakage of the RDVW dowel because of the yield moment in the middle of the dowel. The following figures shows the results of the series 2 and 3.

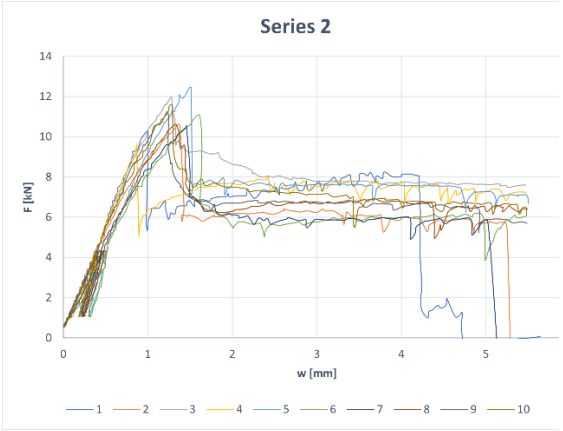


Figure 4: Force-displacement-diagram of series 2

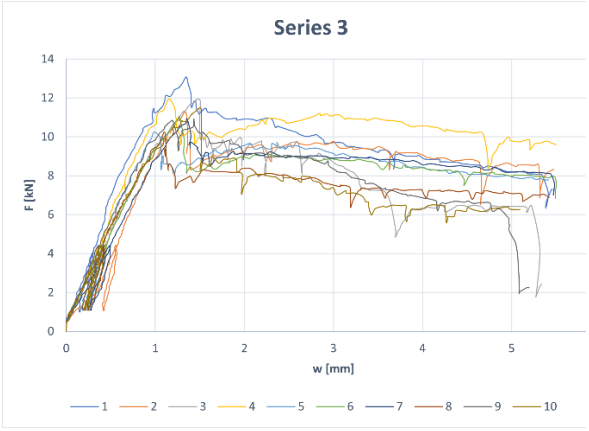


Figure 5: Force-displacement-diagram of series 3

Due to their greater thickness, series 1 and 3 did not exhibit brittle failure to the same extent as series 2 and 4. Although failure in these series was also initiated by the first breakage of the dowel at the midpoint, two additional fractures formed at the inner edges of the external tabs.

To compare the results with the equations, characteristic values were determined according to DIN EN 1990 [4]. In addition to the equations of EC5, two alternative approaches were considered. Ehlbeck et al. [6] proposed a new equation for RDVW dowels in a double shear timber-to-timber connection, while Blaß et al. [3] provided an equation for double-shear timber-to-timber connections with dowels made of timber.

The following table shows the results of the tests and the values according to various approaches. The marked numbers indicate a failure due to the embedment strength.

Table 3: Testing loads and expected loads after various approaches

[kN]	$F_{max,mean}$	$F_{k,tests}$	$F_{k,est,EC5}$	$F_{k,est,Ehlbeck}$	$F_{k,est,Blaß}$
Series 1	*5.59*	4.85	7.70	8.24	6.66
Series 2	*5.50*	4.73	**7.10**	**7.10**	6.66
Series 3	*5.66*	4.89	**7.06**	**7.06**	6.63
Series 4	*5.83*	4.91	**5.38**	**5.38**	**5.38**

It is evident that the load capacity in all series is lower than the embedment strength. The calculation approaches appear to overestimate the load capacity of this specific configuration. The most accurate results are provided by the equation developed by Blaß et al. [3]. This equation does not account for the thicknesses of the timber tabs, but specific thicknesses requirements must be maintained.
To confirm the behaviour of those types of connections more tests with an investigation of more parameters are needed.

4. Conclusions and recommendations

The material properties of RDVW were determined and the embedment strength of glulam with a dowel made of RDVW was observed. The load-bearing behaviour of a double-shear connection using glulam with an interlayer of RDVW and a RDVW dowel was investigated by push-out-tests. The results were compared with the equations of EC5 [1].
The investigations have shown that the usage of RDVW in civil engineering has high potential due to the high load capacity with comparatively low weight.
A new computational model for timber-to-timber connections and fasteners made from RDVW is needed. Due to the brittle behaviour of RDVW dowels, they should not govern the design calculations.
Furthermore, such steel-free connections offer advantages in terms of improved deconstructability and the ability to separate building materials by type.

5. References

[1] DIN EN 1995-1-1:2010, Eurocode 5: Bemessung und Konstruktion von Holzbauten, Teil 1-1: Allgemeine Regeln und Regeln für den Hochbau, Deutsche Fassung EN 1995-1-1:2004 + EN 1995-1-1/AC:2006 + EN 1995-1-1/A1:2008.

[2] DIN EN 383:2007: Betimmung der Lochleibungsfestigkeit und Bettungswerte für stiftförmige Verbindungsmittel, 2007.

[3] H. Blaß und H. W. H. Ernst, Verbindungen mit Holzstiften – Untersuchungen über die Tragfähigkeit, 1999.

[4] DIN EN 1990:2021-10: Grundlagen der Tragwerksplanung; Deutsche Fassung EN 1990:2002+A1:2005+A1:2005/AC:2010.

[5] DIN EN 26891: Verbindungsmittel mit mechanischen Verbindungsmittel, 1991.

[6] J. Ehlbeck und H. Werner, Tragfähigkeit von Laubholzverbindungen mit stabförmigen Verbindungsmitteln. Versuchsanstalt für Stahl, Holz und Steine, Stuttgart: Frauenhofer IRB Verlag, 1992.

Künstliche Intelligenz im Holzbau

Entwicklung und Training eines Künstlichen Neuronalen Netzes zur Vorhersage der Biegefestigkeit von Pappelholz

Pascal Fröhlich
Konstruktionsgruppe Bauen/
Hochschule Biberach
Kempten, Deutschland



Künstliche Intelligenz im Holzbau

1. Einleitung

Die Bestimmung der Biegefestigkeit von Holz spielt in der Bauholzindustrie eine zentrale Rolle, insbesondere bei der Sortierung und Klassifikation des Holzes für spezifische Anwendungsbereiche. Konventionelle Sortiermethoden wie die visuelle Prüfung sind oft begrenzt, da sie auf äußerliche Merkmale abzielen und das innere Potenzial der Holzfestigkeit nicht voll erfassen. Um diese Lücke zu schließen, wurde in dieser Arbeit ein Ansatz mit Künstlichen Neuronalen Netzen (KNN) entwickelt und evaluiert. Der Fokus liegt dabei auf der Erstellung und Optimierung des neuronalen Netzes, um möglichst präzise Vorhersagen über die Biegefestigkeit zu treffen und die Effizienz der Holznutzung zu verbessern.

2. Künstliche Neuronale Netze (KNN)

KNN sind fortgeschrittene rechnerbasierte Modelle bzw. Algorithmen, die der Struktur und Funktionsweise biologischer neuronaler Netzwerke, wie sie im menschlichen Gehirn vorkommen, nachempfunden sind. Sie setzen sich aus zahlreichen miteinander vernetzten Neuronen zusammen, die in der Lage sind, Daten zu empfangen, zu verarbeiten und daraus Vorhersagen zu generieren. Diese Neuronen sind durch gewichtete Verbindungen miteinander gekoppelt, wobei sich die Gewichte im Verlauf des Trainings, basierend auf den Abweichungen der getroffenen Vorhersagen zu den tatsächlichen Werten, anpassen. Dieser dynamische Anpassungsprozess ermöglicht es dem KNN, Muster und Zusammenhänge in Daten zu erkennen, die für den Menschen nicht ersichtlich sind und so komplexe Aufgaben wie die Vorhersage von Biegefestigkeiten zu bewältigen.

Der Erfolg solcher KNN-basierten Systeme ist eng mit der Qualität und dem Umfang der verfügbaren Trainingsdaten verbunden. Aus diesem Grund wurde im Rahmen dieser Arbeit ein umfangreicher Datensatz generiert, indem rund 200 Vierpunktbiegeversuche an 60 cm langen Leisten, mit Querschnittsmaßen von 24 bis 30 mm, durchgeführt wurden.

3. Datenerhebung und Vorbereitung der Probekörper

Die in der Arbeit verwendeten Pappeln stammen aus einer landwirtschaftlichen Anbaufläche aus der Nähe von Ellwangen bei Rot an der Rot, im Landkreis Biberach. Auf dieser Fläche werden drei verschiedene Pappelsorten in Form einer Kurzumtriebsplantage (KUP) angebaut.

3.1. Herkunft und Ernte

Kurzumtriebsplantagen oder auch als Schnellwuchsplantagen bezeichnet, sind Anpflanzungen schnellwachsender Baumarten oder Sträuchern, die nach kurzer Umtriebszeit geerntet werden. Die Gehölze werden auf vormals landwirtschaftlich genutzten Flächen angebaut. Die Bestandsgründung erfolgt mittels maschineller Setzung von 20 cm langen Stecklingen herkömmlicher Pappelarten sowie durch Kreuzungen verschiedener Arten oder Zuchtlinien erzeugten Baumhybriden. Die Umtriebszeit solcher Plantagen, also die Zeitspanne von der Pflanzung bis zur Ernte, beträgt in der Regel 2 bis 20 Jahre, abhängig vom angestrebten Nutzungszweck des Holzes. Es wird zwischen zwei Hauptproduktlinien unterschieden: Industrieholz und Energieholz, wobei der Schwerpunkt auf der Energieholznutzung liegt. Nach jeder Ernte besteht die Möglichkeit, die Flächen durch Mulchen wieder der landwirtschaftlichen Nutzung zuzuführen oder die Bäume durch Stockausschlag erneut austreiben zu lassen. Die Vorteile von Kurzumtriebsplantagen liegen in ihren geringen Kosten, der effektiven Reduzierung von Treibhausgasen, dem schnellen Wachstum und dem hohen Trockenmassenertrag.

Die Anbaufläche umfasst etwa zwei Hektar und ist mit den Sorten Pappel Max Klon 1 und 3 sowie den Pappelhybriden 275, Matrix 24 und 49 bepflanzt. Die Pappelbestände wurden 2014 durch maschinelles Setzen von Stecklingen angelegt. Die Fläche wurde vor etwa 2 – 3 Jahren erstmals vollständig durch Kahlschlag geerntet, woraufhin die Baumstümpfe

durch Stockausschlag erneut austrieben. So entwickelten sich mehrstämmige Bäume mit kräftigen Haupttrieben und kleineren, schräg aus dem Stamm wachsenden Nebentrieben. Auf der Plantage wurden drei optisch unterschiedliche Pappelsorten geerntet. Die gepflanzten Sorten sind zwar bekannt, jedoch wurden ihre Standorte nicht dokumentiert. Normalerweise erfolgt eine Sortenzuordnung anhand der Blätter, doch da die Ernte im Winter stattfand, war dies nicht möglich. Daher wurden die Sorten als A, B und C klassifiziert. Insgesamt wurden etwa 65 Stämme der Sorte A, 16 der Sorte B und 9 der Sorte C geerntet.

3.2. Herstellung der Probekörper

Die Herstellung der Leisten erfolgte nach dem in den Abbildungen 1–6 dargestellten Bearbeitungsschema. Zunächst wurden die 1,30 Meter langen Stammstücke mit einer Zugsäge in 65 cm lange Abschnitte geteilt, um die natürliche Krümmung der Stämme zu reduzieren. Anschließend wurden zwei senkrecht zueinanderstehende Seiten der Abschnitte mit einem Abrichthobel bearbeitet, um ebene Flächen für die weitere Verarbeitung an der Tischkreissäge zu schaffen. Im nächsten Schritt wurden die übrigen Baumkanten an der Tischkreissäge entfernt, um quadratische Leisten zu erzeugen. Diese Leisten wurden schließlich mit einem Dickenhobel auf die finalen Maße von 24 x 24 mm bzw. 30 x 30 mm gebracht.



Abbildung 1: Unbearbeitete 1,30 m Pappelstammstücke vor der Verarbeitung zu Prüfkörpern



Abbildung 2: Resultierende 65 cm lange Stammstücke nach der Halbierung



Abbildung 3: Abgerichtete Stämme mit zwei planen Seiten



Abbildung 4: Quadratische Pappelleisten nach dem Besäumen der dritten und vierten Seite



Abbildung 5: Fertige quadratische Pappelleisten mit den Maßen 24x24 mm bzw. 30x30 mm



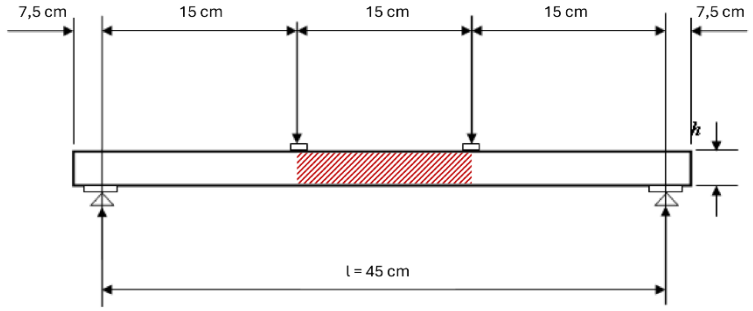
Abbildung 6: Besäumen der dritten Stammseite an der Tischkreissäge

3.3. Sortierung, Prüfung und Auswertung der Probekörper

Das Ziel des im Rahmen der Masterarbeit entwickelten KNN bestand darin, anhand visuell identifizierbarer Merkmale von Pappelholz eine zerstörungsfreie Vorhersage der Biegefestigkeit zu ermöglichen. Für ein effektives Training dieses Netzwerks ist es notwendig, eine angemessene Anzahl an Trainingsbeispielen zu generieren, indem spezifische Holzmerkmale erfasst und anschließend die Biegefestigkeit mittels Vierpunktbiegeversuchen bestimmt wird. Zusätzlich sind Testdaten erforderlich, um die Vorhersagegenauigkeit des Netzwerks zu evaluieren. Die optimale Datenmenge für Training und Test kann jedoch nicht im Vorfeld festgelegt werden. Die Trainingsdatenmenge muss je nach spezifischen Gegebenheiten wie Anwendungsfall, Netzwerkarchitektur und Problemstellung angepasst werden. Ein universell gültiger Richtwert existiert nicht.

Daher wurde ein pragmatischer Ansatz gewählt: Sämtliche hergestellten Probekörper wurden gemäß den festgelegten Kriterien sortiert und mittels Vierpunktbiegeversuchen auf ihre Biegefestigkeit geprüft, um eine umfangreiche Datenbasis zu schaffen. Die Vierpunktbiegeversuche wurden grundsätzlich gemäß DIN EN 408:2012-10 (2012) durchgeführt, jedoch mit einer angepassten Prüfungsordnung. Die Abweichung besteht darin, dass der Abstand zwischen den Auflagepunkten einheitlich auf 150 mm festgelegt wurde, unabhängig von den Querschnittsmaßen der Proben. Diese spezifische Anpassung basiert auf den Richtlinien des Karlsruher Rechenmodells nach Ehlbeck u. a. (1985), einem etablierten Verfahren zur Berechnung der Tragfähigkeit von Brettschichtholzträgern. Das Modell schlägt eine Segmentierung der Holzelemente in Abschnitte von 150 mm vor, die als unabhängige Zellen betrachtet werden, um die strukturellen Eigenschaften präziser zu erfassen. Die Entscheidung, die Segmentierung gemäß dem Karlsruher Modell in die Versuchsanordnung zu integrieren, ist auf die vorgesehene Nutzung der untersuchten Holzleisten für die Herstellung von Brettschichtholzträgern zurückzuführen.

Der Versuchsaufbau, siehe Abbildung 7, positioniert den kritischen 150-mm-Abschnitt, in dem der Bruch erwartet wird, genau zwischen den beiden Prüfstempeln. Zur Vereinfachung der Datenerfassung, Effizienzsteigerung des Versuchsablaufs und Verbesserung der Datenqualität wurde entschieden, sich bei der Klassifizierung, Sortierung und Beurteilung der Proben ausschließlich auf diesen mittleren 150-mm-Abschnitt zu konzentrieren und nur hier die relevanten Merkmale zu erfassen.



(a) Modifizierter Versuchsaufbau für Vierpunktbiegeversuche, angepasst an die spezifischen Anforderungen des Karlsruher Rechenmodells. In rot hervorgehoben der zur Sortierung untersuchte Bereich.

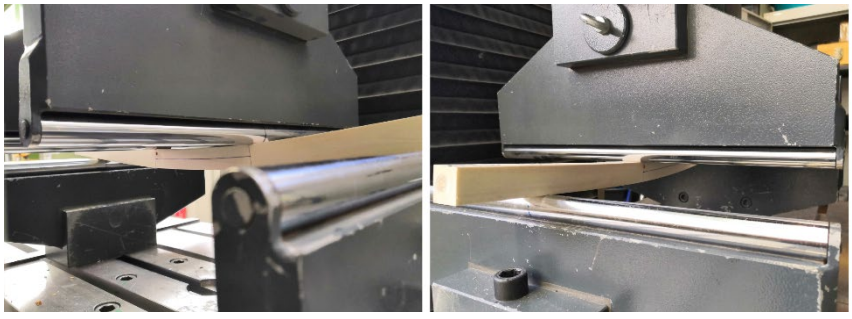


Abbildung 7: Prüfanordnung für die Bestimmung der Biegefestigkeit der Latten/Stäbe

3.4. Visuelle Sortierung der Versuchskörper

Die Prüfkörper mit maximalen Querschnittsmaßen von 24×24 mm bzw. 30×30 mm fallen gemäß DIN 4074-1:2012-06 (2012) in die Schnittholzklasse der Latten. Daher orientieren sich die für die Vorhersage des Netzes herangezogenen Parametern bzw. optischen Merkmalen an den visuellen Sortierkriterien für Latten. Berücksichtigt wurden die Merkmale Astigkeit, Faserneigung, Jahrringbreite, Baumkante und Krümmung. Die Merkmale Insektenfraß, Verfärbung, Fäule, Druckholz, Blitzrisse und Ringschäle wurden nicht in die Sortierung einbezogen, da sie in den Prüfkörpern nicht auftraten. Auch das Sortiermerkmal Markröhre wurde nicht angewandt, da es bei Pappelholz aus Kurzumtriebsplantagen aufgrund des geringen Stammdurchmessers unvermeidbar ist, Latten ohne Markröhre herzustellen. Das Sortiermerkmal Faserneigung, welches üblicherweise durch den Verlauf der Schwindrisse im trockenen Holz bestimmt wird, konnte aufgrund des Fehlens solcher Risse bei den Prüfkörpern nicht erfasst werden, obwohl es einen signifikanten Einfluss auf die Biegefestigkeit hat. Stattdessen wurde der Verlauf der Markröhre als Ersatzkriterium herangezogen, in der Annahme, dass die Angabe der Krümmung und des Markröhrenverlaufs indirekt die Faserneigung abbildet. Zusätzlich wurden die Astflächen in der oberen und unteren Querschnittshälfte, der Anteil der Markröhre am Gesamtquerschnitt, die Rohdichte, die Holzfeuchte, die Pappelsorte sowie die Herstellungsart berücksichtigt.

3.5. Durchführung der Versuche

Für die Versuche wurden ausschließlich Leisten verwendet, die nach dem Trocknungsprozess keine zweiaxiale Verformung aufwiesen. Die Vorschubgeschwindigkeit des Prüfstempels betrug bei allen Versuchen einheitlich 6 mm/min. Die Querschnittsabmessungen variierten zwischen 22,51×22,38 mm und 29,85×29,88 mm, bei einer einheitlichen Länge von 600 mm.

Gemäß DIN EN 1912:2013-10 (2013) können den visuellen Sortierklassen bestimmte Festigkeitsklassen zugeordnet werden. Für das in der Arbeit verwendete Pappelholz entspricht die Sortierklasse S10 bzw. LS10 der Festigkeitsklasse C22, während die Sortierklasse S13 bzw. LS13 der Festigkeitsklasse C27 zugeordnet ist. Nach DIN EN 338:2016-07 (2016) ergeben sich daraus erwartete charakteristische Biegefestigkeiten von 22 N/mm² für Leisten der Sortierklasse S10 und 27 N/mm² für Leisten der Sortierklasse S13.

Tabelle 1: Übersicht der gemittelten Werte der Sortiermerkmale und Biegefestigkeit

Sorte	Rohdichte $[kg/m^3]$	Äste nach DIN 4074-1	Astfläche oben $[mm^2]$	Astfläche unten $[mm^2]$	Jahrringbreite $[mm]$	Baumkante nach DIN 4074-1
Sorte A	346,49	0,17	20,07	19,73	4,59	0,04
Sorte B	432,28	0,21	32,90	19,01	3,43	0,00
Sorte C	418,20	0,15	16,84	14,37	3,46	0,09
Gesamt	363,81	0,17	21,12	19,06	4,34	0,04

Sorte	Anteil Markröhre $[\%]$	Holzfeuchte $[\%]$	Krümmung nach DIN 4074-1 $[mm]$	Markröhrenneigung $[\%]$	Biegefestigkeit $[N/mm^2]$
Sorte A	2,87	11,24	2,25	0,39	44,74
Sorte B	1,02	11,91	3,15	0,29	55,63
Sorte C	1,91	11,98	2,79	0,57	55,90
Gesamt	2,56	11,40	2,41	0,40	47,18

Während der Versuchsreihe traten Bruchstellen auf, die auf Fehlstellen außerhalb des untersuchten 15-cm-Bereichs zurückzuführen waren. Da diese Fehlstellen bei der Sortierung nicht erfasst wurden, wurden die vier betroffenen Probekörper bzw. Datensätze aus der

Datenbasis für das Training und Testen des neuronalen Netzes ausgeschlossen. Abbildung 8 zeigt die Bruchbilder der verschiedenen Sorten: Sorte A zeigte ein sprödes Bruchverhalten, Sorte B ein überwiegend duktiles Verhalten und Sorte C eine Mischform mit tendenziell sprödem Verhalten.



(a) Bruchbild der Sorte A



(b) Bruchbild der Sorte B



(c) Bruchbild der Sorte C

Abbildung 8: Bruchbilder der unterschiedlichen Sorten

Gemäß den in Tabelle 1 aufgeführten Versuchsdaten beträgt die durchschnittliche Biegefestigkeit aller Proben 47,18 N/mm². Detaillierter betrachtet ergaben sich für die verschiedenen Sorten spezifische Mittelwerte von 44,74 N/mm² für Sorte A, 55,63 N/mm² für Sorte B und 55,90 N/mm² für Sorte C. Die charakteristischen Biegefestigkeiten betrugen für alle Sorten auf 36,01 N/mm² ermittelt, für Sorte A auf 36,11 N/mm², für Sorte B auf 48,48 N/mm² und für Sorte C auf 48,44 N/mm².

4. Entwicklung und Training eines KNN zur Festigkeitsvorhersage

Auf Grundlage des erstellten Datensatzes aus Sortiermerkmalen und Biegefestigkeit wurden vier unterschiedliche neuronale Netzwerke entwickelt: eines für jede der drei untersuchten Pappelsorten und ein übergreifendes Netzwerk, das alle Sorten gemeinsam betrachtet. Die Programmierung und Anwendung dieser Netzwerke erfolgte in der Programmiersprache Python in PyCharm, wobei die zuvor in Excel vorbereiteten Daten in die Entwicklungsumgebung importiert wurden, um als Trainingsgrundlage für die KNN zu dienen. Nach der Programmierung und dem Training der Modelle wurde ihre Leistungsfähigkeit mithilfe eines separaten Testdatensatzes evaluiert, der nicht im Trainingsprozess verwendet wurde. Diese Methode erlaubte eine objektive Beurteilung der Vorhersagegenauigkeit der Netzwerke anhand von Daten, die den Modellen zuvor unbekannt waren.

4.1. Optimierung Künstlicher Neuronaler Netzwerke (KNN)

Die Leistungsfähigkeit und Vorhersagegenauigkeit eines KNN werden maßgeblich durch spezifische Konfigurationseinstellungen, bekannt als Hyperparameter, bestimmt. Diese Hyperparameter, wie die Anzahl an versteckten Neuronen, definieren die grundlegende Struktur und das Trainingsverhalten des Netzwerks und sind von den während des Trai-

ningsprozesses angepassten Modellparametern, wie Gewichten und Biasen, zu unterscheiden. Im Gegensatz zu diesen dynamischen Parametern verändern sich die Hyper-parameter über die gesamte Trainingsdauer hinweg nicht und müssen daher vor Beginn des Trainings vom Anwender festgelegt werden. Die Wahl dieser Parameter ist entscheidend für eine effiziente und effektive Durchführung des Trainings und beeinflusst somit maßgeblich die Vorhersagegenauigkeit und die Leistungsfähigkeit des Netzwerks.

Zu den wesentlichen Hyperparametern, die für ein MLP für Regressionsaufgaben festgelegt werden müssen, gehören:

- **Eingabeneuronen:** Die Auswahl der Eingangsmerkmale bestimmt, welche Informationen das Modell nutzt. Zu viele irrelevante Merkmale verlängern das Training, während zu wenige möglicherweise nicht genug Informationen liefern.
- **Anzahl versteckter Schichten und Neuronen:** Ein Netzwerk mit mehr Schichten und Neuronen kann komplexere Muster in den Daten erkennen, ist jedoch anfälliger für Überanpassung (Overfitting).
- **Standardisierung der Eingabedaten:** Vor dem Training ist zu entscheiden, ob und wie die Eingaben standardisiert werden. Standardisierungsarten, wie die z-Transformation beeinflussen, wie das Netzwerk die Daten interpretiert. Sie können die Trainingsgeschwindigkeit und die Stabilität des Modells erheblich verbessern.
- **Lernrate:** Die Lernrate bestimmt, wie oft das Netzwerk seine Gewichte anpasst. Eine zu hohe Rate kann Instabilität verursachen, während eine zu niedrige das Training verlangsamt. Moderne Lernalgorithmen passen die Lernrate adaptiv an.
- **Batch-Größe:** Die Batch-Größe bestimmt, wie viele Trainingsbeispiele in einer Trainingsiteration verarbeitet werden. Kleinere Batches fördern die Generalisierungsfähigkeit, während größere den Prozess stabilisieren, aber in lokalen Minima der Fehlerfunktion verharren können.
- **Anzahl der Epochen:** Zu wenige Trainingsdurchläufe (Epochen) führen zu Underfitting, bei der das Modell nicht die gesamte Komplexität der Daten erlernt. Zu viele Epochen verstärken die Gefahr des Overfittings, bei dem das Modell auf die Trainingsdaten spezialisiert ist, aber keine Generalisierungsfähigkeit besitzt.
- **Aktivierungsfunktionen:** Die Aktivierungsfunktion beeinflusst, wie das Netzwerk nichtlineare Zusammenhänge erkennt und verarbeitet. Häufig werden sigmoidale oder unipolare Funktionen eingesetzt.
- **Gewichtsinitialisierung:** Die Anfangswerte der Gewichte der Neuronen sind für die Konvergenz des Modells entscheidend. Methoden wie die Glorot- oder He-Initialisierung schaffen stabile Startpunkte, die speziell auf die Aktivierungsfunktionen abgestimmt sind und den Trainingsprozess verbessern.
- **Datenaufteilung:** Die Art und Weise, wie die Daten in Trainings-, Validierungs- und Testsets aufgeteilt werden, ist bedeutend für ein erfolgreiches Training. So kann z.B. eine umfangreichere Validierungsdatenmenge die Generalisierungsfähigkeit und damit die Performance des Netzes auf unbekannte Daten verbessern, während eine zu knapp bemessene Trainingsdatenmenge die Leistungsfähigkeit einschränkt, da nicht ausreichend Informationen für den Lernprozess zur Verfügung stehen.

Neben der richtigen Wahl und Festlegung der Hyperparameter ist auch die Datenmenge und -qualität, obwohl technisch nicht als Hyperparameter klassifiziert, von entscheidender Bedeutung. Da diese Elemente die Grundlage bilden, auf denen das neuronale Netz lernt, haben sie einen direkten Einfluss auf das Endresultat des Trainings und beeinflussen somit die Fähigkeit des Netzes, präzise und zuverlässige Vorhersagen zu treffen.
Bei der Erstellung eines KNN besteht die Herausforderung somit nicht allein in der Auswahl der technischen Parameter, sondern auch in der Beschaffung und Aufbereitung qualitativ hochwertiger Daten, der Identifikation relevanter Eingangsvariablen, der Definition der Netzwerkstruktur und der Festlegung geeigneter Größen der Hyperparameter. Für die Wahl dieser Größen und Freiheitsgrade der Netzgestaltung existieren in der Fachliteratur lediglich Gestaltungsvorschläge oder Empfehlungen, aber keine wissenschaftlich fundier-

ten Regeln, die eine optimale Modellkonfiguration garantieren, insbesondere bei komplexen Problemstellungen. Vielmehr wird auf die «Erfahrung» des Modelldesigners für eine effiziente Anwendung verwiesen oder das systematische Ausprobieren unterschiedlicher Möglichkeiten empfohlen.

Die Konsequenz ist, dass die effektive Anwendung von KNN und anderen KI-Modellen in der Praxis nicht, so wie vielerorts propagiert, als «Black-Box»-Ansatz betrachtet werden kann, sondern ein tiefgreifendes Verständnis sowie eine Anpassung an den spezifischen Kontext notwendig ist. In vielen Anwendungen neuronaler Netze fehlen klare Handlungsanweisungen und definierte Vorgehensweisen, sodass Anwender bislang gezwungen sind, sich heuristischer Vorgehensweisen zu bedienen [Walde (2005), Ernst u. a. (2020) und Sonnet (2022)].

4.2. Beschreibung und Festlegung der Netzwerkarchitektur

Auf Grundlage der besonderen Eignung für Regressionsprobleme wurde als Netzwerkarchitektur das mehrschichtige Perzeptron (MLP) gewählt. Die Netzwerktopologie und die Hyperparameter orientieren sich an den in Walde (2005) genannten Empfehlungen zur Eingabeschicht, zur verborgenen Schicht und zur Ausgabeschicht.

Die quantifizierten Holzmerkmale dienen als Eingabeneuronen und bilden eine Eingabeschicht mit 14 Neuronen für das Gesamtnetzwerk, während sortenspezifische Netzwerke jeweils 12 Neuronen nutzen. Eine Transformation symbolischer Attribute entfällt, da die Merkmale bereits in numerische Formate konvertiert wurden. Um die Diversität der Maßeinheiten und Wertebereiche der Merkmale zu berücksichtigen, wurde beschlossen, die Daten mithilfe einer Normalisierungsschicht zu skalieren. Diese Schicht ermittelt während des Trainings den Mittelwert und die Standardabweichung der Eingabedaten und transformiert diese in ein Format mit einem Mittelwert von null und einer Standardabweichung von eins. Die Eingabemerkmale werden homogenisiert, was Verzerrungen durch unterschiedliche Wertebereiche reduziert und die Konvergenz des Trainings verbessert.

Das Netzwerk wurde mit nur einer verborgenen Schicht konzipiert. Da angenommen wurde, dass eine einzige versteckte Schicht ausreicht, um die Muster in den Daten zu erfassen, da ein MLP mit einer versteckten Schicht nachweislich jede nichtlineare Funktion approximieren kann und das Risiko für Overfitting durch geringe Komplexität reduziert wird. Die Neuronenzahl in der verborgenen Schicht wurde mit 14 im Gesamtnetzwerk und 12 in den spezialisierten Netzwerken festgelegt. Als Aktivierungsfunktion für die Neuronen der verborgenen Schicht wurde der Tangens Hyperbolicus (Tanh) gewählt, da dieser sich laut Walde (2005) besonders für Regressionsaufgaben eignet.

In der Ausgabeschicht wurde ein Neuron verwendet, um die Biegefestigkeit der Leisten als kontinuierlichen Wert zu prognostizieren. Eine lineare Aktivierungsfunktion ermöglichte den direkten Vergleich der Netzwerkausgabe mit den Zielwerten. Für das Training des neuronalen Netzwerks wurde die Verlustfunktion Root Mean Squared Error (RMSE) verwendet, die Abweichungen zwischen Soll- und Ist-Werten quadriert, um eine gegenseitige Aufhebung positiver und negativer Abweichungen zu vermeiden. Größere Fehler werden stärker gewichtet, was die Konvergenz des Trainingsprozesses unterstützt.

Die Initialisierung der Anfangsgewichte der verborgenen Neuronen wurde in Übereinstimmung mit der Aktivierungsfunktion durch die Glorot-Uniform-Methode, auch bekannt als Xavier-Initialisierung, vorgenommen. Dabei werden die Anfangsgewichte willkürlich aus einer gleichförmigen Zufallsverteilung, deren Grenzen auf der Anzahl der Eingangs- und Ausgangsverbindungen der jeweiligen Neuronen basieren, festgelegt.
Für das Training der vier zu entwickelnden Netze wurde der in der Arbeit erstellte Datensatz verwendet, der die erfassten Holzmerkmale und die Biegefestigkeiten der 190 geprüften Leisten umfasst. Das Gesamtnetz, das alle Daten der verschiedenen Sorten berücksichtigt, wurde mit dem vollständigen Versuchsdatensatz trainiert. Für die sortenspezifischen Netze wurde der Gesamtdatensatz in drei separate Datensätze aufgeteilt: 148 Einträge für Sorte A sowie jeweils 21 für die Sorten B und C. Der Datensatz wird in 80 % für das Training, 10 % für die Validierung und 10 % für die Testphase aufgeteilt.

4.3. Optimierung von Hyperparameter mittels Trial and Error

Für das beschriebene neuronale Netz sollen geeignete Werte für die Hyperparameter Lernrate und Batch-Größe mittels des Trial-and-Error-Verfahrens bestimmt werden. Dabei werden verschiedene Kombinationen dieser Parameter systematisch getestet, um die optimalen Werte für das Netzwerk zu finden. Zunächst wird eine Reihe vordefinierter Werte für die Lernrate und die Batch-Größe festgelegt. Anschließend wird das Netzwerk mit jeder Kombination trainiert und die Leistung des Modells anhand der Abweichungen zwischen den Vorhersagen und den tatsächlichen Testdaten bewertet. Kombinationen, die zu besseren Ergebnissen führen, werden für weitere Versuche ausgewählt und verfeinert. Dieser Prozess wird so lange wiederholt, bis eine signifikante Verbesserung der Netzleistung erreicht wird.

Vor Beginn des Optimierungsprozesses sind klare Kriterien zur Bewertung der Modellleistung festzulegen. Die Leistung des Modells kann anhand zweier Fehlermetriken beurteilt werden: dem Trainingsfehler und dem Validierungsfehler.

- **Trainingsfehler**: Dieser zeigt die Anpassung des Modells an die Trainingsdaten und dient als Indikator für den Trainingserfolg, jedoch ohne Aussage zur Generalisierungsfähigkeit.
- **Validierungsfehler**: Dieser Wert zeigt die Modellleistung auf einem unabhängigen Datensatz und gibt Hinweise auf die Vorhersagegenauigkeit neuer Daten. Ein geringerer Validierungsfehler deutet auf eine verbesserte Generalisierungsfähigkeit hin.

Hohe Trainings- und Validierungsfehler deuten auf Underfitting hin, bei dem das Netzwerk die zugrunde liegenden Muster in den Daten nicht ausreichend erfasst hat. Die Ursachen für Underfitting können in einer zu geringen Modellkomplexität, einer unzureichenden Hyperparameterwahl oder in einer schlechten Datenbasis liegen. Allerdings können auch niedrige Trainings- und Validierungsfehler problematisch sein, wenn das Modell überangepasst wurde. Overfitting tritt auf, wenn das Modell die Trainingsdaten zu gut lernt, aber bei neuen Testdaten versagt. Dies kann durch lange Trainingszeiten, eine mangelnde Variabilität der Daten oder durch Testdaten verursacht werden, die Merkmale aufweisen, die in den Trainingsdaten nicht vorhanden sind. Daher wurde auch die Leistung auf Testdaten anhand zweier Metriken bewertet:

- **Gesamtabweichung** zwischen Vorhersagen und tatsächlichen Werten: Diese gibt die durchschnittliche Modellgenauigkeit an.
- **Maximale Einzelabweichung**: Zeigt das größte Vorhersageabweichungsrisiko und dient zur Vermeidung extremer Abweichungen.

Daher ist es essenziell, bei der Optimierung des neuronalen Netzes nicht nur den Trainingsprozess zu überwachen, sondern auch die Leistung auf den Testdaten sorgfältig zu evaluieren, um fundierte Entscheidungen über die Verbesserung des Modells zu treffen.

In Tabelle 2 sind exemplarisch die Ergebnisse von neun der etwa 40 getesteten Parameterkombinationen des Gesamtnetzes zusammengefasst. Dieses Netzwerk umfasst alle ausgewählten Sortiermerkmale sowie die Versuchsdaten aller Pappelsorten. Mithilfe des entwickelten Programmcodes wurden verschiedene Kombinationen von Batch-Größe, Lernrate und der Anzahl verborgener Neuronen getestet. Die Ergebnisse wurden hinsichtlich Validierungsverlust und Abweichungen auf den Testdatensatz ausgewertet. Der Testdatensatz umfasste 19 repräsentative Beispiele aus den Versuchsdaten mit mindestens zwei Proben jeder Sorte.

Die Experimente zeigten, dass niedrige Lernraten und kleine Batch-Größen nicht zwangsläufig zu optimalen Ergebnissen führen. Mit sinkendem Validierungs- und Trainingsverlust steigt die Prognosefähigkeit des Netzwerks und die Abweichungen auf den Testdatensatz nimmt ab. Eine Ausnahme bildeten die Versuche 8 und 9, bei denen trotz hoher Verluste in der Trainingsphase, bedingt durch die hohe Anzahl verborgener Neuronen, gute Ergebnisse auf den Testdaten erzielt wurden. Als «beste» Parameterkombination stellte sich Versuch 4 dar, da diese Kombination sowohl im Trainingsverlauf als auch in der Generalisierungsfähigkeit auf die ungesehenen Testdaten überzeugte. Dieses Verfahren wurde ebenfalls auf die drei spezifischen Netzwerke der einzelnen Sorten angewendet.

Tabelle 2: Ergebnisübersicht der Trial and Error Methode für das Gesamtnetz

Trial Nummer	1	2	3	4	5	6	7	8	9
Layer 1 Anzahl Neuronen	14	14	14	14	14	14	14	50	60
Aktivierungsfunktion (Layer 1)	tanh	tanh	tanh	tanh	tanh	tanh	tanh	tanh	tanh
Lernrate	0,01	0,01	0,02	0,02	0,03	0,03	0,04	0,05	0,06
Batch-Größe	151	75	75	100	100	75	50	50	25
Validation Loss	16,51	19,26	20,02	13,56	15,40	18,47	21,04	18,14	23,26
Training Loss	11,15	11,30	11,19	8,22	11,49	13,29	9,51	11,71	13,16
Gesamtabweichung	66,09	64,06	68,01	55,46	60,94	58,07	58,76	57,33	56,58
Anzahl der Vorhersagen	19	19	19	19	19	19	19	19	19
Schlechteste Vorhersage (%)	21,52	18,92	25,29	24,46	21,22	16,81	21,00	24,78	32,35

Die optimalen Parameterkonfigurationen für die vier Netzwerke sind in Tabelle 3 dargestellt. Für die Ermittlung wurde grundsätzlich der gleiche Netzaufbau und Programmieransatz verwendet. Durch das Trial and Error Verfahren konnten bereits erfolgs-versprechende Parameterkombinationen identifiziert werden, die im Durchschnitt Vorhersagen mit weniger als 10 % Abweichung von den tatsächlichen Werten lieferten.

Tabelle 3: Übersicht der durch Trial and Error ermittelten Netzwerkparameter

Netzwerktyp	Gesamt-netz	Sorte A	Sorte B	Sorte C
Layer 1 Anzahl Neuronen	14	14	20	80
Aktivierungsfunktion (Layer 1)	tanh	tanh	tanh	tanh
Lernrate	0,02	0,23	0,09	0,02
Batch-Größe	100	25	16	16
Validation Loss [N/mm^2]	13,56	13,92	3,89	10,98
Training Loss [N/mm^2]	8,22	5,10	3,46	57,78
Gesamtabweichung [N/mm^2]	55,46	58,11	3,95	6,19
Anzahl der Vorhersagen	19	19	3	3
Mittlere absolute Abweichung [N/mm^2]	2,92	3,87	1,32	2,06
Mittlere Abweichung (%)	6,27	8,31	2,13	3,85
Schlechteste Vorhersage (%)	24,46	16,85	5,68	5,03

4.4. Hyperparameter Tuning Strategien und Methoden

Die Erfahrungen aus dem manuellen Hyperparameter-Tuning zeigen die Notwendigkeit, den Prozess der Hyperparametersuche effektiver, effizienter und zielgerichteter zu gestalten. Der Keras Tuner, eine in TensorFlow integrierte Bibliothek, bietet hierfür wertvolle Unterstützung, indem er verschiedene Algorithmen zur automatisierten Suche nach der optimalen Konfiguration bereitstellt und die bislang experimentell und möglicherweise willkürlich durchgeführte Suche systematisiert und automatisiert. Bevor der eigentliche Suchprozess initiiert werden kann, sind zunächst grundlegende Schritte erforderlich:

- **Definition des Suchraums:** Der Anwender muss die zu optimierenden Hyperparameter festlegen und den Suchbereich (Wertebereiche oder Wertelisten) definieren, innerhalb derer der Tuner seine Suche ausführt.
- **Auswahl der Tuning-Strategie:** Im nächsten Schritt wählt der Anwender eine Tuning-Strategie wie Random Search, Hyperband oder Bayesian Optimization.
- **Konfiguration der Tuner-Einstellungen:** Je nach gewählter Strategie werden spezifische Konfigurationen festgelegt, wie Suchrichtung (z.B. Minimierung oder Maximierung), Zielmetrik oder die Anzahl der Epochen.

Nach der Festlegung der Randbedingungen erfolgt der in Abbildung 9 veranschaulichte Tuning-Prozess. Der Tuner wählt eine mögliche Parameterkonfiguration basierend auf den gewählten Hyperparametern und dem vordefinierten Raum aus, trainiert das Netzwerk auf dem Trainingsdatensatz und bewertet die Leistung mithilfe eines Validierungsdatensatzes. Der Prozess wiederholt sich, bis eine festgelegte Anzahl an Durchläufen erreicht ist oder die Verbesserungen der Zielmetrik unter einen bestimmten Schwellenwert fallen. Das Modell wird anschließend mit den optimalen Hyperparametern gegen den Testdatensatz evaluiert, um seine Generalisierungsfähigkeit zu überprüfen.

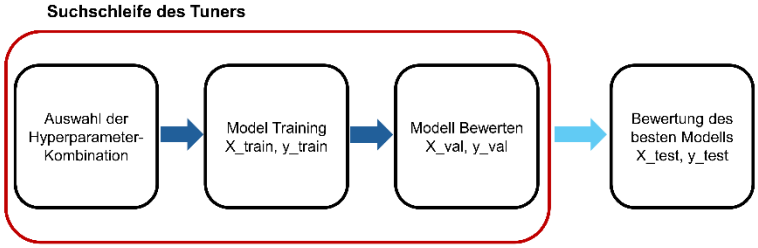


Abbildung 9: Hyperparameter Tuning Prozess mit dem Keras Tuner

Tuning-Strategien im Überblick:

- **Random Search:** Der Algorithmus wählt zufällige Kombinationen an Hyperparametern aus einem vorher definierten Wertebereich aus. Dies ist eine einfache Methode, jedoch wenig systematisch und ineffektiv bei größeren Modellen.
- **Grid Search:** Hier wird jede mögliche Kombination von Hyperparametern aus einem vordefinierten Satz getestet. Dies führt zu einem hohen Rechenaufwand, garantiert jedoch, dass keine mögliche Kombination übersehen wird.
- **Hyperband:** Diese Methode optimiert die Ressourcennutzung, indem anfänglich viele Möglichkeiten getestet und in späteren Runden nur die vielversprechendsten Konfigurationen intensiver evaluiert werden. Sie spart Zeit und Rechenressourcen, indem sie ineffektive Konfigurationen frühzeitig aussortiert [Run:ai (2024), Keras (2024)].

Für die Optimierung der vier Netzwerke wurde der Hyperband-Tuner ausgewählt, da er eine gute Balance zwischen Effizienz und Implementierbarkeit bietet.

4.5. Optimierung von Hyperparameter mittels Hyperband Tuner

In der Tabelle 4 werden die mit Hilfe des Hyperband-Tuners ermittelten besten Hyperparameter-Kombinationen dargestellt. Im Vergleich zu den durch das Trial-and-Error-Verfahren gefundenen Werten in Tabelle 4 ist zu erkennen, dass die im Tuning ermittelten Lernraten durchweg höher sind, während die Batch-Größen geringer ausfallen, was auf einen effizienteren und schnelleren Trainingsprozess hinweist.

Tabelle 4: Ergebnisse des Hyperparameter Tunings ermittelten besten Netzwerkparameter

Netzwerktyp	Gesamt-netz	Sorte A	Sorte B	Sorte C
Layer 1 Anzahl Neuronen	70	134	94	142
Aktivierungsfunktion (Layer 1)	tanh	tanh	tanh	tanh
Lernrate	0,28	0,32	0,41	0,09
Batch-Größe	16	64	16	6
Epochen Anzahl Tuner	50	25	25	25
Validation Loss [N/mm²]	3,10	2,80	2,68	5,01
Training Loss [N/mm²]	1,95	5,28	18,35	3,85
Gesamtabweichung [N/mm²]	48,52	42,51	10,62	9,78
Anzahl der Vorhersagen	19	15	3	3
Mittlere absolute Abweichung [N/mm²]	2,55	2,83	3,54	3,26
Mittlere Abweichung (%)	5,98	6,19	6,51	5,63
Schlechteste Vorhersage (%)	27,81	18,27	8,91	10,58

Die Abbildung 10 zeigt einen direkten Vergleich der Trainings- und Validierungsverluste sowie der Vorhersagegenauigkeit der Netzwerke, die mithilfe der zwei unterschiedlichen Optimierungsmethoden feinjustiert und trainiert wurden. Der Vergleich zeigt, dass die meisten Netzwerke deutliche Verbesserungen bei den Trainings- und Validierungsverlusten erfahren haben. Eine Ausnahme bildet das Netzwerk für Sorte B, bei dem keine signifikante Verbesserung, sondern eine Verschlechterung erreicht wurde.
Die Genauigkeit in der Vorhersage der mittleren Abweichung konnte für das Gesamtnetz um 12,67 % und für das Netzwerk der Sorte A sogar um 26,87 % gesteigert werden. Für die Netze der Sorten B und C konnten keine signifikanten Verbesserungen erzielt werden, was ggf. auf die im Vergleich geringe Menge an verfügbaren Trainingsdaten zurückzuführen ist.

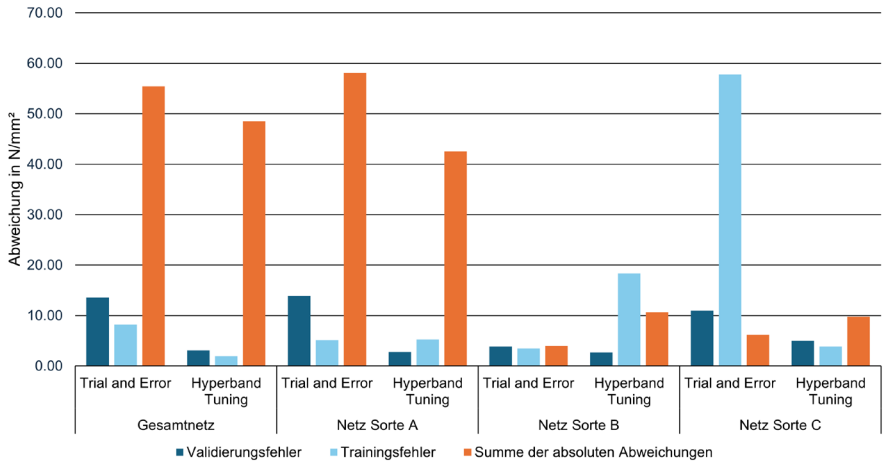


Abbildung 10: Vergleich der Hyperparameter Optimierungsverfahren

Beim Gesamtnetz und dem Netzwerk für Sorte A gelang es, durch eine sorgfältige Anpassung der Validierungsmenge und der Anzahl der Tuning-Epochen, stets Konfigurationen zu ermitteln, die weder zu Overfitting noch zu Underfitting führten. Im Gegensatz dazu ließen sich für die Netzwerke der Sorten B und C, insbesondere für Sorte B, keine zufriedenstellenden Einstellungen finden. Bei Sorte C konnten Verbesserungen im Trainingsprozess erzielt werden, jedoch nicht in der Gesamtabweichung.
Eine detaillierte Betrachtung der einzelnen Prognosen offenbart, dass die ungenauesten Vorhersagen oft Werte am unteren oder oberen Spektrum des Datenbereichs betreffen. So liegt beispielsweise die am weitesten abweichende Prognose des Gesamtnetzes nahezu 30 % über dem tatsächlichen Wert von 31,90 N/mm². Angesichts einer durchschnittlichen Biegefestigkeit von 47,18 N/mm² im Datensatz, der für das Training des Gesamtnetzes herangezogen wurde, erscheint dieser Wert als besonders niedrig. Dieses Muster weist darauf hin, dass die trainierten Netzwerke Herausforderungen bei der Vorhersage von Extremwerten haben. Das Gesamtnetz verzeichnete eine durchschnittliche prozentuale Abweichung von 5,98 %. Würde man den besagten Datensatz ausschließen, könnte diese Abweichung auf 4,76 % reduziert werden. Da diese Werte nicht als Ausreißer betrachtet werden können, unterstreichen sie das Problem einer unzureichenden Trainingsdatenmenge, die nicht die gesamte Bandbreite der Merkmale und Biegefestigkeiten der Testdaten widerspiegelt. Es fehlt insbesondere an einer ausreichenden Anzahl von Datenpunkten mit extremen Versuchsergebnissen, die für eine akkurate Vorhersage solcher Extremwerte nötig wären. Daher könnte eine Vergrößerung des Datensatzes maßgeblich dazu beitragen, die Prognosegenauigkeit der Netzwerke zu verbessern.

4.6. Zusammenfassung der Ergebnisse

In Tabelle 5 sind die optimierten Konfigurationen der entwickelten Netzwerke aufgeführt, die durch die zwei beschriebenen Optimierungsmethoden ermittelt wurden. Für das umfassende Gesamtnetz sowie das spezifische Netz für Sorte A erwiesen sich die mit dem Hyperband-Tuner gefundenen Hyperparameterkombinationen als überlegen. Im Gegensatz dazu lieferte das Hyperband-Tuning-Verfahren für die Netzwerke der Sorten B und C

keine zufriedenstellenden Ergebnisse, weshalb in diesen Fällen auf, die durch das Trial and Error Verfahren identifizierten Konfigurationen zurückgegriffen wurde.

Tabelle 5: Zusammenstellung der optimierten Netzwerkkonfigurationen

Netzwerktyp	Gesamt-netz	Sorte A	Sorte B	Sorte C
Layer 1 Anzahl Neuronen	70	134	20	80
Aktivierungsfunktion (Layer 1)	tanh	tanh	tanh	tanh
Lernrate	0,28	0,32	0,09	0,02
Batch-Größe	16	64	16	16
Optimierungsverfahren	Hyperband	Hyperband	Trial & Error	Trial & Error
Validation Loss [N/mm^2]	3,10	2,80	3,89	10,98
Training Loss [N/mm^2]	1,95	5,28	3,46	57,78
Gesamtabweichung [N/mm^2]	48,52	42,51	3,95	6,19
Anzahl der Vorhersagen	19	15	3	3
Mittlere absolute Abweichung [N/mm^2]	2,55	2,83	1,32	2,06
Mittlere Abweichung (%)	5,98	6,19	2,13	3,85
Schlechteste Vorhersage (%)	27,81	18,27	5,68	5,03

4.7. Fazit

Im Rahmen der Abschlussarbeit wurde bewiesen, dass der Einsatz Künstlicher Neuronaler Netze als leistungsfähiges Werkzeug zur präzisen Vorhersage der Biegefestigkeit von Pappelholz grundsätzlich möglich ist und bereits mit einem relativ kleinen Datensatz von nicht einmal 200 Einträgen gute Vorhersagergebnisse mit einer mittleren Abweichung von unter 10 %, erzielt werden konnten. Trotz der erreichten Erfolge und der vielversprechenden Ergebnisse bleibt jedoch noch Raum für weitere Forschung und Entwicklung. Insbesondere das Problem der Abweichungen auf besonders hohe und niedrige Daten könnte durch eine Erweiterung des Trainingsdatensatzes und der weiteren Optimierung des Trainingsprozesses sowie der Netzwerkarchitektur reduziert werden. Dennoch stellt diese Arbeit einen weiteren Schritt in Richtung der Integration moderner Technologien in das Bauwesen dar.

5. Literaturverzeichnis

[1] [DIN 4074-1:2012-06 2012] DIN 4074-1:2012-06: Sortierung von Holz nach der Tragfähigkeit–Teil 1: Nadelschnittholz. DIN-Deutsches Institut für Normung e.V., 2012

[2] [DIN EN 1912:2013-10 2013] DIN EN 1912:2013-10: Bauholz für tragende Zwecke-Festigkeitsklassen-Zuordnung von visuellen Sortierklassen und Holzarten. DIN-Deutsches Institut für Normung e.V., 2013

[3] [DIN EN 408:2012-10 2012] DIN EN 408: 2012-10: Holzbauwerke – Bauholz für tragende Zwecke und Brettschichtholz – Bestimmung einiger physikalischer und mechanischer Eigenschaften. DIN-Deutsches Institut für Normung e.V., 2012

[4] [Ehlbeck u. a. 1985] Ehlbeck, J. ; Colling, F. ; Görlach, R.: Einfluss keilgenzinkter Lamellen auf die Biegefestigkeit von Brettschichtholzträgern-Entwicklung eines Rechenmodells. Versuchsanstalt für Stahl, Holz und Stein, Abt. Ingenieurholzbau, Universität Karlsruhe, 1985

[5] [Ernst u. a. 2020] Ernst, Hartmut; Schmidt, Jochen; Beneken, Gerd: Grundkurs Informatik-Grundlagen und Konzepte für die erfolgreiche IT-Praxis-Eine umfassende, praxisorientierte Einführung. Springer Verlag, 2020

[6] [Sonnet 2022] Sonnet, Daniel: Neuronale Netze kompakt – Vom Perceptron zum Deep Learning. Springer Verlag, 2022

[7] [Walde 2005] Walde, Janet F.: Design Künstlicher Neuronaler Netze-Ein Leitfaden zur effizienten Handhabung mehrschichtiger Perzeptrone. Deutscher Universitäts-Verlag, 2005

[8] [Run:ai 2024] Run:ai: What Is Hyperparameter Tuning. https://www.run.ai/guides/hyperparameter-tuning. Version: 2024. – [Online; aufgerufen 15-März-2024]

[9] [Keras 2024] Keras: KerasTuner API. https://keras.io/api/keras_tuner/. Version: 2024. – [Online; aufgerufen 07-März-2024]

Sustainable Development and Adaption of the Historic Tachenhausen Farm Estate

Eliese Helmig
Frankfurt University of Applied Sciences
Frankfurt am Main, Germany



Sustainable Development and Adaption of the Historic Tachenhausen Farm Estate

1. Site/Task

Tachenhausen farm estate is picturesquely situated on a hill outside the town and offers an impressive view of the surrounding landscapes. It serves as an agricultural teaching and experimental facility and is referred to as a «Laboratory in the Green» at the Nürtingen-Geislingen University of Applied Sciences (HfWU). For many years, the estate has been a central location for practical training and research in various study programs. It is primarily used by the fields of Agricultural Science, Equine Science, and Sustainable Agricultural and Nutritional Sciences. Students of Landscape Architecture, Environmental Science, and Urban Planning also benefit from the diverse opportunities for agricultural and environmental research available on the grounds. A key objective of the university is to sustainably develop the site and transform it into a forward-looking hub for teaching, research, and innovation. The facility is to be both functionally and aesthetically enhanced, while preserving the existing historic structures.

A distinctive feature of the farm estate appearance is its large, red gable roofs, which are visible from afar and define the historical structure of the site. The central courtyard is framed by buildings from the 19th century, creating a closed courtyard area. This main courtyard is characterized by a clearly defined inside-outside appearance, created by the positioning of the buildings and the enclosing greenery. To the north lies another area with buildings from the 1980s, which are similarly enclosed by vegetation and thus create the impression of a second courtyard. However, the structural layout of the farm estate poses some challenges. While the residential and storage buildings can be used without significant modifications, the buildings for animal husbandry, machinery storage, and teaching must be renovated or newly constructed to meet changing requirements. The objective of the design task is to examine which buildings can be preserved and effectively utilized, and where additional structures are necessary.

2. Planning Concept/Project Goals

The design approach for the Tachenhausen farm estate project is based on a clearly defined sustainability concept that takes into account both the material usage and the long-term flexibility of the buildings. The idea follows the principle of «as little as possible but as much as necessary»: New buildings are only erected where the existing structures cannot meet the requirements, and the new structures are positioned so that no additional access areas are needed. A central goal is to make the best possible use of existing pathways and access areas and to minimize the sealing of new surfaces. Through the deliberate arrangement of the buildings, the typical structure of the farm estate with clearly defined inside-outside appearance is maintained.

The design solution envisions two courtyard areas: The historic main courtyard is defined by the existing buildings and remains in its original form. The newly planned machine hall, together with existing structures, forms a second courtyard area, enhancing and reinforcing the overall structure of the farm estate. The new stables are positioned in optical alignment and close proximity to the machine hall, with some distance maintained between them. This arrangement ensures a logical and efficient operational structure, as it facilitates short paths for accessing pasture areas and moving machinery and vehicles.

The analysis of the existing structures shows that the narrow support structures of the historic buildings make repurposing for many new requirements difficult or impossible. Large volumes beneath the gable roofs remain largely unused due to the compartmentalized layout, making them unsuitable for machine storage or stables. The existing machines and vehicles require more space, and there is also a lack of facilities for cow and goat stables for research purposes.

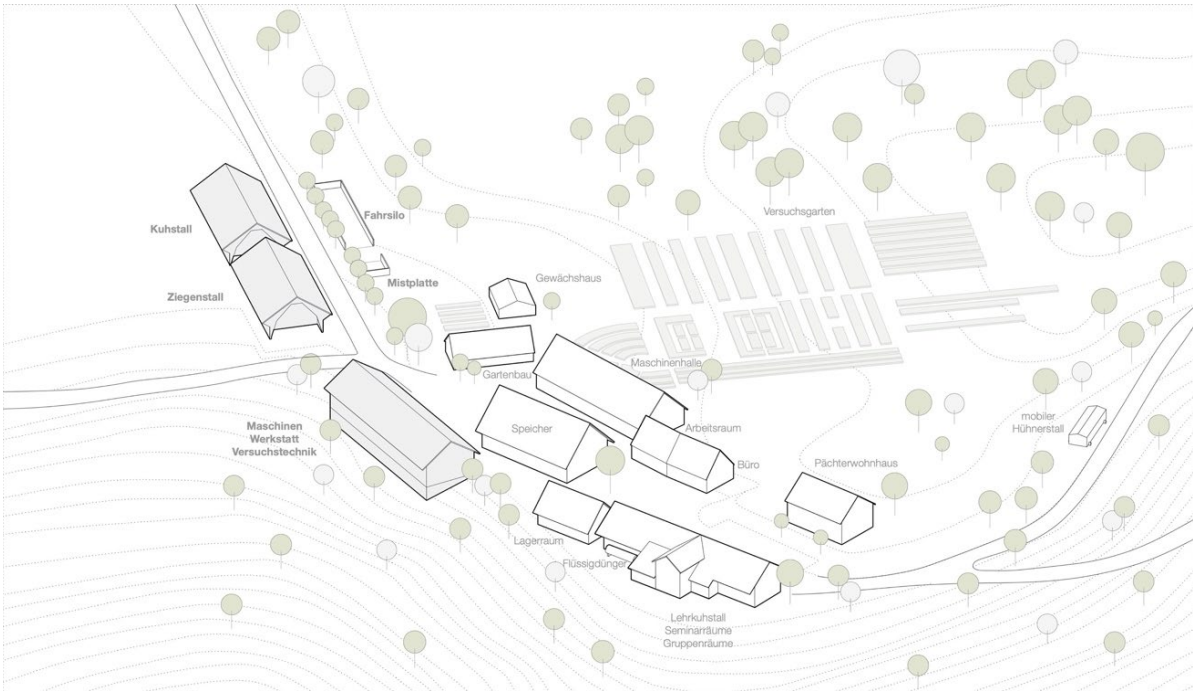


Figure 1: axonometry Tachenhausen farm estate, added buildings in gray

3. Former Pigsty: Conversion into a Teaching Facility

The former pigsty, a historic building with a strong architectural identity, will be transformed into a teaching facility as part of the project. The conversion concept involves a careful energy-efficient renovation that respects the historic structure while meeting the requirements of a modern educational facility. On the ground floor, all existing fixtures will be removed, and the walls in the entrance area will be set back to create a larger foyer that serves as the central access point to the building. The new entrance area will include a ramp for barrier-free access. A newly created atrium above the foyer introduces a new spatial quality, providing views of the upper level and enhancing the building's overall experience. A new staircase and elevator provide access to the upper floor, which houses seminar rooms, group workspaces, and the Smart Farming Lab.

The historic structure is largely preserved by limiting thermal upgrades to the occupied areas. The massive 65 cm-thick walls on the ground floor offer sufficient insulation for temporarily used rooms, eliminating the need for additional insulation. The walls remain in their original form, emphasizing the historic character of the building. The former slatted floor will be insulated from below, while the vaulted ceiling on the ground floor will remain visible to maintain the authentic stable appearance. In the upper floor, floor insulation is applied from above.

On the courtyard-facing half-timbered facade, the infill will be removed and replaced with recessed glazing. This measure brings daylight into the building, creating an open and bright atmosphere with a visual connection to the courtyard. Some glass elements are operable for ventilation, providing natural air circulation. The seminar and group workspaces are housed within insulated timber-frame boxes that are acoustically decoupled, offering a comfortable learning environment. By using a box-in-box structure, circulation areas remain unheated.

The building exemplifies the project's approach of carefully modernizing old structures and creating new, flexible uses that respect and secure the future of the farm estate.

4. Machine Hall: Machine Hall with Workshop and Experimental Areas

The new machine hall expands the existing facilities of Tachenhausen farm estate with a modern structure that serves not only as storage space for agricultural machinery but also includes a workshop and areas for field experiments. The concept for the machine hall emphasizes a clear structure and maximum flexibility to accommodate diverse uses. The goal is to create a hall that meets current requirements while remaining adaptable to future needs.

The hall is supported by a two-hinged frame structure that enables a column-free space, offering significant flexibility in space utilization. This design allows for easy adaptation of the building to new uses if necessary. The wooden structure visually integrates with the existing buildings, creating a cohesive connection with the historical surroundings.

The machine hall is designed for ground-level access, providing easy entry for large vehicles and machinery. Since the terrain slopes slightly, the ground surface is raised on the hillside to ensure the entire hall is built on one level. This creates a spacious maneuvering area, optimizing machinery operations and ensuring short distances between different work areas. The hall is equipped with large doors that allow direct entry and exit for machinery of any size.

Parts of the hall are reserved for the workshop and experimental fieldwork. The temporary workshop previously housed in the old machine hall is replaced by a new and better-equipped facility. This workshop includes maintenance pits, workbenches, storage space for spare parts, and a small, heated room used as an office for technical work. The workshop enables quick and efficient maintenance of all machines on-site. Additionally, the machine hall offers space for the university's field experiments. On a second level, heated boxes serve as social rooms, a kitchen, WC, and changing areas. The platform is suspended within the frame structure and accessible via a staircase, allowing for spatial separation between different uses and optimal utilization of the hall’s large volume.

The facade of the machine hall is clad with a lath covering made of rough-sawn, untreated wood. On the valley side of the hall, the boards of the cladding are omitted, leaving only the laths. Behind this permeable cladding is simple glazing, providing natural light and ventilation. The darker-colored substructure recedes visually into the background. There is also a large, glazed surface at the front of the platform, bringing daylight into the social spaces on the second level and creating a pleasant working environment.

The machine hall is a modern, functional building designed to meet the requirements of sustainable and flexible use.



Figure 2: site plan farm estate



Figure 3: view of the added machine hall

5. Stables: Composting Stables for Cows and Goats

The new stalls at Tachenhausen farm estate follow the open-stable concept, placing special emphasis on animal welfare, environmental friendliness, and efficient space utilization. The goal is to create stables that meet the needs of the animals while remaining flexibly usable in the long term.

The stables are designed as composting stables, meaning that the animals are kept on a bedding layer made of compostable material. The bedding consists of chopped green waste that is already produced on the farm and reused for the stables. This type of bedding initiates a natural composting process, creating a dry and smell-reducing resting area. The bedding is replaced approximately every six months and can then be used as organic fertilizer on the fields. The cows feed at an outside feeding table, separated from the feeding aisle by a feed fence. The arrangement of the feeding table under an overhanging roof allows for the distribution of silage using a tractor. The feeding aisle is regularly cleaned by a manure removal robot, which transports the manure into an underground slurry pit embedded in the ground. This structure minimizes labor in the stables and ensures efficient animal care.

The stables feature ramps at both gable ends, enabling tractor access. A unique aspect of the stables is the second level, which serves as a storage area for hay and straw, optimizing the use of the available volume. This upper level is loaded via gable-end doors can using a telescopic loader. A single-rail hay crane has been installed to facilitate hay distribution on the upper level. Roof openings ensure effective air circulation, improving the stable’s indoor climate and preventing heat accumulation in the summer months.

On cold winter days or during strong winds, the stables can be closed off with curtains on the west side. The goat stable is similarly designed but features specific adaptations to meet the unique needs of the goats.



Figure 4: view of the added stables

6. Stable Construction: Flexible Structure

The construction of the new stables follows the principles of flexibility and sustainability, aligning with the overarching goals of the project. The structure is based on a two-hinged frame that allows for large, column-free spaces, providing significant flexibility in spatial design. The building's base consists of a 35 cm-wide concrete plinth, serving as the foundation for the wooden structure and protecting it from rising moisture, ground dampness, and dirt. Above the concrete base lies a wooden framework composed of 16 x 16 cm beams. In certain areas, the structure is executed as a scissor construction, with ties measuring 8 x 16 cm—half the thickness of the main beams. This design saves material and, unlike glued laminated beams, does not require environmentally harmful adhesives. Moreover, standard dimensions are used, eliminating the need for custom fabrication.

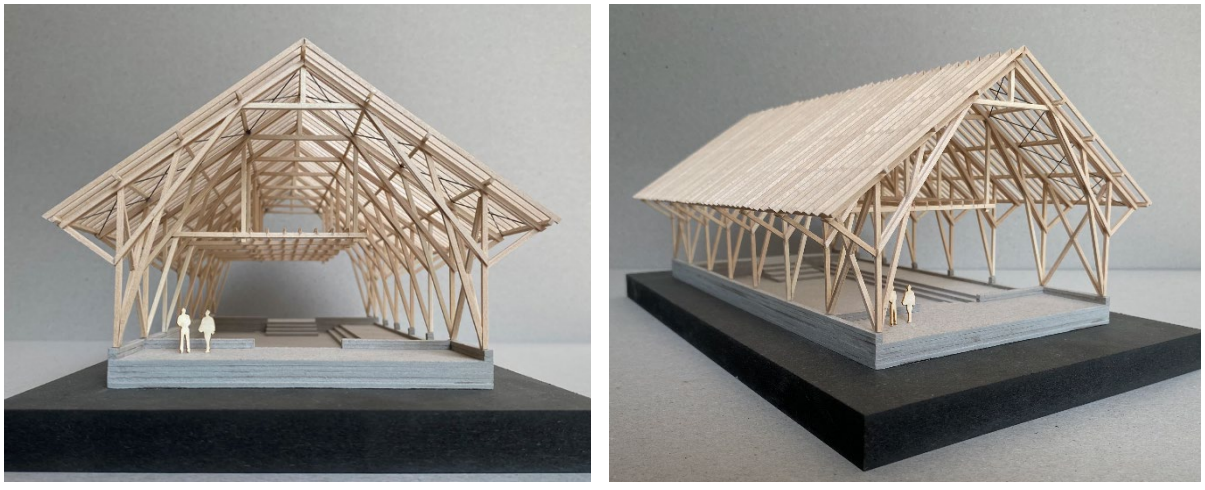


Figure 5: construction model 1:50

The purlins rest on the frame elements and support the roof structure. The purlins carry notched rafters, which in turn hold the battens for the roofing made of natural red PV tiles. The roof overhang adheres to the 60° rule, protecting the sides of the structure that are not clad. A key element of the flexible stables is the is the second level positioned above the resting space. It is attached to hanging beams and secured between the wooden scissors with bolts, allowing for easy disassembly or expansion.
The cladding of the stables consists of rough-sawn, untreated spruce wood slats. The slats cladding is interrupted and offset at the height of the doors, adding structure to the facade. The foremost frame is fully clad to protect the wooden structure from weather exposure. Skylights in the roof are set within a wooden frame with glass at the top. The wooden frame is open at both the top and bottom, ensuring good ventilation and reducing heat accumulation in the summer. The skylights are designed to bring light and air into the interior of the stall without compromising the structural integrity. Above the wooden frames, a gutter directs water away, protecting the wooden structure from moisture.

In summary, both the stables and the machine hall are built on a unified structural system designed as a flexible wooden shell. This shell can be adapted for various functions and has been specifically tailored through targeted measures such as different cladding, roof overhangs, versatile structures on the roof, and flooring adjustments. This flexibility allows the buildings to be adapted to future changes in use with minimal effort, ensuring the sustainable and long-term operation of the Tachenhausen farm estate.

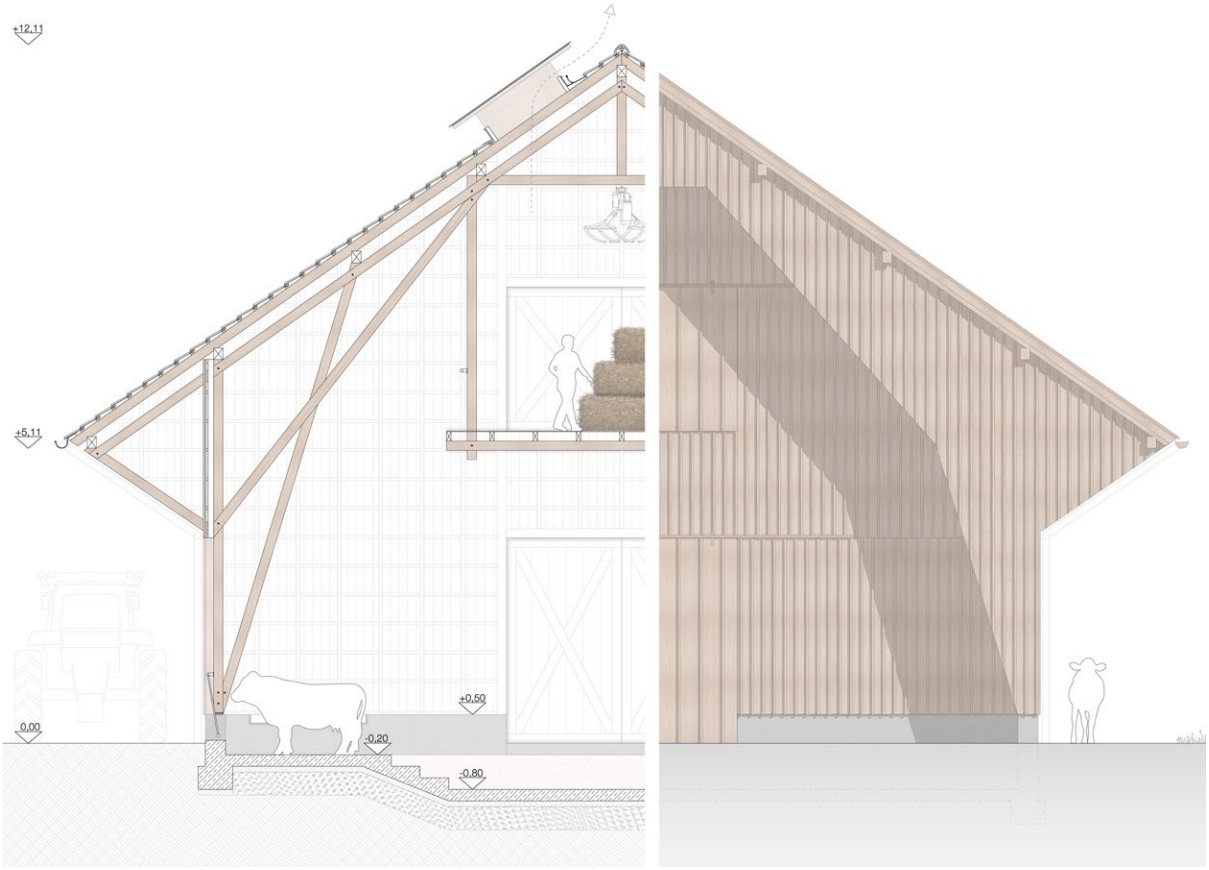


Figure 6: detail section and detail elevation

A Systems Thinking Approach to Production Optimisation in the Prefabricated Housing Industry

Lorenz Weiß
TH Rosenheim/Rubner Haus GmbH
Bruneck, Italien



A Systems Thinking Approach to Production Optimisation in the Prefabricated Housing Industry

Abstract

Optimising production in the prefabricated housing industry is challenging due to the complexity of human and technical systems. The need for customised products based on a modular platform, combined with the floating bottleneck in mixed-model assembly lines, creates a complex optimisation scenario. This paper presents a systems thinking approach that incorporates systems engineering and the soft systems view, considering both quantifiable «hard facts» and «soft facts» derived from the knowledge and experience of production workers. To test the approach, a case study is conducted in a company that produces prefabricated single-family houses. The approach, which was tailored to the specific case company, involved the analysis of the current state, the identification of improvement opportunities and the derivation of specific improvements. It included the use of methods such as product family matrix analysis, business process management notation, digital data collection and evaluation using the Microsoft Power Platform, and survey-based assessments. The efficacy of these solutions is evaluated using a payback period–net present value matrix, which guides the implementation strategy. Continuous improvement ensures the sustainability of the implemented solutions. This approach provides a general solution for discovering and implementing efficient production optimisation strategies in the prefabricated housing industry.

Keywords

Industrial House Building (IHB), Systems Thinking, Mass Customisation, Product Platform, Systems Engineering, Assessment of Optimisation Potentials

1. Introduction

In the industrialised house building (IHB) sector, companies have shifted from a project-oriented organisation towards a product-oriented one, aligning products and processes through a platform providing the solution space for a cost efficient product (Popovic et al. 2021, 4). In terms of variability and economic efficiency, mass customisation describes a strategy using modern manufacturing systems to optimise these opposite factors delivering a product which meet the needs of the customer at a reasonable price (Jiao and Tseng 1999).

Due to the increase of the year to year growth rate of construction costs in Europe of 6,53 % in 2021 and 12,65 % in 2022 (Statista 2024) in combination with increasing interests from 2021 to 2023 from 1,09 % to 3,92 % (Statista 2024) and the resulting decrease in orders, construction firms strive for optimisation to improve their profit (Quin Investment 17.08.2023).

To improve their performance and ultimately their margins, it is imperative to comprehensively analyse all the processes involved in creating goods that are sold to customers and thus generate revenue.

To facilitate this analysis and to abstract the complex process linking the company's market position with individual actions in production, it is possible to describe the process with a conceptual model consisting of different interacting systems to evaluate cause and effect (Haraldsson and Sverdrup 2021, 15).

Moreover, production optimisation is also about understanding and incorporating the soft information that exists among the employees in the company (Checkland and Poulter 2020, 202). This includes their knowledge, experience, and insights, which can play a crucial role in identifying and addressing inefficiencies in the production process (Lies 2023).

The paper focuses specifically on improving the efficiency of the industrial production of building components for residential construction. The optimisation of production in industrialised housing is multifaceted, requiring the coordination of various elements such as design, procurement, manufacturing, and assembly. These complexities are compounded by factors such as existing floor plans in built-up areas, required return on capital, material costs, employee availability, required flexibility for future products, and potential capacity increases.
Given the interdependence of investment costs for improvements or newly built factories, reduced production costs, and overall margin, an approach is needed to analyse the current state of production as a foundation for future decisions and to identify tangible opportunities for increasing efficiency.
The study aims to investigate the possibility of a systems thinking approach to production optimisation in IHB. This will be achieved by combining measurable indicators with the knowledge and experience of the company's personnel. To ensure the general applicability of the results, a basic analysis of the products and processes typical for IHB is carried out. This analysis will allow for a theoretical classification of the monitored activities.
An approach to combine systems engineering theory with soft systems methodology is developed and implemented in a case study to verify the practical application of the theory. The study aims to provide an objective overview of production and a tangible optimisation strategy to reduce costs and increase margins.

2. Systems thinking approach for product centred production development and optimisation

To develop an optimal production solution or optimise an existing facility for IHB, a hybrid approach in the context of systems thinking is created as visualised in Figure 1. Therefore, the systems engineering approach (SE) is combined with soft systems methods (SSM) to form a solution comparable to critical systems heuristics (CSH). To discover potentials and to define the solution space, the SE approach is used to investigate the process and to describe the requirements of different interacting systems as well as providing optimisation potentials based on measured data.
SSM is used to secure experience and learnings due to problems in the existing production solutions. The results are combined to the solution space for the optimisation. The different potentials are assessed in terms of efficiency. An optimisation strategy is derived from the solution space forming a basis to continuously improve the system using the learning cycle of the SSM.

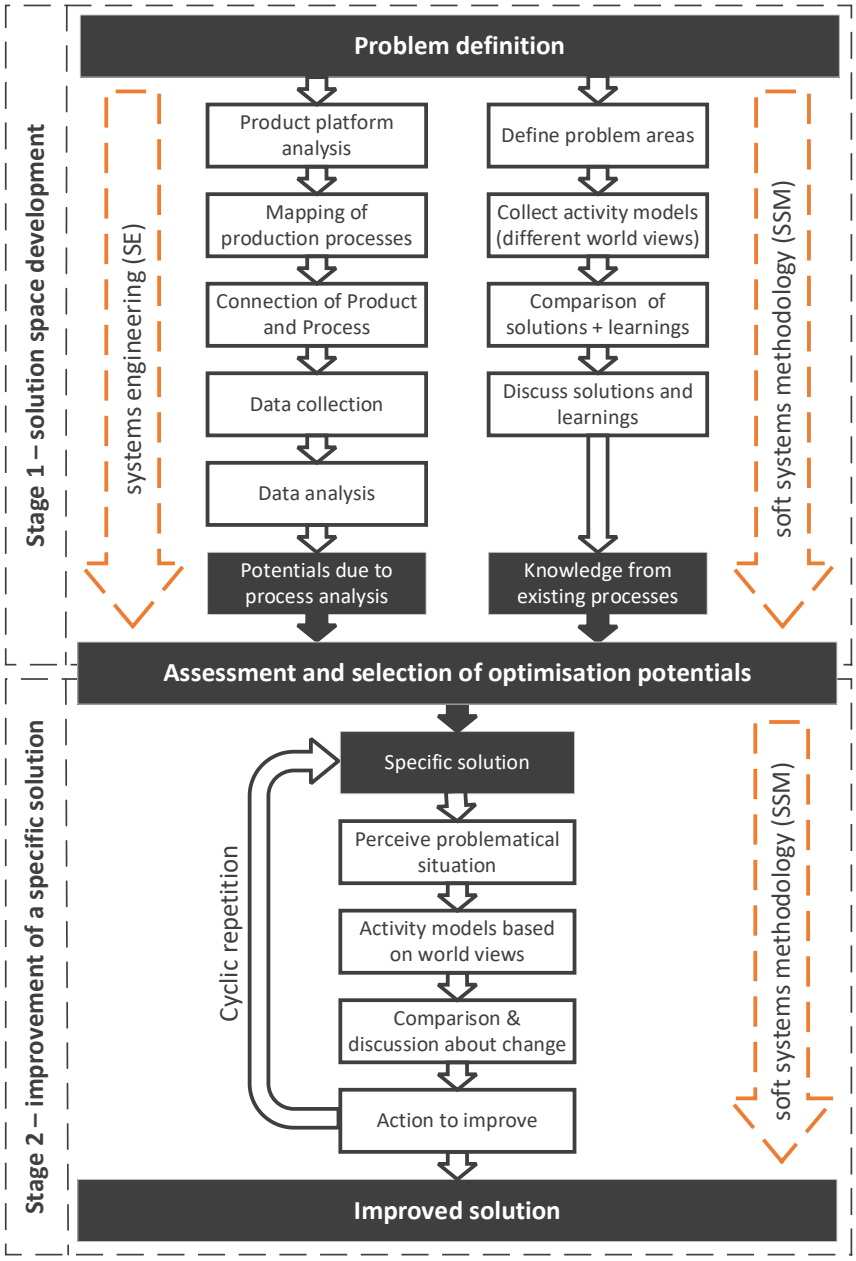


Figure 1: 2-stage hybrid approach to production planning using systems thinking

3. Methodology to perform the systems thinking approach in practice

To verify the approach, it was applied to an actual case company that aimed at optimising an existing solution for wall element production in the prefabricated housing industry. Therefore, the applicability of different methods was assessed resulting in a set of methods used to perform the systems thinking approach in praxis.

Prior to the analysis of the processes, the product portfolio is structured to allow for the connection of the process data with the product characteristics. Therefore, the approaches «dissolution of product families to product variants (Bauer et al. 2014b, 736)» and the «product platform based on robust and flexible modules» according to Bauer et al. (2014a) are combined. This dissolution of the product category to the specific customised product variant along the modular product platform defines the capability of the product solution space offered by the company. To design the chart, the visualisation software Microsoft Visio is used.

To analyse the structure and sequence of the current production processes as a basis for quantitative analysis and future production improvement, it is necessary to map out these processes. BPMN is identified as a suitable method for mapping complex processes and process variants within the context of processes in IHB. Additionally, the case company has access to a software license for SAP Signavio, a process mapping software that utilises the BPMN notation, at no extra cost.

To establish the link between the manufactured products and the necessary processes, a product process matrix (Erlach 2020, 39) was developed.

In order to collect and evaluate quantitative data efficiently, a digital solution is created using Microsoft PowerApps, to provide a clear and user-friendly interface for collecting data at the process level. The collected data is recorded in a connected SharePoint database allowing for an interactive Microsoft PowerBI, report directly available to the analyst, allowing visualisations of the latest measurement data, based on transformed relational data model.

To incorporate the knowledge and experiences of the production staff, interviews were conducted using a combination of open and closed questions. A multilingual form was created using Microsoft Forms to facilitate the execution of the interviews and the collection of results.

The «spaghetti diagram» can be used to conduct a qualitative analysis of material flow in order to identify waste areas in transportation and movement.

For the prioritisation of the optimisation potentials discovered, a Payback Period – Net Present Value Matrix is established. Therefore, the different potentials are supplemented with a possible solution, the actions and costs necessary to achieve the solution, the benefits generated, and the data used to calculate the worth of the actions. To compare the different possible actions, the NPV of the investment is calculated for a duration of 5 years with a discount rate of 10 %. To present the potentials in a single matrix, a logarithmic scale is used on the y-axis.

After classification, the identified potentials defining the solution space of stage 1 are discussed with the stakeholders to determine the next steps.

Depending on the implementation strategy chosen on with the stakeholders, the potentials are implemented, revised, or postponed.

To ensure a good solution, the soft systems approach stage 2 using the learning cycle (Checkland and Poulter 2020, 217) can be used. This way, the proposed solution is discussed with the different stakeholders and improved until it is possible to agree on a solution fulfilling all requirements.

4. Implementation of the case study

The modelled variant of the systems thinking approach for product centred production development and optimisation, is applied in practise to analyse the production of the case company.
Historical data is analysed to determine the average cycle time of the past to evaluate implemented improvements. A time study, using the Microsoft PowerApps application developed, is conducted to analyse the composition of the cycle sequence, process times, and the floating bottleneck, examining the causes for the cycle time.
The results are reported using the prepared data model, resulting in an interactive Microsoft Power BI report presenting the results. These results are justified with observations made during the practical execution of the studies and by analysing the report visuals.
Interviews are then conducted with the production staff to incorporate their knowledge and experiences, and the results are summarised and compared with potentials identified during the systems engineering stage.
Summarising the results, potentials can be outlined. Concrete solutions based on the outlined potentials are constructed and further developed through workshops with the integration of leading production staff resulting in concrete solutions for the optimisation / reengineering of the production.
By realising the first stage of the systems thinking approach, different optimisation potentials were discovered, summarised in Table 1, forming the basis for production improvements. As displayed in Table 1, most of the potentials were discovered with the systems engineering approach, the soft systems methodology approach in addition discovered the potentials «sorting of beams in wall lots for the supply at the framing station to reduce searching times, as well as «collaboration and teamwork»».

Table 1: Summary of potentials discovered with the different approaches used

ID	potentials	systems engineering approach	soft systems thinking approach
1	Common waiting time of table 2 and table 3	x	
2	Delayed start in cycle time	x	
3	Occurance of machine and Planning errors	x	x
4	Material supply Table 3 - Electrical installation material	x	x
5	Material supply Table 4 - Materials needed to close the outer wall side	x	x
6	Material supply Table 5 - supply of materials	x	x
7	Waste disposal Table 4 - cork	x	
8	Supply of information needed in Production	x	
9	Digital Quality Check	x	
10	Digital feedback of used materials	x	
11	Reduction of Machine Downtime	x	x
12	Collaboration & Teamwork		x
13	Sorting of beams in wall lots for the supply at the framing station		x

4.1. Evaluation of the strategy based on the detected potentials

To enhance production, it is necessary to implement the identified optimisation potentials. Therefore, the solutions are evaluated based on their costs and benefits. This evaluation requires a detailed description of the costs and benefits to provide a realistic estimate of the impact.
To achieve this, past project experiences and concrete costs are researched and taken into consideration. To assess the economic efficiency of the implementation, the net present value and payback period is calculated. The matrix, shown in Figure 2, excludes potentials with a calculated payback period greater than 10 years. It displays the efficiency of the potentials. Nine out of the 13 observed potentials have a payback period shorter than one year, providing varying levels of efficiency in terms of the NPV calculated over a period of five years.
Based on Figure 2, the most efficient optimisation potentials to be implemented are line balancing for table 2 and table 3, digital quality checks using a custom application, and an error handling strategy for machine and planning errors.

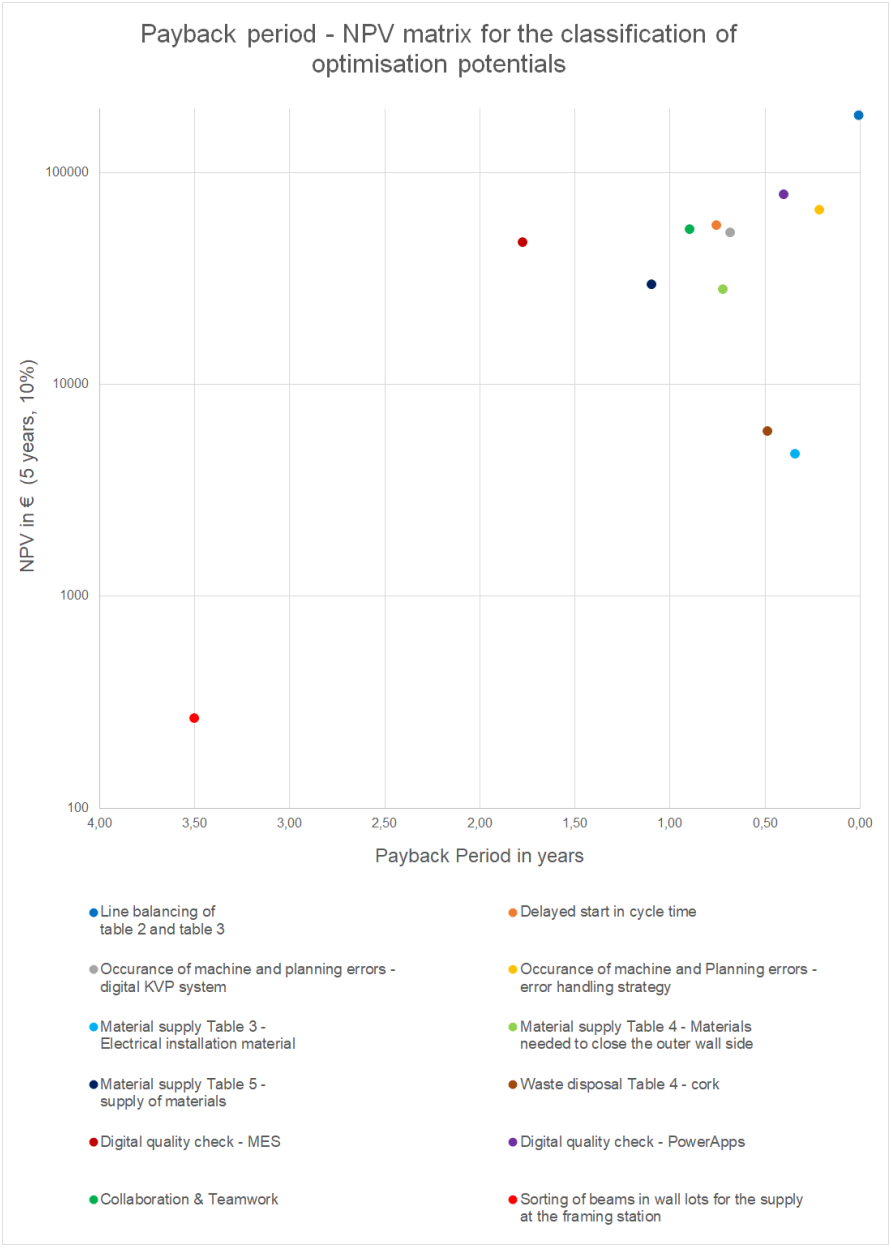


Figure 2: Payback Period – NPV matrix to rate optimisations in production in terms of efficiency (click on diagram to access data)

4.2. Optimisation strategy based on the discovered potentials

After assessing the different solutions, the further proceeding was discussed with the production managers, resulting in a clear optimisation strategy as shown in Table 2.

Table 2: Approach based on the proposed optimisation potentials

ID	optimisation suggestions	immediate implementation	to be discussed with Group IT	to be revised	implementation postponed
1	tact optimisation using line balancing	x			
2	delayed start in cycle time				x
3	introduction of a continual improvement process (CIP)		x		
4	Introduction of a process of handling errors occurring during tact				x
5	material supply table 3 (electrical installations)	x			
6	material supply table 4	x*			
7	waste disposal of cork at table 4	x			
8	material supply table 5	x*			
9	supply of information needed in production		x		
10	digital quality check		x		
11	digital feedback of used materials		x		
12	reduction of machine downtime				x
13	collaboration & teamwork				x
14	sorting of beams for the supply at the framing station			x	

* prototype is made to test the concept

4.3. Improvement of the solution through Soft Systems Methodology (SSM)

The production managers implemented the workplace optimisations immediately after discussing the optimisation strategy. Due to the short time frame between the discussion and implementation, it was not possible to improve the solution using soft systems thinking before the practical implementation. Experiences with the adopted workplaces were collected, and potential optimisations were discussed.
Due to the motivation of the production managers on the implementation of the improvements, the learning cycle had to be adopted including the practical implementation of the solution.

5. Summary

The practical implementation of the systems thinking approach provides a concrete strategy for optimising the production of the case company.

5.1. Application of Systems Engineering

Focusing on the systems engineering approach of stage one, historical data enabled the determination of an average cycle time of approximately 75 minutes for the year 2022. Furthermore, to identify areas for optimisation, we conducted a detailed time study using Applications of the Microsoft Power Platform.
A mean cycle time of 66,2 minutes was observed, with a standard deviation of 14,6 minutes, which differs from the historical average of 2022. The limited personal resources and cycle time led to the observation of 45 evaluable work cycles, with a maximum of two observed workplaces at a time. Focusing on specific shares of the measured data can provide targeted information for a particular product family and workstation but results in a decrease in sample size and limits the ability to perform a statistical analysis. The collected data allowed for the analysis of individually observed cycles in terms of composition using a Gantt chart integrated in the PowerBI report.

By collecting 48 comments about irregularities that occurred during time measurements in production, an unexpected opportunity to extract optimisation potentials was discovered. Utilising the comments, it was possible to assess observations objectively, such as the potential «tact start <> work start», which was mentioned 12 times. The ability to collect comments during measurement, with a connection to the measured data, enables the allocation of irregularities and the ability to adapt to unexpected occurrences during observation.

5.2. Application of Soft Systems Methodology

A survey, available in Italian and German was conducted in production collecting 19 responses. In contrast to the measured and calculated average cycle time, the survey estimated a cycle time of 55 minutes with a standard deviation of 19,5 minutes.
The estimated frequency of floating bottlenecks of 44 % at table 3 and 33 % at table 4 did not align with the median of the measured cycle times. This discrepancy may be attributed to the small sample size of the process time measurement, as well as potential biased perceptions by the workers.
Open questions were used to collect knowledge and experiences about existing optimisation potentials among the workers. The most significant cause of delays, mentioned 15 times, was planning errors, followed by complex processing, mentioned eight times, and «machine errors», mentioned seven times. Special attention should be given to the answer «teamwork and collaboration», which is mentioned twice, in response to the question «how can we reduce cycle time», a potential difficult to detect using a systems engineering approach. Additionally, the conducted survey may be biased due to the employees' overestimated reading and writing capabilities. This circumstance reduces the quality of the responses of the soft systems approach but provides valuable knowledge about the workers' capabilities to interact with written information.

Assessment of potentials to create an optimisation strategy

Thirteen concrete optimisation potentials were stated based on the research conducted, 38 % were discovered by both approaches, 46 % only by the systems engineering method, and 15 % only by the soft systems approach. The soft systems approach demonstrated its ability to identify difficult-to-measure potentials, such as a lack of teamwork and collaboration.
Specific solutions based on optimisation potentials are created and evaluated in terms of their realisation effort and benefits for the company, measured in costs. The data for the assessment is estimated based on concrete costs, previous projects, and experiences. The payback period and NPV were calculated based on the effort-benefit evaluation and visualised in a payback period – NPV matrix. This provides insight into the efficiency of capital use for and indicates that nine out of the 16 solutions have a payback period of less than one year, with varying performance for capital use.
The solutions were discussed with stakeholders to create an implementation strategy. Four solutions were chosen for immediate implementation, two solutions were revised, and the further proceeding of four solutions was discussed with the IT department (Table 2).
To use the full potential of the solutions proposed, it is necessary to apply the learning cycle to the implemented solutions. Furthermore, further potentials discovered in the production can be added to the payback period – NPV matrix to assess the efficiency, as well as to prioritise the implementation.

6. Conclusion

The approach identifies a concrete optimisation strategy by utilising soft systems thinking and systems engineering within the context of critical systems thinking considering both «soft facts» and «hard facts» as available information to describe a complex production system. The approach created provides a general framework for production optimisation and is equipped with methods selected to meet the characteristics of the case company. This allowed for the application of a customised methodology in the case study to verify its general applicability. Various optimisation potentials were detected, nine were evaluated with a payback period of less than one year.
The implementation of solutions was evaluated in cooperation with production managers, resulting in five potential solutions to be implemented immediately with a net present value of around 250.000 € (5 years; 10% discount rate). Further potential solutions concerning information flow will be evaluated with the company's IT department.
The created approach proves its capabilities during the execution of the case study. It has a positive impact on all stakeholder groups. Management benefits from reduced production costs and the therefore improved margin. The production manager gains from enhanced predictability of production time and flow, as well as reduced personnel requirements for production operations. Workers in production benefit from a consistent workload that is manageable without the need to rush. By utilising the learning cycle of the systems thinking approach in stage two, the aim is to resist bad solutions and continuously strive for efficiency.
Utilising critical systems thinking, it was possible to improve a complex system. The production of batch size one products with varying dimensions, complexity, random occurring errors and the resulting floating bottleneck characteristics, result in a system difficult to predict and simulate to optimise efficiency. This relates to the work of Grenzfurtner et al. (2023) which describes the challenges related to the quantity and quality of available data, which require simplifications and assumptions. The created approach focusing on the implementation of efficient improvements provides a general applicable methodology to improve the production efficiency and therefore the company’s margin. This strategy is in line with the general attempt to optimise situations with critical systems thinking as stated in the «critical systems practice» by Jackson (2021, 13).

7. Outlook

To control the impact of implemented optimisation solutions, it is essential to establish an automated method for measuring the current cycle time. The learning cycle can be used to further improve the implemented solutions.
Additionally, machine learning can be employed to combine product attributes and historical data to predict future bottlenecks. This allows for optimisation to avoid bottlenecks.
Furthermore, as detected in the thesis, errors have an impact on the cycle time. Therefore, the creation of an efficient system to monitor the quality and error occurrence can improve the company's profitability. Machine learning could be used to analyse to prevent future errors.
Before assessing potential future investments in the production line, it is necessary to evaluate and adapt the current product portfolio in the context of the company's market position and competitors' offerings. This will ensure a sustainable production solution, securing the company's ability to generate profit in the future.

8. Acknowledgement

I would like to express my gratitude to my supervisor, Martin Wolfsgruber (Rubner Haus), as well as my professors, Andreas Heinzmann and Christian Kortüm of TH Rosenheim, for their support.

9. References

[1] Bauer, Wolfgang/Chucholowski, Nepomuk/Elezi, Fatos (2014a). Zyklenorientiertes Modul- und Plattformdenken. Ein Leitfaden für Praktiker. Garching.

[2] Bauer, Wolfgang/Werner, Christopher/Elenzi, Fatos/Maurer, Maik (2014b). Forecasting of Future Developments Based on Historic Analysis. Proceedings of the DESIGN 2014 13th International Design Conference.

[3] Checkland, Peter/Poulter, John (2020). Soft Systems Methodology. In: Sue Holwell/Martin Reynolds (Eds.). Systems Approaches to Making Change: A Practical Guide. London, Springer, 201–253.

[4] Erlach, Klaus (2020). Wertstromdesign. Berlin, Heidelberg, Springer Berlin Heidelberg.

[5] Grenzfurtner, Wolfgang/Pichler, Elena/Gronalt, Manfred (2023). Increasing the Output of Mixed-Model Assembly Lines for Industrialised Housebuilding: Learnings from a Case-Based Simulation Study.

[6] Haraldsson, Hördur/Sverdrup, Harald (2021). Systems science and system thinking in practice- How to develop qualitative and numerical models for evolving understandings of challenges and responses to complex policies.

[7] Jackson, Michael (2021). Critical systems practice 2: Produce – Constructing a multi-methodological intervention strategy. Systems Research and Behavioral Science 38. https://doi.org/10.1002/sres.2809.

[8] Jiao, Roger/Tseng, Mitchell (1999). Methodology of developing product family architecture for mass customization. Journal of Intelligent Manufacturing 10, 3–20. https://doi.org/10.1023/A:1008926428533.

[9] Lies, Jan (2023). harte und weiche Faktoren. Available online at https://wirtschaftslexikon.gabler.de/definition/harte-und-weiche-faktoren-52688/version-275806 (accessed 10/26/2023).

[10] Popovic, Djordje/Schauerte, Tobias/Elgh, Fredrik (2021). Product platform alignment in industrialised house building. Wood Material Science & Engineering 17, 1–14. https://doi.org/10.1080/17480272.2021.1903993.

[11] Quin Investment (2023). Krisenanalyse 2023: QUIN Investment – Berliner Immobilienmakler. QUIN Investment | Makler für Wohn- und Gewerbeimmobilien Berlin of 8/17/2023. Available online at https://quininvestment.com/berliner-immobilienmakler-quin-investment-befragt-projektentwickler-zur-krisensituation/ (accessed 2/6/2024).

[12] Statista (2024). Home construction cost in Western Europe countries 2022 | Statista. Available online at https://www.statista.com/statistics/1380225/growth-of-housing-construction-cost-in-selected-western-europe-countries/ (accessed 2/6/2024).

[13] Statista (2024). Zinssätze für Wohnungsbaukredite an private Haushalte bis 2023 | Statista. Available online at https://de.statista.com/statistik/daten/studie/1263033/umfrage/zinssaetze-fuer-wohnungsbaukredite-an-private-haushalte-in-deutschland/ w(accessed 2/6/2024).

Enhancing design and production in modular timber architecture with computational design tools

Joaquim Escoda Llorens
Institute for Digital Construction and Wood Industry,
Bern University of Applied Sciences
Biel/Bienne, Switzerland



Enhancing design and production in modular timber architecture with computational design tools

1. Introduction

Off-site construction and modular building systems both lead to fast production, economic solutions regarding material and processes, more accuracy and higher overall quality. This research investigates the integration of computational design tools to enhance both design process and production methods within the context of modular timber architecture.
The focus is specifically on two aspects. Firstly, the integration of various existing analysis tools into the design process to achieve a more informed design. Secondly, automating the modelling, analysis, and CNC fabrication of different architectural design variations (geometry, shape, materials, etc) using a range of bespoke computational tools.
The utilization of computational design tools in modular timber construction has the potential to enhance both quality and productivity without sacrificing architectural uniqueness. The resultant flexibility achieved by such computational methods enables the creation of distinctive and unique solutions with the same level of effort required for standardized, repetitive ones. This represents a paradigm shift in modular architecture transitioning from mass production to mass customization of buildings or building components.
To achieve these goals, this research has developed bespoke computational tools including structural analysis, energy simulations, cost evaluation, weight assessment, environmental impact analysis and design-to-production processes. All these tools have been integrated into a parametric planning platform that has been iteratively improved and extended by the learning-by-doing design process and validated by different series of 1:1 prototypes.
This is exemplified by the research project «àDisposition» led by the BFH with the goal to develop a modular timber construction kit optimized for easy transport, assembly, adjustment, and dismantling, particularly for the temporary use of vacant buildings and sites.
Finally, research outcomes are showcased by a configurator, designed to be used at an end-user level, that allows to plan, visualize, analyze, and prepare production files for various proposals utilizing the above-mentioned modular kit.

1.1. Research motivation and goals

In recent years, the focus on sustainable building methods has increased, bringing modular timber architecture to the forefront. Modular building systems and off-site construction both lead to fast production, economic solutions regarding material and processes, more accuracy and higher overall quality.
Nevertheless, modular architecture has often been criticized in popular opinion for being impersonal, of inferior quality, or lacking in [1]. Amidst the growing emphasis on customization and improved performance, architects are challenged to create designs that align with the unique requirements of clients and local regulations. Computational design and automated fabrication emerge as empowering tools, enabling to create bespoke solutions, allowing design, analysis, and manufacture automatization without compromising individuality.
Simultaneously, the market demands adaptable and flexible building solutions to answer evolving needs. The integration of modular architecture with computational design is set to meet this demand by providing scalable, quickly deployable solutions that are applicable in various contexts, significantly reducing both delivery times and costs. [1, p. 76], [2, p. 13].

With these motivations in mind, this investigation had the following goals:
- Study the role played by computational design in the domain of architecture, with a particular focus on its capacity to generate bespoke context-sensitive tools, for modular construction.
- Investigate the integration of automation, by means of different computational tools into the design and manufacturing processes of modular architecture.

- To propose a set of methods to enable an integrative design process that improves both the design and manufacture of an example of modular timber architecture.
- Employ these methods in a real case study to develop a modular timber construction kit optimized for easy transport, assembly, adjustment, and dismantling, particularly for the temporary use of vacant buildings and sites, with computational tools, in the context of project «àDisposition» (Innosuisse, 59217.1 IP-SBM) led by the BFH.



Illustration 1: Second round of prototypes: defining a minimal 3x3 walls room at DISPO hall.

1.2. Relevance of the study and contribution

In the contemporary context, the production and functioning of buildings account for a substantial 36% of worldwide energy consumption and contribute significantly to 39% of carbon dioxide emissions [3]. Although progress has been made in recent years in reducing operational emissions of buildings, the reduction of embodied emissions involved of construction, assembly and transport of materials remains an essential challenge to achieve near-zero emission cities and societies.
Concurrently, the construction industry is undergoing unprecedented growth, driven by a rapidly increasing population and a shortage of affordable housing [4]. As the demand for new buildings intensifies, the resulting growth carries inherent consequences. Consequently, there is an increasing need for substantial innovation throughout the architecture, engineering, and construction (AEC) value chain to meet the evolving challenges posed by this growing sector.
Moreover, the construction sector is well known for its low productivity growth over the past few decades, with an increase of only 0.4% in real gross value added per hour worked, compared to 3% in the manufacturing sector and 2% in the overall economy [5]. Therefore, the relevance and contribution of this research lies in the field of modular timber construction enabled by computational design methods.

This research focuses on three key aspects that collectively address the need for more sustainable and efficient construction practices.

The first focus is the use of wood as a construction material. Wood is one of the oldest materials used in building, but it also offers significant potential in the context of decarbonizing the built environment. It provides an alternative to more environmentally impactful materials such as concrete and steel. Additionally, using wood in construction supports the natural carbon cycle by allowing for the regrowth of trees, which can continue to sequester carbon. Furthermore, wood acts as a long-term carbon storage solution when incorporated into buildings, helping to mitigate the impact of carbon emissions.
The second theme centers on modular architecture. Modular construction has proven to be more affordable [2], higher in quality [6], and quicker to implement [2] than traditional building methods. The use of modular components not only enhances flexibility and customization in design but also facilitates easier disassembly and reuse of materials. This adaptability makes modular architecture an ideal fit for the principles of a circular economy, as it reduces waste, minimizes the consumption of resources, and lowers the environmental footprint of buildings.
The third area of exploration is computational design and digital planning. The construction industry is often hindered by inefficiencies arising from outdated processes. The application of digital planning and computational design tools is critical to addressing these challenges (2). By improving accuracy, reducing fabrication time, and minimizing material waste, these technologies can significantly enhance the efficiency of construction projects. Moreover, they enable a seamless integration of modular building principles, further optimizing sustainability in the construction process.
The relevance and contribution of this master's thesis lie in its exploration of modular timber construction, enhanced by computational design methods. By combining the environmental benefits of wood with the flexibility and efficiency of modular architecture, alongside the precision of digital tools, this work aims to contribute to advancing sustainable building practices and driving innovation in the construction sector.

2. Methods

To answer the research question described above different methods are required. The methods proposed for the development of the case study are the following:

- An integrative design process and an iterative evaluation.
- The development of computational design system for the exploration design and analysis of a modular timber construction kit.
- Prototyping.

2.1. Integrative and iterative design process

The integration of all the disciplines involved in the project in one same platform is one of the main methods of this research. Integrating multiple disciplines in parallel and facilitating feedback exchange between them is expected to lead to better and more informed design decisions, enabling a multi-disciplinary decision-making process. In the field of architecture this has been previously referred to as «integrative design» by Achim Menges [7, p. 72] or total architecture by Ove Arup [8].
All the disciplines involved in the design and manufacture of the modular building system were integrated into a parametric platform. This parametric platform brings together the computational design system created for this project, covering the entire parametric data flow, from early design exploration to the performance analysis and the generation of manufacturing instructions.
At the same time, this integrative development process has been applied incrementally. This means that not all the features were developed at the same time and some of them were implemented at a later point in the project.
This incremental development had two main purposes. The first one was to manage the complexity of integrating different disciplines by breaking the problem into smaller parts, allowing for partial and incremental verification of each feature's proper functioning. The second purpose was to align its development with the design timeline of the modular building system. The design of the modular building system was not pre-defined at the beginning of the project but developed concurrently with the computational design system.

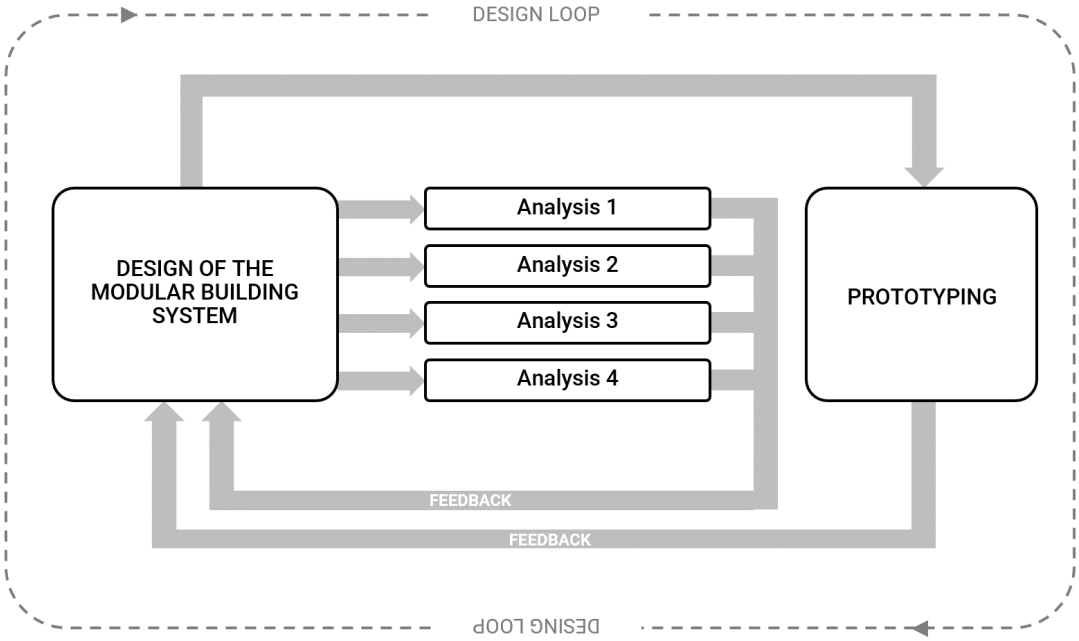


Illustration 2: Integrative and iterative planning tool diagram.

Each iteration of this integrative and iterative design process constituted a design loop. With each loop, the platform was refined based on insights from the previous cycle. Simultaneously, each loop allowed for the inclusion of more complexity, thereby expanding the platform's scope and capacity.
To succeed in the incremental development, it was crucial to set the design boundaries of the modular building system to properly define the computational design system.
A roadmap was established from the beginning to anticipate design limitations and their implications for developing computational tools. This design boundaries were reviewed in each design loop.
Finally, iterative prototyping and testing are key features of this development process. Each design loop was finalized with a prototype or mockup to evaluate the design decisions.

2.2. Development of the computational design system

From the early phases of the design process, computational design tools were used to explore design options and produce prototypes. Small algorithms were developed to model the first modular systems, afterwards, following the iterative design process explained before, they were extended, adding more design options, new features like the connection to the data base, the visualization, and the different measurements. At the end, these small algorithms have become the computational design system that enables the integrative design-to-production methodology.

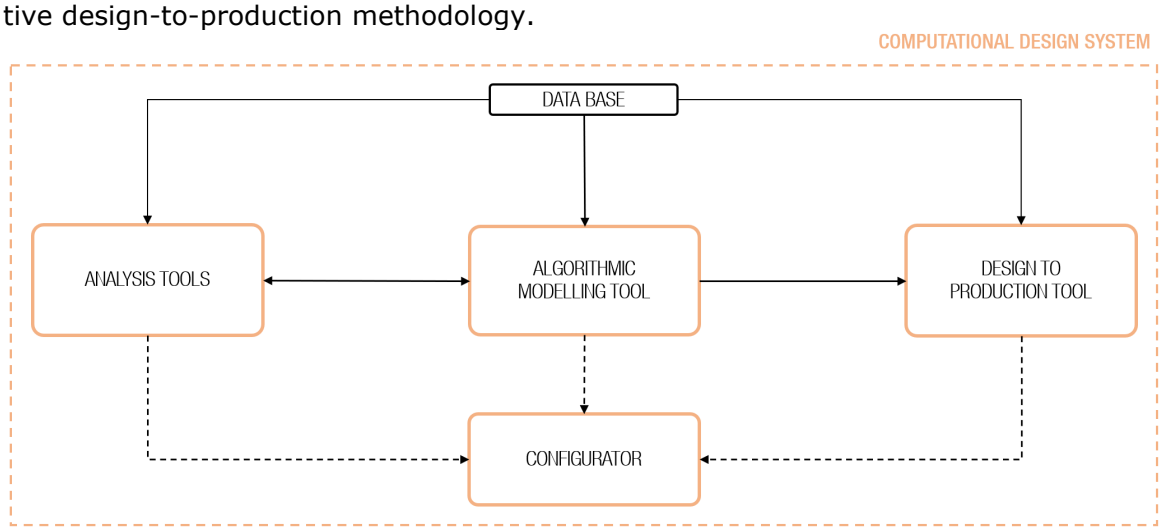


Illustration 3: Simplified diagram of the developed computational design system

The main tool used is the geometry modeler Rhinoceros by McNeel [9] and its addon Grasshopper [10], a visual programming language, aiming for more consistency of the data-flow. Other grasshopper plugins were used, like Karamba3D[11], Ladybug tools [12] Woodpecker [13], and eleFront [14] to extend Rhino7 functionalities

The tool development strategy was distributed in 4 main modules, that at the same time are divided into parts.
The first one is the algorithm modelling and visualization tool. This script was the first one to be developed and the one that has experienced more changes since it had to absorb all the design variations proposed by the design team. The goal of this script is to model, inform and export the geometric information of all the components used for any variation of the modular system. Also, it generates the abstract base model used for different performance analysis.
The second one handles the performance analysis and evaluation of the proposed modular system from different aspects. The first one are the measurements of weight, cost and embedded $C0^2$ emissions, allowing also to export a Bill of Quantity. Another one is the structural analysis and compliance. Future developments will include energy balance analysis (currently under development) and acoustic performance in the future.
The third computational tool developed deals with the design-to-production seamless integration. From the geometry extracted from Rhino, manufacturing process instruction, in BTL format, are automatically generated for every part to be produced. This script automatically bridges the CAD/CAM link, allowing the machining instructions to be obtained very quickly from any modular design variant.
And finally, the fourth computational tool developed is the so-called Configurator. This tool is addressed to the end-user and allows to visualize, measure, and adapt different variations of the modular systems in a web-based platform according to the user's need.
The tools were developed gradually. From the start of the project, a roadmap was established for the three-year duration. The computational design tools were developed in alignment with the project's progression. The first year focused primarily on exploring the modular system design and verifying its feasibility. Consequently, the initial tools developed were for algorithmic modelling and some analysis tools, such as the structural analysis tool. In the second year, with the modular system more clearly defined, manufacturing was introduced into the design process, and the automatic translation of the design to manufacturing was developed. Concurrently, further progress was made in defining the layers of the modular system, leading to the initiation of the energy simulation tool development. Finally, the last year will be dedicated to the final definition of the modular system and the development of its commercialization through the configurator.

2.3. Prototyping

Iterative prototyping and testing is the last method. It is considered an essential part to inform the design process and demonstrate the effectiveness of proposed solutions. This methodology involves the creation of prototypes at different scales and for different purposes, facilitating the validation of design ideas. Through systematic experimentation and evaluation, critical insights were gained, leading to more effective solutions.
The «learning by doing» approach facilitated the understanding of the limitations of the proposed designs, tools, supply chains and partner capabilities, and the integration of these constraints into the design of the modular building system. At the same time, involving the designers in the execution of the prototypes allowed for direct learning, which translated into immediate feedback for the design.
The evaluation of prototypes was crucial to the decision-making process, with concrete data and feedback guiding subsequent design adjustments. Each iteration contributed to the continuous improvement of the design of the modular building system.
The feedback obtained from the prototyping was both qualitative and quantitative. For each one a report was written summarizing the learning.



Illustration 4: Images of the different series of prototypes

3. Case Study: àDISPO

àDisposition is an Innosuisse-based research project led by BFH together with five project partners (C2 Beat Cattaruzza GmbH, Beer Holzbau AG, Pius Schuler AG, Bauart Architeckten und Planer AG). The main goal of the project is to temporarily transform unused industrial halls into useful and flexible spaces. For this purpose, the research project aims to develop a rentable modular system that can be adapted to different activities and space requirements.
The modular building system, or «construction kit», the end user has at its disposal an online configurator to easily test and present project ideas for the temporary use of their vacant buildings and sites, and to implement them in a time and resource efficient manner, demonstrating the viability of their projects.
The modular system is based on the principle of do-it-yourself assembly, using prefabricated lightweight timber components with dismountable yet robust joints to create adaptable rooms that can be assembled quickly and easily by non-professionals builders using as few tools as possible.
The aim of the project is to provide comfortable spaces for many different usage scenarios. For this reason, the modular system allows for multiple configurations with different dimensions, features and finishes.
To achieve this goal, the project has two main developments. On the one hand, the development of a parametrically defined modular building system that can be easily transported, assembled, adjusted and dismantled. On the other hand, the development of an integrative planning and visualization tool that allows for the rapid design and analysis of the modular building system and, at the final stage, the preparation of files for production.

3.1. Modular building system

The first development of this project is the design of a modular building system that offers an optimized approach to constructing temporary and adaptable spaces, with simplicity and efficiency at its core. It is mainly made up of two parts: the components and the layers. The components act as the main structure providing the global stability while also defining the architectural morphology and aesthetics, while the layers define the bioclimatic performance and the finishes. Engineered for non-professional assembly, the building system employs lightweight components and layers, limited to a maximum of 25 kg of weight carried per one person, to ensure safety and ease of handling during the assembly.
The assembly process is straightforward and intuitive, utilizing a plug-and-play concept. No adjustments are necessary, making it simple for anyone to put the components together quickly and efficiently.
The component is the basic part of the modular building system. A minimal number of different components is used to simplify the modular building system. They are parametrically defined, so, for any given rectangular reference surface, any component can automatically be modelled. There are two main components, the vertical ones, the wall components, and the horizontal ones, the floor or roof components. Both components can be filled with different layers.



Illustration 5: Eall and horizontal components are joined creating segments.

The components are joined together using metal demountable connector, forming segments, and a group of segments constitutes a room. The minimal room is a 3x3 walls configuration (or three segments). The construction time is very short, it takes about 20 minutes to build one segment, and this can be done, without special tooling by 2 unskilled workers.

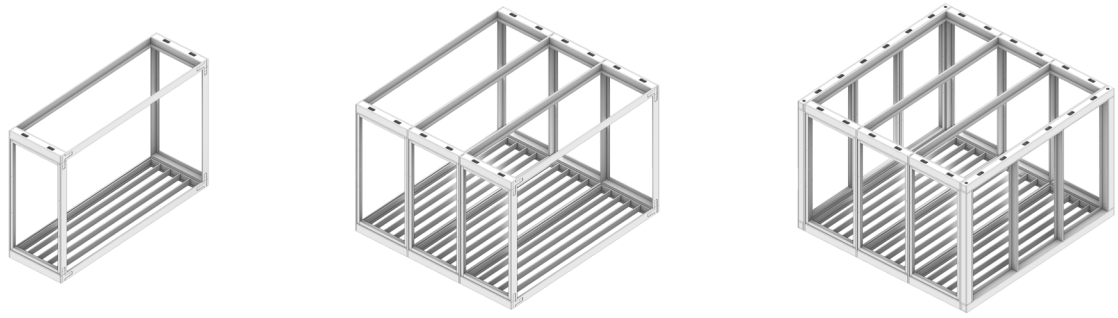


Illustration 6: Assembly sequence of the structure from the segment to the final room.

The Modular Building System is designed to adapt to rooms' changing thermal needs across seasons, allowing users to customize panels by mixing and matching materials for finishing, insulation, and fire protection. These layers can be rented, cut to shape, or even reused from existing materials, thanks to integrated connectors in the frames that securely hold the panels. The spaces are designed to adapt to various scenarios, each with unique requirements for user capacity, area per person, acoustics, and thermal comfort. To meet these diverse needs, the system not only provides flexible building components but also includes a streamlined process for the rapid design of varied unit types.

Global Parameters	Range [mm]
Segment Width	500 to 1200
Segment Height	1100 to 2400
Segment Length	1 to 4 Segment Width
Roof Type	Flat / Doubly pitch
Nº of Frames	1 to …

Structure Parameters	Range [mm]
Cross-section Height	120 to 200
Cross-section Width	10 to 25
T Off-set	0 to Cross-section Height
T Length	30 to 90

Illustration 7: By changing the global parameters, it is possible to respond to specific needs, bringing versatility to the system.

The parametric configurator enables quick customization of the system, allowing adjustments to global parameters to meet specific needs and enhancing its versatility. Basic element dimensions can be easily modified to adapt to a wide range of situations.



Illustration 8: Different variations of the modular building system at the segment level.

At the segment level, diverse roof configurations can be created to offer varied spatial experiences, while rooms and finishing layers can also be modified. This parametric approach allows users to generate a wide variety of arrangements within the modular system's structured rules. In summary, the configurator and building system combine a systematic approach with customization, enabling unique and cost-effective constructions with minimal effort.

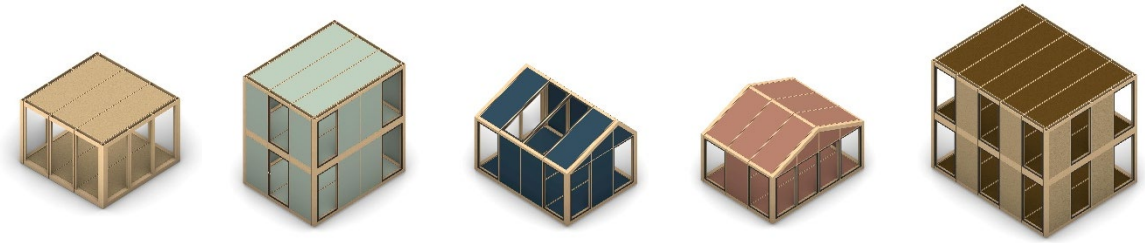


Illustration 9: Possible configurations of the àDISPO modular building system considering future developments.

3.2. Integrative planning and design tool

The second development of this project is an integrative planning and design tool that is the direct consequence of the integrative an iterative method and the computational design system. It allows the rapid design and analysis of the modular building system, at the final stage, the preparation of files for production.
From the beginning of the research project the goal was to design a modular construction kit in timber that allowed for the fast deployment of temporary rooms. However, the design of the modular building system was not pre-defined at the project's outset but was developed concurrently with the computational design system. With each iteration of the design process, new parts of the computational design system were developed.
The integrative planning and design tool is clearly divided into two parts. The first one, also called the «back end», refers to the tool used by the researcher for the development of the project. It includes all the tools used for the design, analysis and manufacturing of the modular building system. It is called back end because it is exclusively accessible to these researchers who at the same time use it and expand its possibilities and refine the design of the modular building system.
On the other hand, there is the configurator or front-end. The ultimate aim of this tool is to make the modular building system accessible to end users, allowing them to design their temporary use module according to their needs within clearly defined limits. The configurator is fed by the results of the integrative planning and design tool and presents them in a user-friendly way to potential customers interested in buying or renting the modular building system.

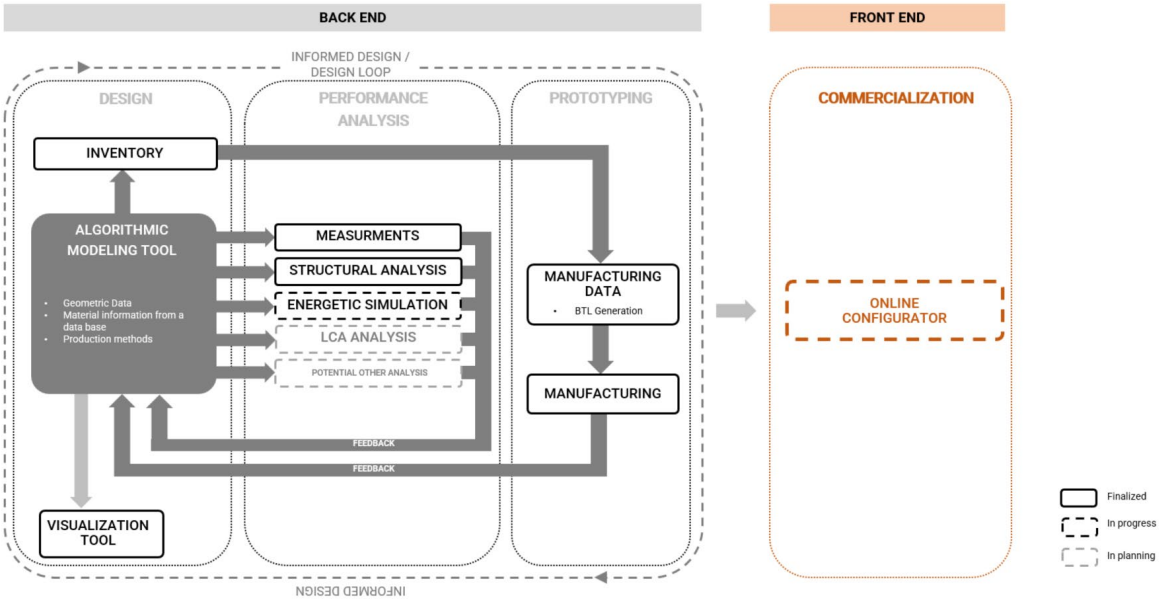


Illustration 10: The design methodology is based on integrative planning and design tool.

3.2.1. Analysis tools

The analysis tools evaluates the performance of the proposed modular system from various aspects. The first aspect includes measurements of weight, cost and embedded CO^2 emissions, and allows the export of a Bill of Quantities. Another aspect is structural analysis and compliance and the energy balance and comfort level analysis.

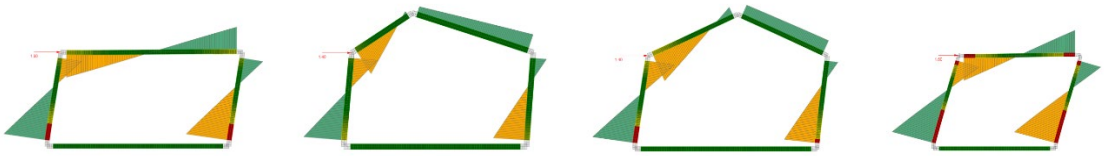


Illustration 11: Example of 4 out of 1200 analyzed segments with different parameters combination.

The structural analysis tools allow for resolving minor structural issues and identifying the structural implications of design decisions. The primary aim of this analysis is to evaluate how the L-shaped metal bracket influences the frame's stiffness, as stability in this plane depends entirely on these brackets. The tool successfully analyzed over 1,200 possible segment combinations, plotting the results based on their compliance with EC5 standards.

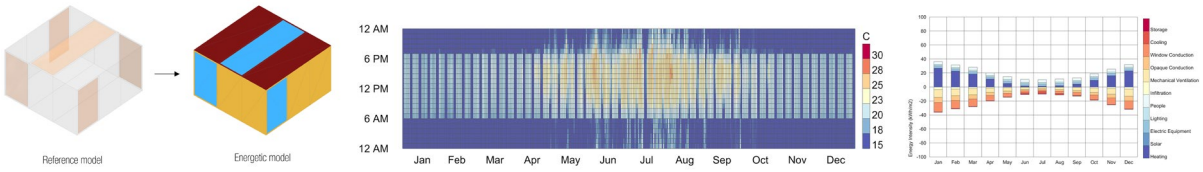


Illustration 12: Abstract model of the analysed room, highlighting the glazed walls in orange (left). Representation of the analysed model in Ladybug (middle). Total monthly loads (right).

The primary objective of the energy simulation tool is to enable automated calculations of the energy balance and assess comfort levels across numerous modular system variations. Using the available materials, new composites with their relevant properties can be automatically defined as Ladybug materials through the database.

3.2.2. Design-to-Production tool

The Design-to-Production tool goal is to automatically transform geometry data into BTL [15] operations in preparation for the CNC manufacture. BTL serves as a descriptive language for timber fabrication. It offers parametric definitions for a wide range of timber elements, from general cuts to more complex details.
Softwares like Cadwork, from just a «dumb» geometry, can automatically generate BTL instructions by recognizing features and deciding which machining operation is needed to arrive at the final shape. This has been proven to work for simple geometry but as soon

as the geometry is a bit complex with parametric dependencies this process is unsuccessful, and it has to be done manually in the CAM software. To bridge this gap the Woodpecker[13] plug-in for Grasshopper is used. This plugin enables to extend the parametric models seamlessly into fabrication directly defining from the cad model what features are used for the fabrication. It offers several GH components that can turn input geometry into fabrication data in BTL(X) format.

Step by step, the design-to-production tool will be introduced with an example:

First, the desired components to build are selected from the inventory. The global manufacturing parameters must be established at the outset, depending on the machinery utilized since the BTL instructions depend on those parameters. In this case, a HOMAG CENTATEQ P-500/600 CNC Machining Center was used.

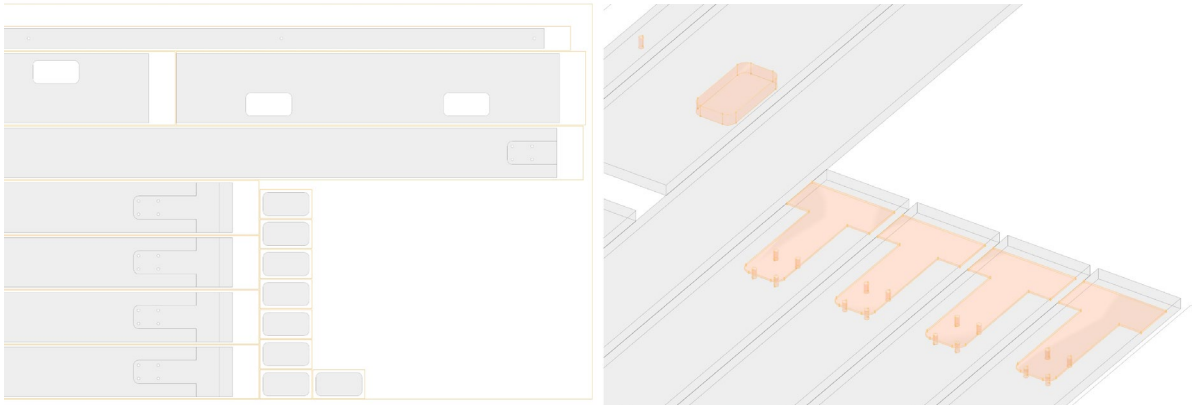


Illustration 13: In gray, the parts to mill. In orange, the tolerance added to avoid unwished cuts (left). Pockets and drills are extracted from the geometry with a solid difference with the bounding box of each part(right).

The next step is to sort all the parts by type so that they can be nested correctly. Each CNC operation needs its own tolerance, so the nesting must reflect this to avoid damage to the neighboring parts. For example, the longitudinal cut always needs an extra space at the end of the cut. The nesting is done using the OpenNest [16].
Once all parts are nested, the fabrication features must be identified. The goal is to find the most suitable fabrication feature (engraving, drilling, pocket, free contour, saw cut and longitudinal cu) from the dumb geometry within the BTL standard operations list.
Once the big parts, drillings and pockets have been separated the goal is to extract the fabrication feature dimensions and their location from the «dumb» geometry. This involves performing a series of geometric operations specific for each operation.

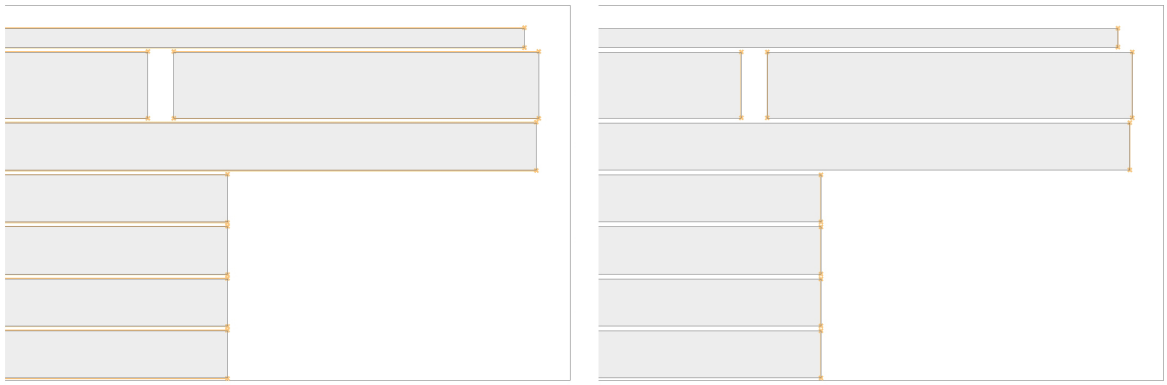


Illustration 14: The long cuts are done with the longitudinal cut and the short ones with the saw cut.

The big parts are cut using longitudinal (0-010-4) cut for those parallel to the x-axis and saw cuts (3-013-4) for the cuts parallel to the y-axis. In this case, it is necessary to determine the starting point, the length, and the depth of the cut. All this information is obtained from the bounding box of each part.

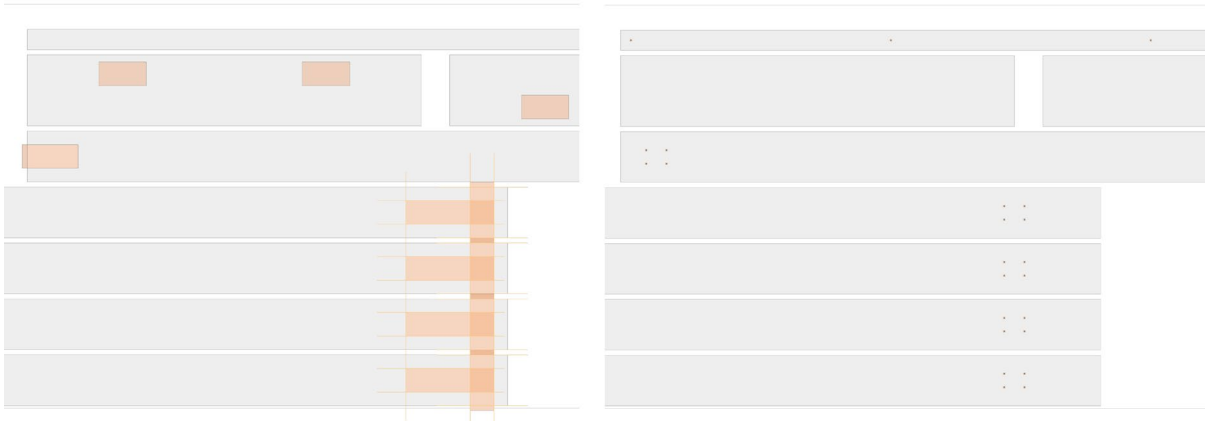


Illustration 15: Identified pockets and extended edges of the T-pockets (left). Identified drillings (right).

Defining pockets is a more labor-intensive process. There are two types of pockets: rectangular and non-rectangular (or T-pockets). Rectangular pockets can be defined as a single pocket operation, while T-pockets require two combined pocket operations.

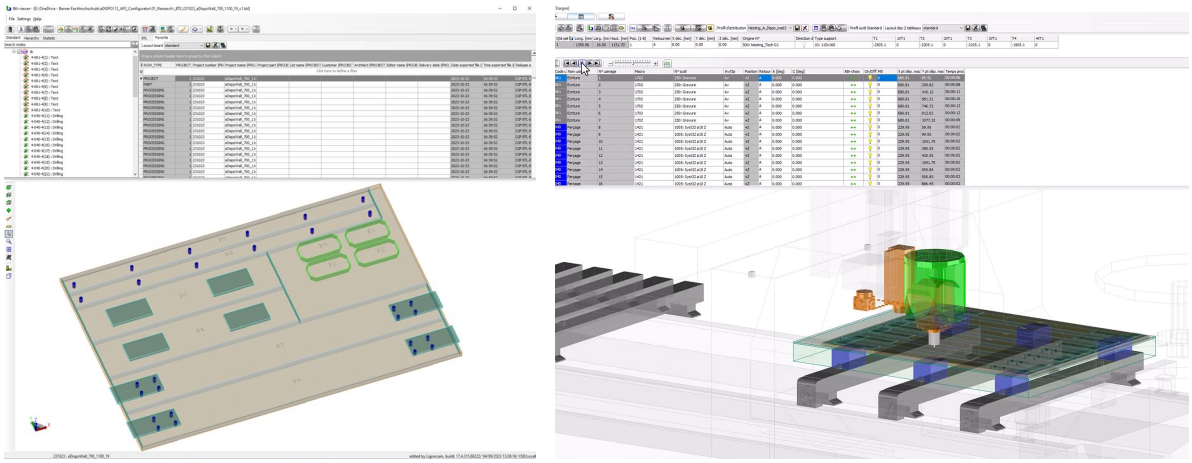


Illustration 16: BTL export of the previously presented mockup from the BTL Viewer (left).
G-code simulation in Lignocam(right).

With all the necessary information, including points, lines, thicknesses, and lengths, the operations can be defined using the Woodpecker plugin. When the native components are not enough to define the operations the UserDefinedOperations component is used, since it allows to use any BTL operation in the standard. Finally, all the Woodpecker components are merged into one list of operations and exported to BTL. To conclude the process, the BTL file was imported into Lignocam to create the G-code used by the HOMAG CENTATEQ P-500/600 CNC Machining Center. Before fabrication, the tool priority macros need to be reviewed to ensure they match those defined previously.



Illustration 17: CNC mock-up of a reduced wall component produced with the HOMAG CENTATEQ P-500/600 CNC Machining Centers from BFH Techpark.

4. Conclusions

This research had the goal to evaluate to what extent can the design and production of modular timber architecture be enhanced by computational design tools. Based on the case study embedded in this specific context, it was possible to test all the methods presented previously and to evaluate their impact.

The results show that the implementation of computational design tools has, under certain conditions, significantly aided the design and manufacturing processes of the proposed modular building system.

The modular building kit presented in the case study is based on the repetitive use of components to generate rooms. However, what is repeated is not just the components themselves (such as walls or roofs) but their design rules. The modular building kit does not have specific dimensions; instead, it relies on design rules applied to reference surfaces.

It is clear from this baseline that the parametric definition of the modular building system is highly beneficial because, once the parametric definition is set, all variants within the set limits can be modeled automatically.

Essentially, the design improvements were achieved by extending this parametric definition to the analysis phase, allowing for near real-time feedback. This approach informed the design process, making it easier to validate or discard options compared to traditional methods, leading to better decision-making.

Implementing these methods has significantly benefited production. The primary advantage arose from extending algorithmic modeling to facilitate the automatic generation of manufacturing information in BTL format. For any proposed module dimensions within design boundaries, manufacturing instructions were automatically generated.

As a result, the digital manufacturing of parts became highly efficient, enabling mass customization. Simultaneously, precision improved due to the use of CNC technology, allowing greater freedom and complexity in detailing without increasing costs.

Finally, all these computational tools could be integrated into an online configurator, making them accessible to end users and further reinforcing the implementation of mass customization.

However, in both design and production, the proposed methods also had several disadvantages. The most significant was the time-consuming process of implementing design updates or modifications into the computational design system. This was primarily due to the complexity of translating each design feature into its corresponding BTL definition. Additionally, frequent debugging was required throughout the computational system to accommodate potential changes in the data structure.

Furthermore, the BTL-to-CAM process always required minor adjustments. While the CAD-to-BTL bridge worked effectively, small adjustments to the CAM software macros were required to reflect preferred tools or other BTL parameters that were not accessible through the Woodpecker plugin.

In conclusion, while the methods proposed in this thesis may not be universally suitable for all types of modular timber architecture, they offer significant advantages for product-based modular building systems such as the one presented in this paper. This type of architecture is consistent with the findings of the thesis, as its clearly defined design boundaries help to maximize the benefits, minimize the drawbacks and ensure the robustness of the computational design system. The repetitive nature and controlled customization of these product-based kits make them highly compatible with the computational design methods demonstrated in this research.

5. Bibliography

[1] M. Aitchison, *Prefab housing and the future of building: product to process*. London: Lund Humphries, 2018.

[2] N. Bertram, S. Fuchs, J. Mischke, R. Palter, G. Strube, and J. Woetzel, «Modular construction: From projects to products | McKinsey.» Accessed: Mar. 26, 2024. [Online]. Available: https://www.mckinsey.com/capabilities/operations/our-insights/modular-construction-from-projects-to-products#/

[3] G. UNEP, «2022 Global Status Report for Buildings and Construction,» UNEP – UN Environment Programme. Accessed: Feb. 12, 2024. [Online]. Available: http://www.unep.org/resources/publication/2022-global-status-report-buildings-and-construction

[4] UNECE, «Housing2030: Effective policies for affordable housing in the UNECE region | UNECE.» Accessed: Feb. 12, 2024. [Online]. Available: https://unece.org/info/Housing-and-Land-Management/pub/360530

[5] Filipe Barbosa *et al.*, «Reinventing construction through a productivity revolution | McKinsey.» Accessed: Feb. 10, 2024. [Online]. Available: https://www.mckinsey.com/capabilities/operations/our-insights/reinventing-construction-through-a-productivity-revolution

[6] R. E. Smith, *Prefab Architecture: A Guide to Modular Design and Construction*. John Wiley & Sons, 2011.

[7] J. M. Taron, *ACADIA 2011: Integration Through Computation: Proceedings of the 31st Annual Conference of the Association for Computer Aided Design in Architecture (ACADIA)*. Association for Computer Aided Design in Architecture, 2011.

[8] «Ove Arup Key Speech – Arup.» Accessed: Feb. 02, 2024. [Online]. Available: https://www.arup.com/perspectives/publications/speeches-and-lectures/section/ove-arup-key-speech

[9] Robert McNeel &, «Rhinoceros 3D,» www.rhino3d.com. Accessed: Feb. 10, 2024. [Online]. Available: https://www.rhino3d.com/

[10] David Rutten, «Grasshopper.» Accessed: Feb. 10, 2024. [Online]. Available: https://www.grasshopper3d.com/

[11] «Karamba3D,» Food4Rhino. Accessed: Feb. 14, 2024. [Online]. Available: https://www.food4rhino.com/en/app/karamba3d

[12] «Ladybug Tools.» Accessed: Jun. 21, 2024. [Online]. Available: https://www.ladybug.tools/

[13] «Woodpecker,» Food4Rhino. Accessed: Jan. 22, 2024. [Online]. Available: https://www.food4rhino.com/en/app/woodpecker

[14] «eleFront,» Food4Rhino. Accessed: Feb. 14, 2024. [Online]. Available: https://www.food4rhino.com/en/app/elefront

[15] «design2machine – the data transfer interface for wood constructions.» Accessed: Jan. 22, 2024. [Online]. Available: https://design2machine.com/index.html

[16] «OpenNest,» Food4Rhino. Accessed: Jun. 25, 2024. [Online]. Available: https://www.food4rhino.com/en/app/opennest

Vertrieb FORUM **HOLZBAU**
Bahnhofplatz 1, 2502 Biel/Bienne, Schweiz
T +41 32 327 20 00
info@forum-holzbau.com
www.forum-holzbau.com

ISBN 978-3-906226-69-9